

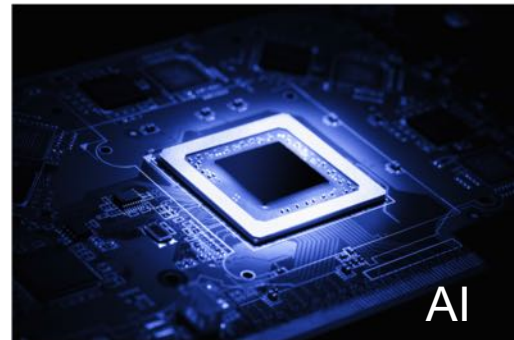
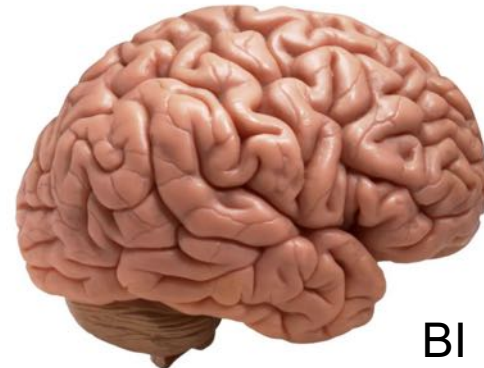
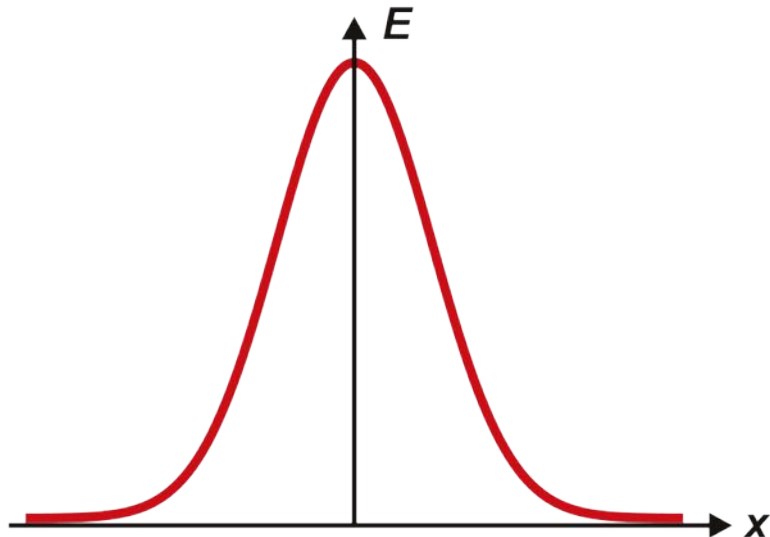
# 机器学习与脑科学

*Interaction and convergence*

洪 波

[hongbo@tsinghua.edu.cn](mailto:hongbo@tsinghua.edu.cn)

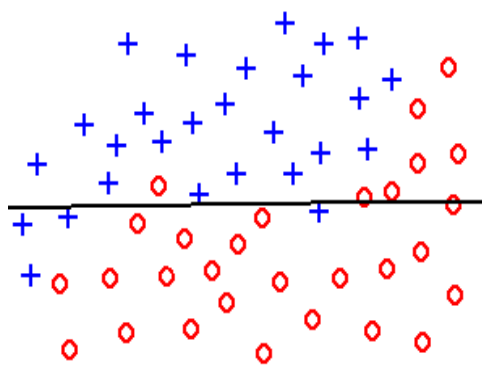
# BI and AI are facing the same challenge



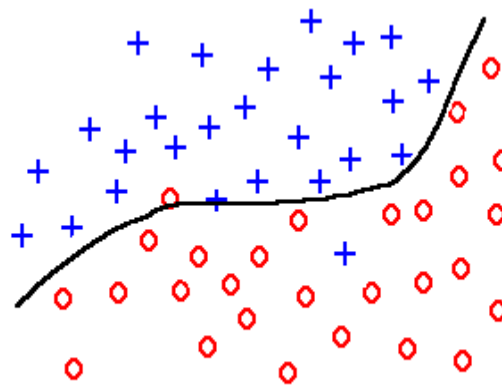
智能 - 应对确定性和不确定性的能力

*Certainty and Uncertainty!*

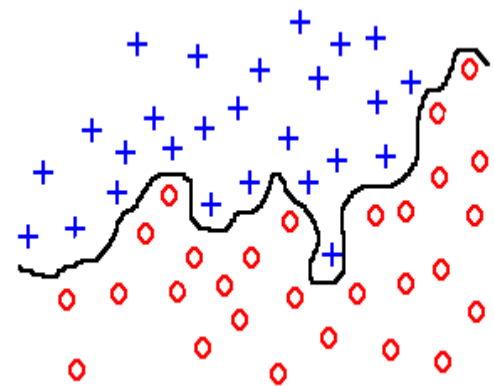
# Certainty and Uncertainty in Classification



Under-fitting

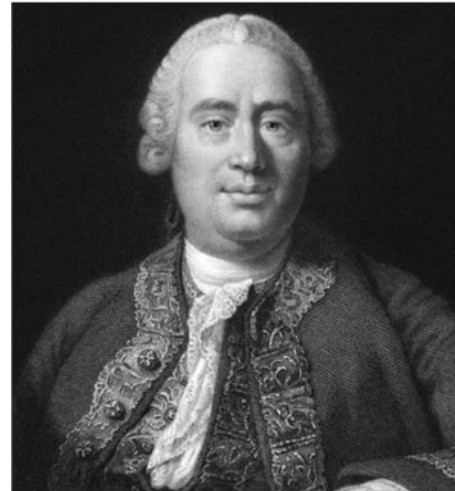


Good fitting



Over-fitting

# 明知“不可知”而知之



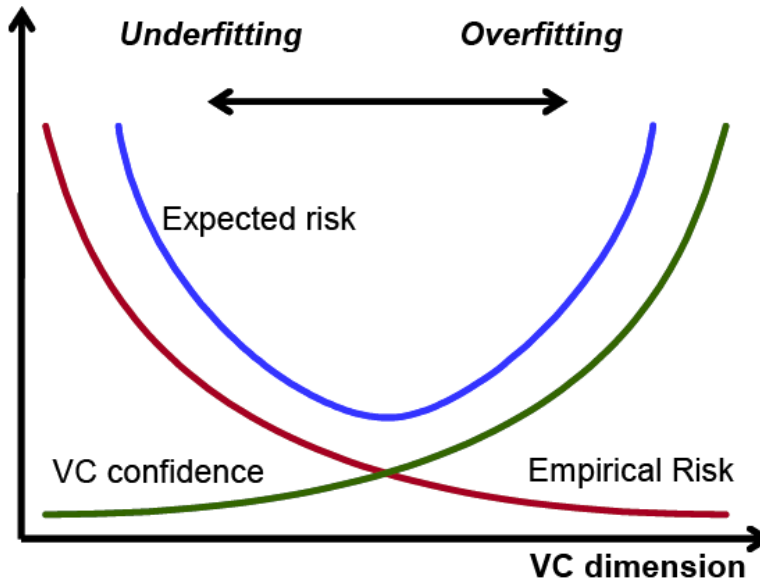
“我们无从得知因果之间的关系，只能得知某些事物总是会连结在一起，而这些事物在过去的经验里又是从不曾分开过的。我们并不能看透连结这些事物背后的理性为何，我们只能观察到这些事物的本身，并且发现这些事物总是透过一种经常的连结而被我们在想像中归类。”

—大卫·休谟 David Hume, 1740

# 认识和解决泛化问题 Generalization

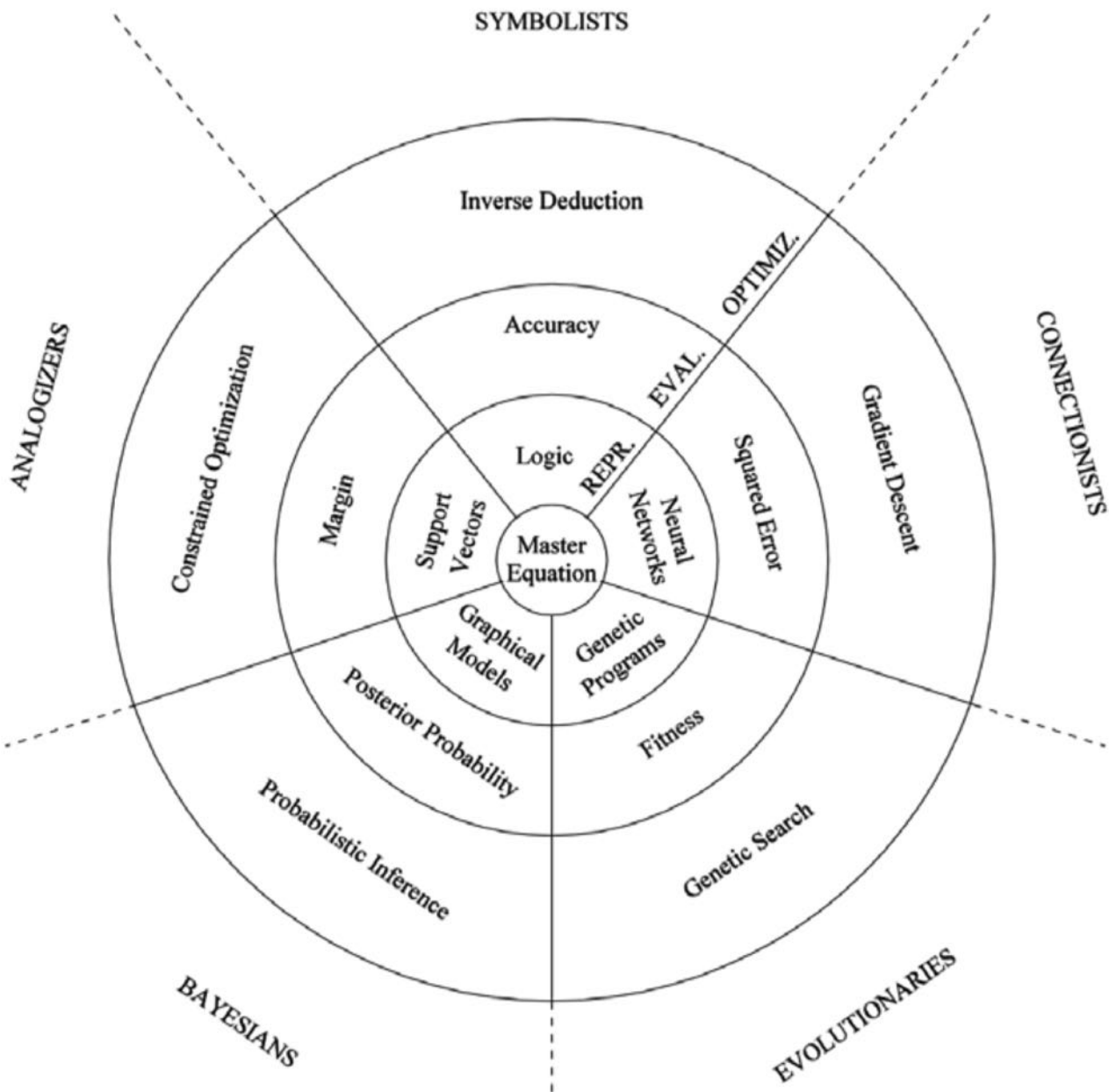
通常情况下，我们总是努力在有限样本的训练集上能找到使得经验风险最小的分类器，而且希望当样本数增多时，经验风险趋近于期望风险：

$$R_{emp} \xrightarrow[n \rightarrow \infty]{?} R$$



# 机器学习的核心方法

- 模型选择 Model selection
- 代价函数 Cost function
- 优化算法 Optimization algorithm
- 正则化 Regularization
- 核函数升维 Kernel trick



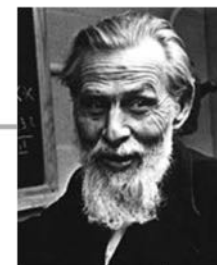
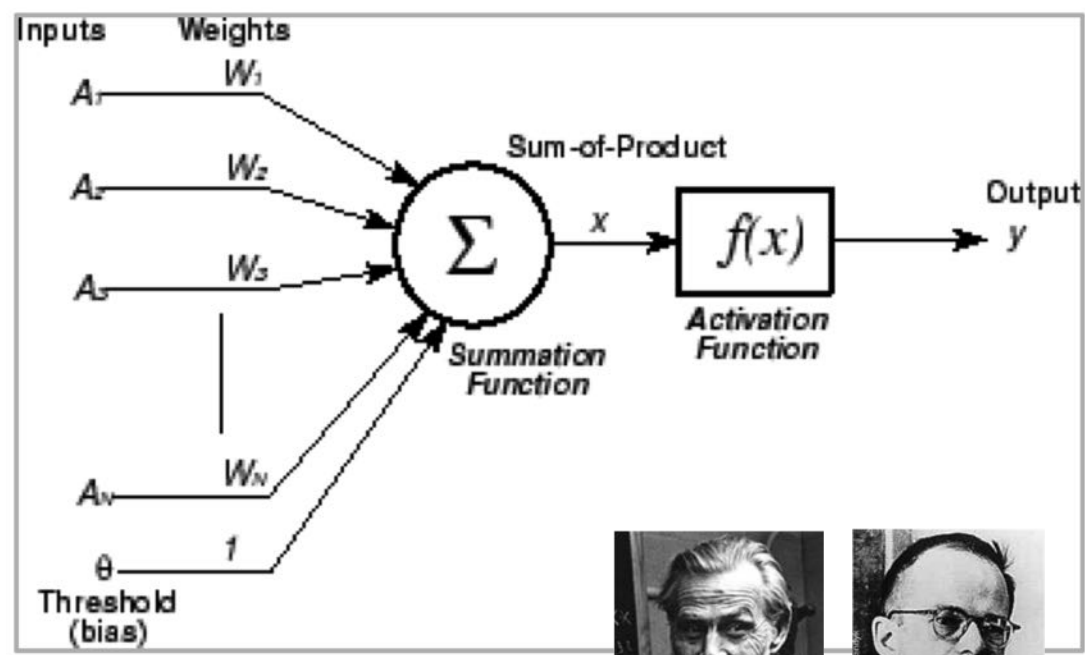
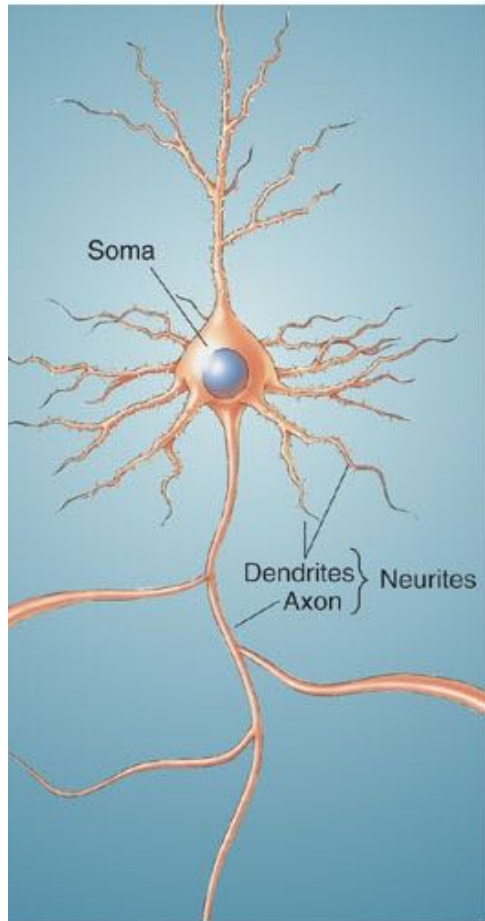
# 机器学习的经典方法

- ☑ 线性分类器 Linear Classifier
- ☑ 支持向量机 Support Vector Machine
- ☑ 贝叶斯分类 Bayesian classifier
- ☑ 主分量分析 Principal component analysis
- ☑ 无监督聚类 Clustering

脑科学帮助人工智能  
BI inspires AI

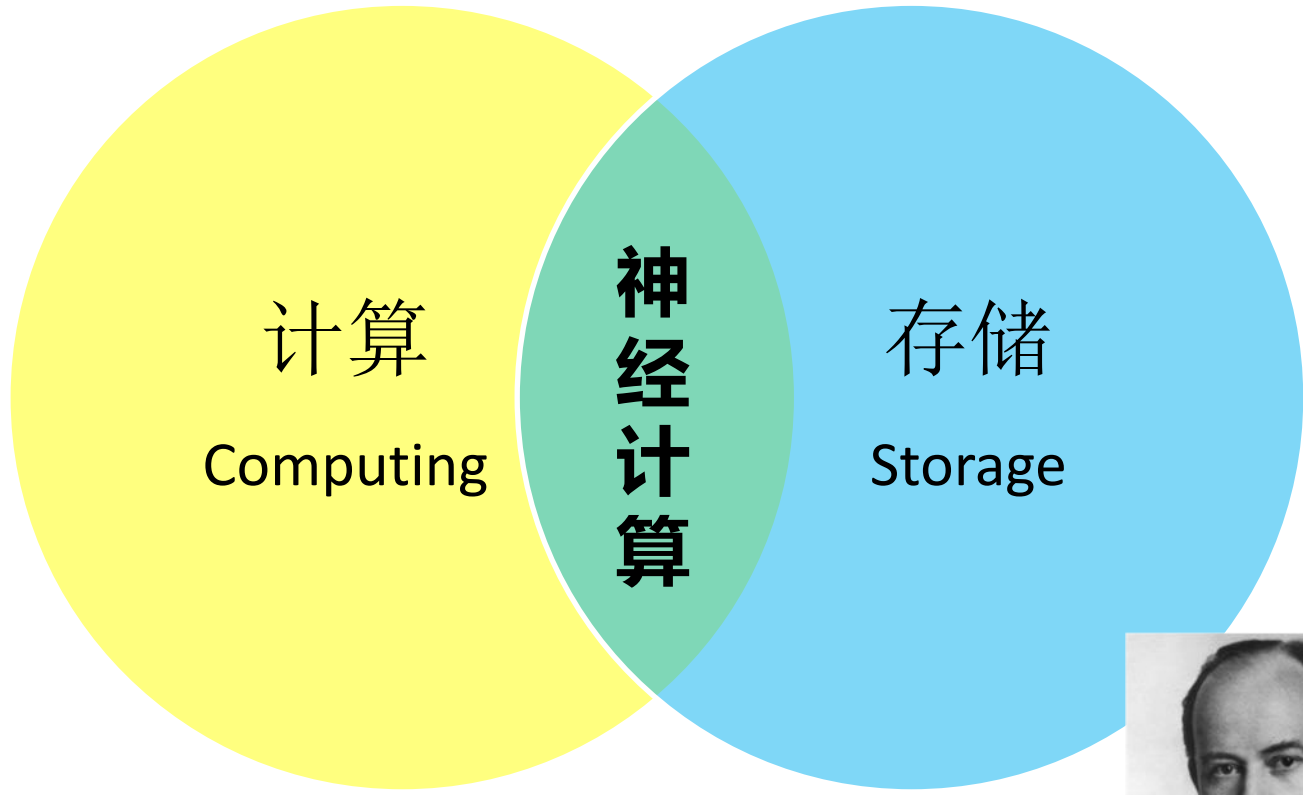
# Leap 1#: Artificial neuron

Inspired by neuron firing and synaptic transmission



McCulloch–Pitts  
1943

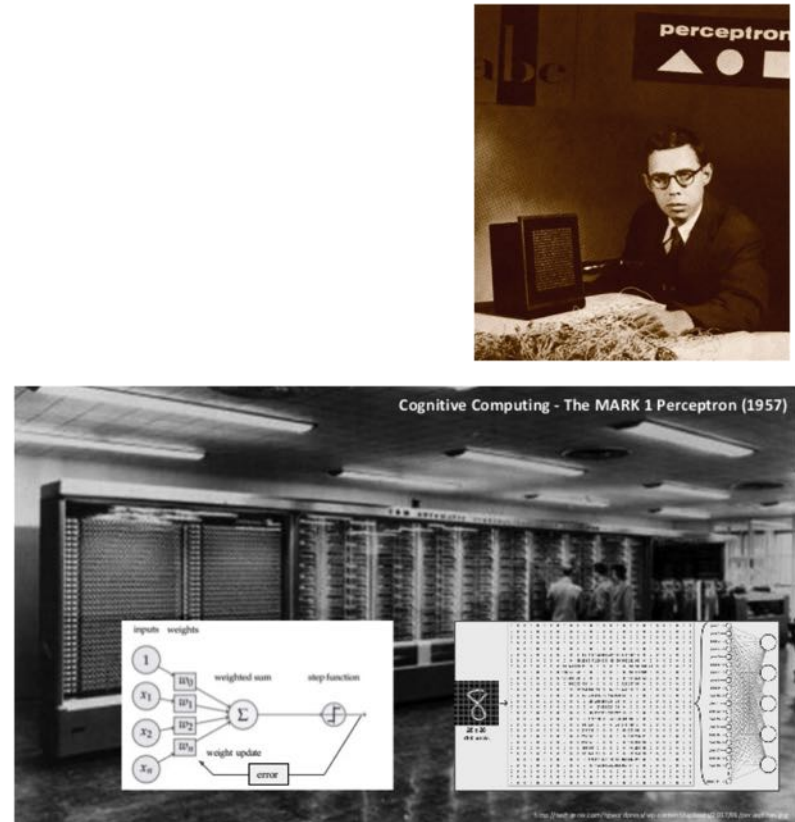
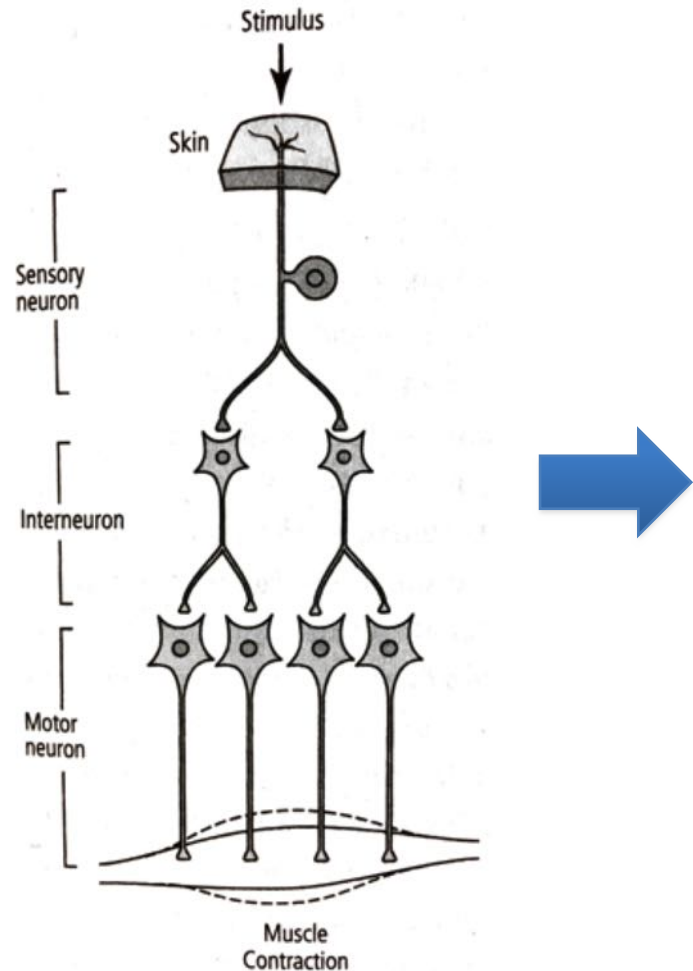
# 神经计算：计算与存储合二为一



John von Neumann

# Leap 2#: Perceptron 感知机

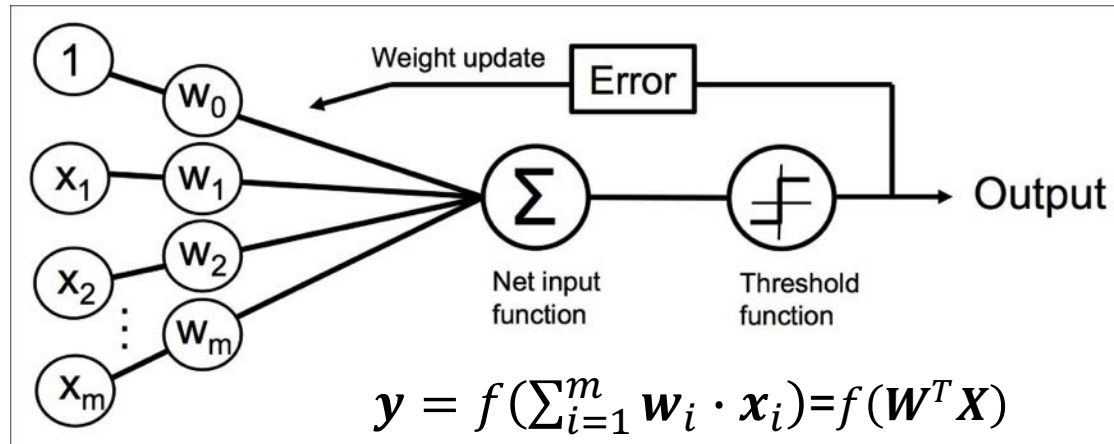
Inspired by the structure and function of interneuron



Frank Rosenblatt, 1957

Rumelhart 1985; Werbos, 1974

# 感知机 Perceptron



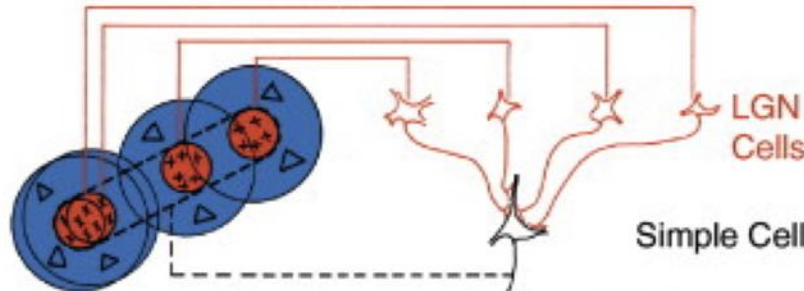
The perceptron, invented in the late 1950s, was considered a **paradigm shift**. For the first time, a machine could be taught to perform certain tasks using examples. This surprising invention was almost immediately followed by an equally surprising theoretical result, the **perceptron convergence theorem**, which states that a machine executing the perceptron algorithm can effectively produce a decision rule that is compatible with its training examples. A youthful wave of optimism took over the research community. Although it only dealt with a very specific category of tasks, namely pattern recognition tasks, the perceptron was widely publicized as the **forerunner of more general learning machines**.

Léon Bottou, 1988

## Leap 3#: Convolution Neural Network(CNN)

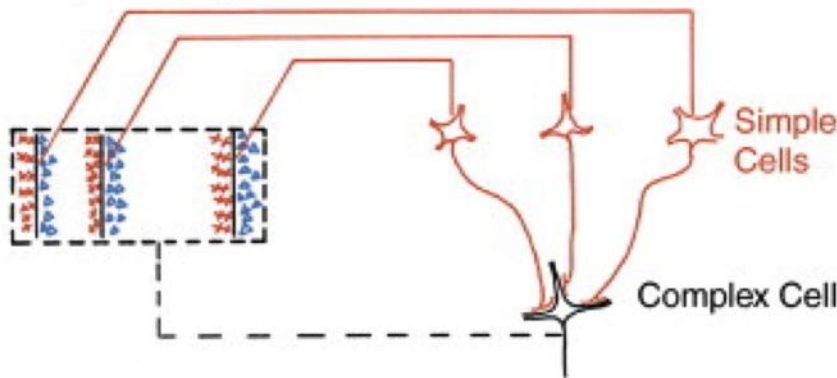
Inspired by Simple and Complex Cell in Visual Cortex

Circuit Building a Simple Cell from LGN Cells



**Convolution**

Building a Complex Cell from Simple Cells



**Pooling**

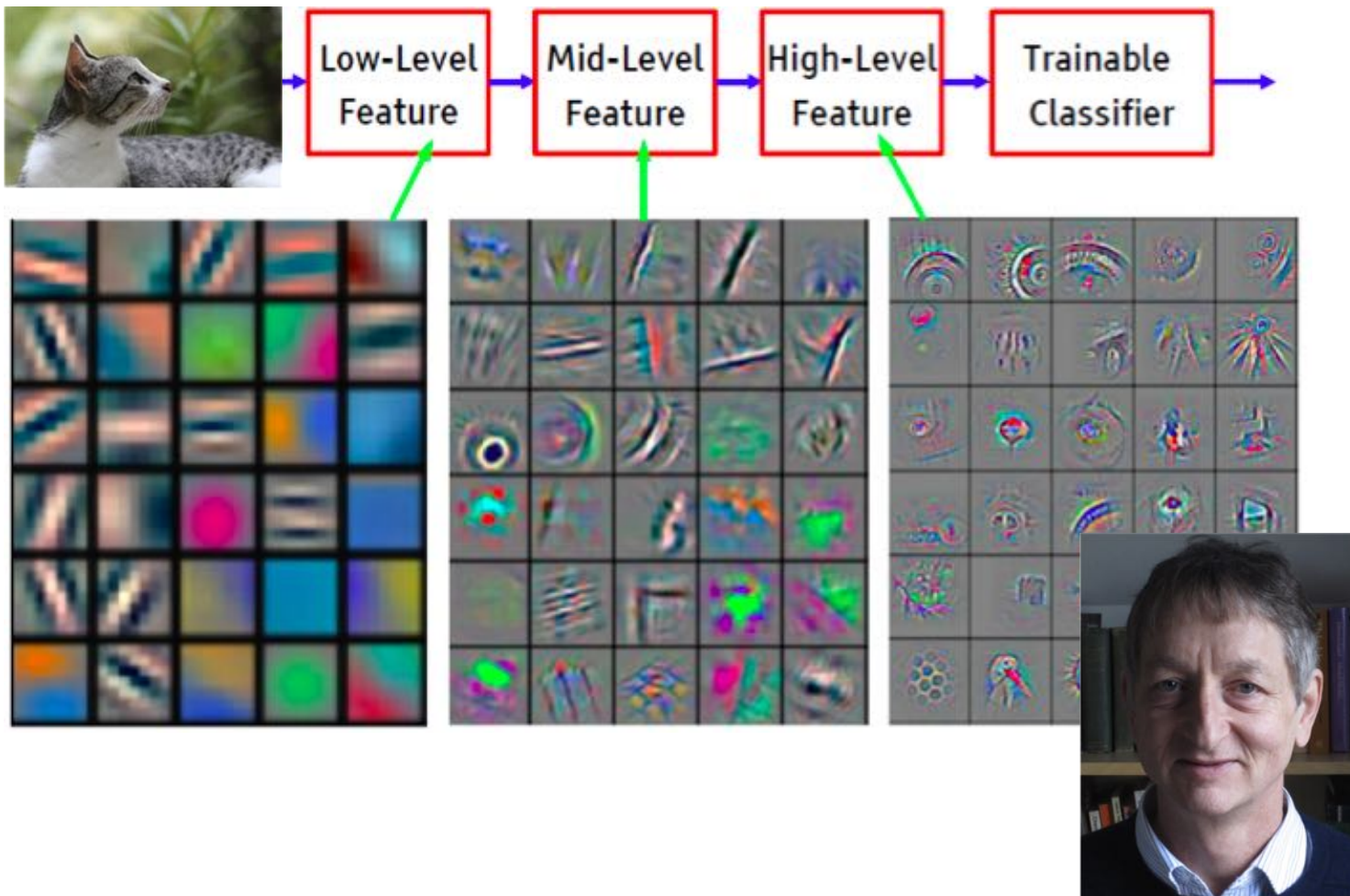


David H. Hubel

Torsten N. Wiesel

1981 Nobel Prize

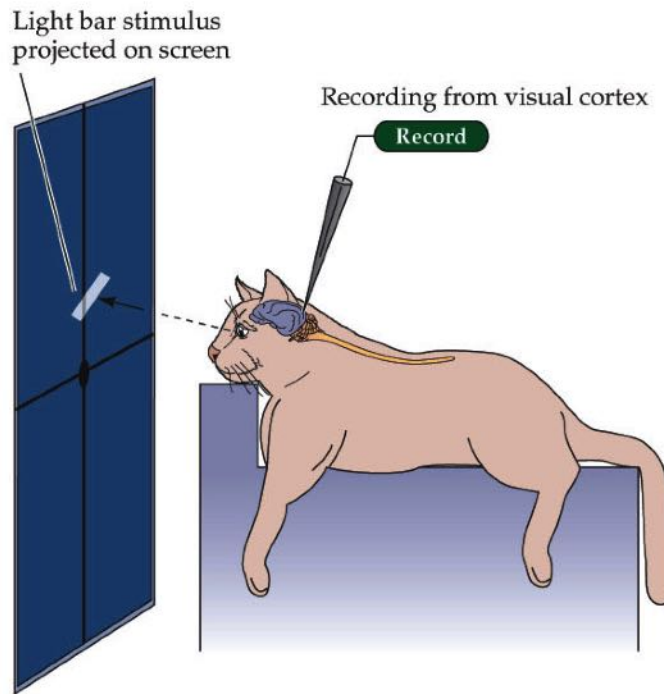
# Feature map of low levels



Geoffrey E. Hinton

# Preferred stimulus of a visual cortex neuron

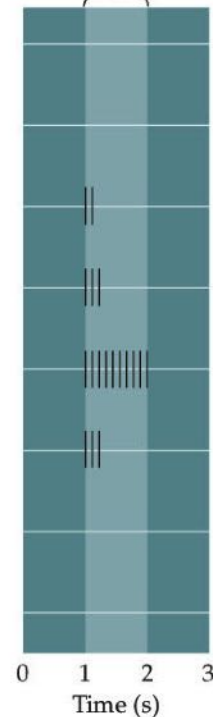
(A) Experimental setup



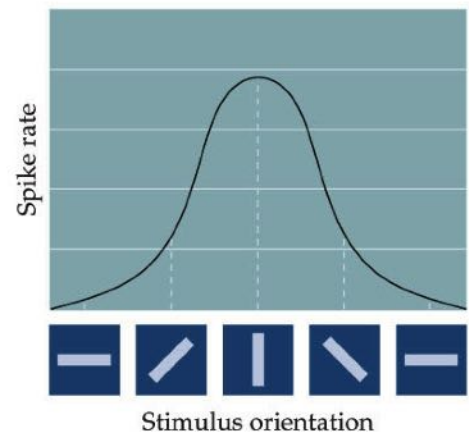
(B) Stimulus orientation



Stimulus presented

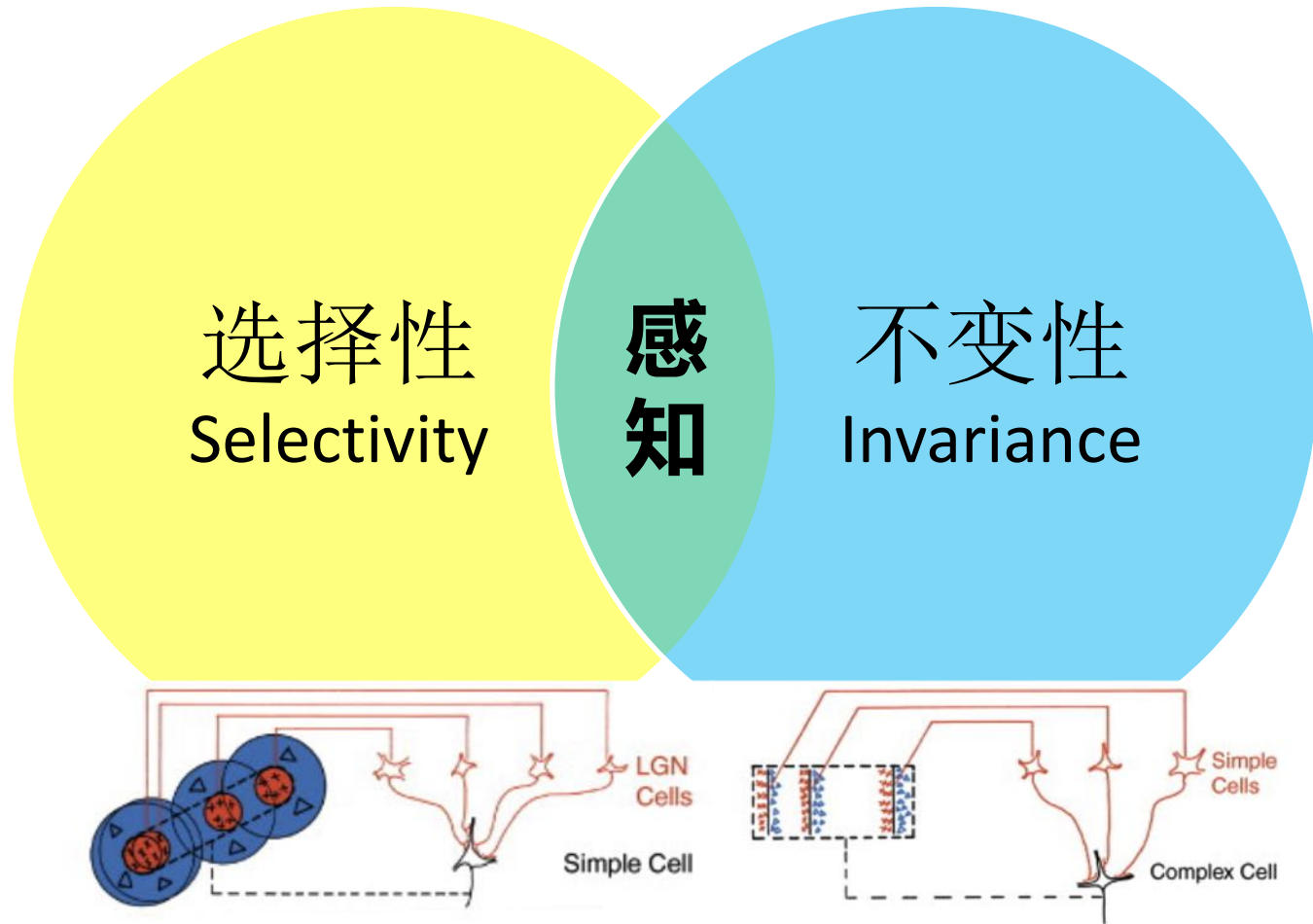


(C)



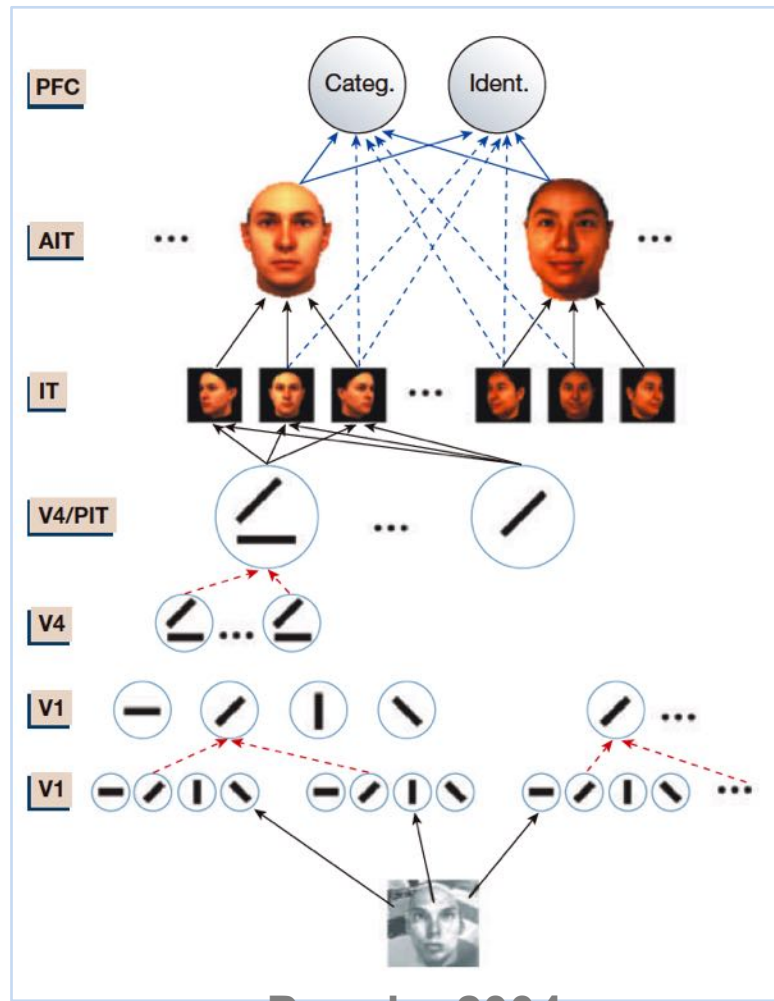
Part of Nobel prize (1981) work by Hubel and Wiesel

# 感知的难题：选择性和不变性

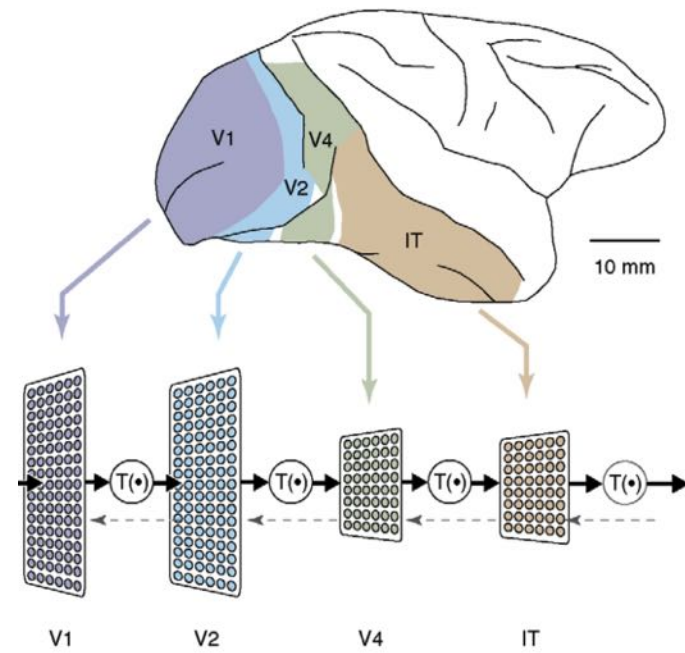


# Leap 4#: Feed-forward Deep Learning Network

Inspired by hierarchical processing in visual cortex



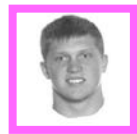
Poggio, 2004



DiCarlo, Cox, 2007



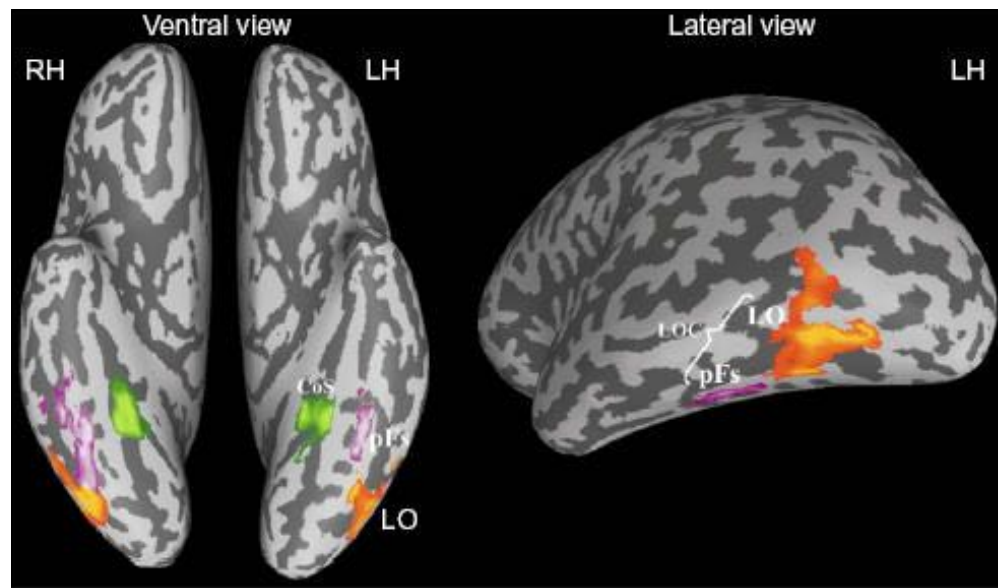
objects



faces



places



*Malach, 2002, TICS*

# 深度网络识别图像中的物体

Samoyed (16); Papillon (5.7); Pomeranian (2.7); Arctic fox (1.0); Eskimo dog (0.6); white wolf (0.4); Siberian husky (0.4)

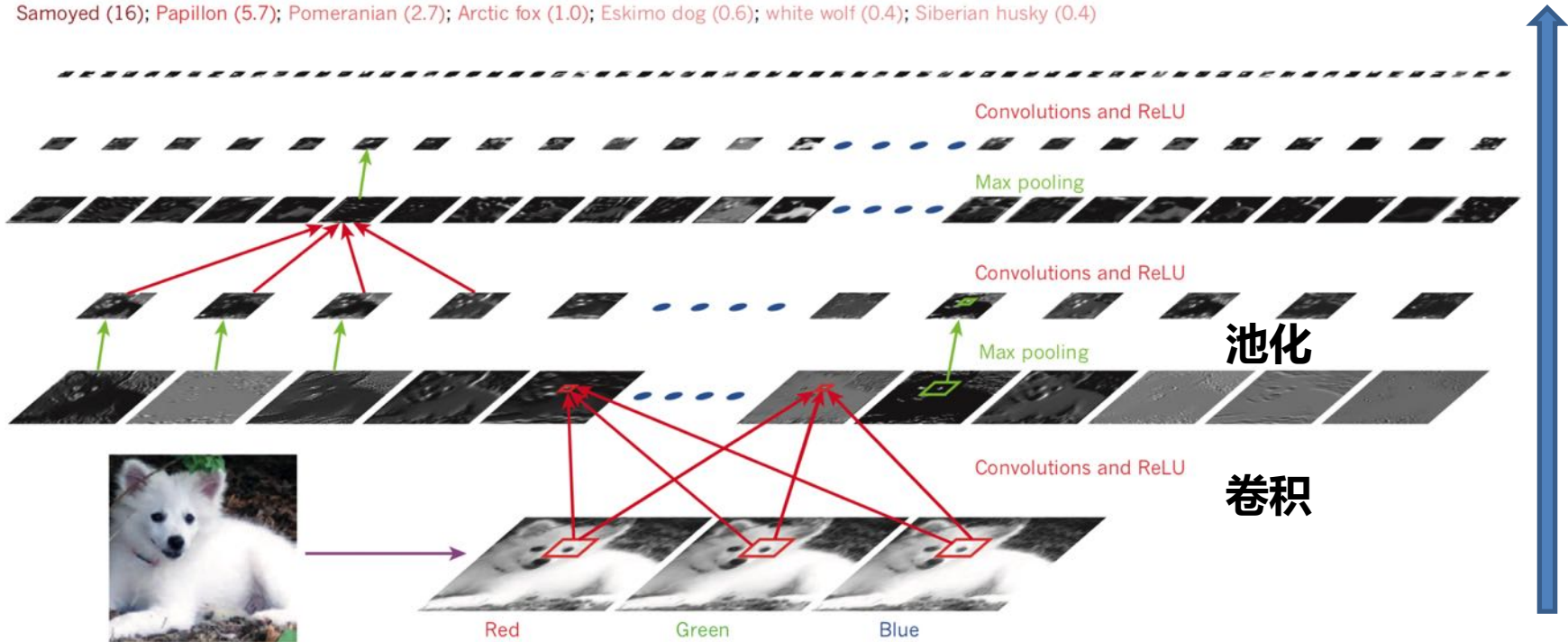
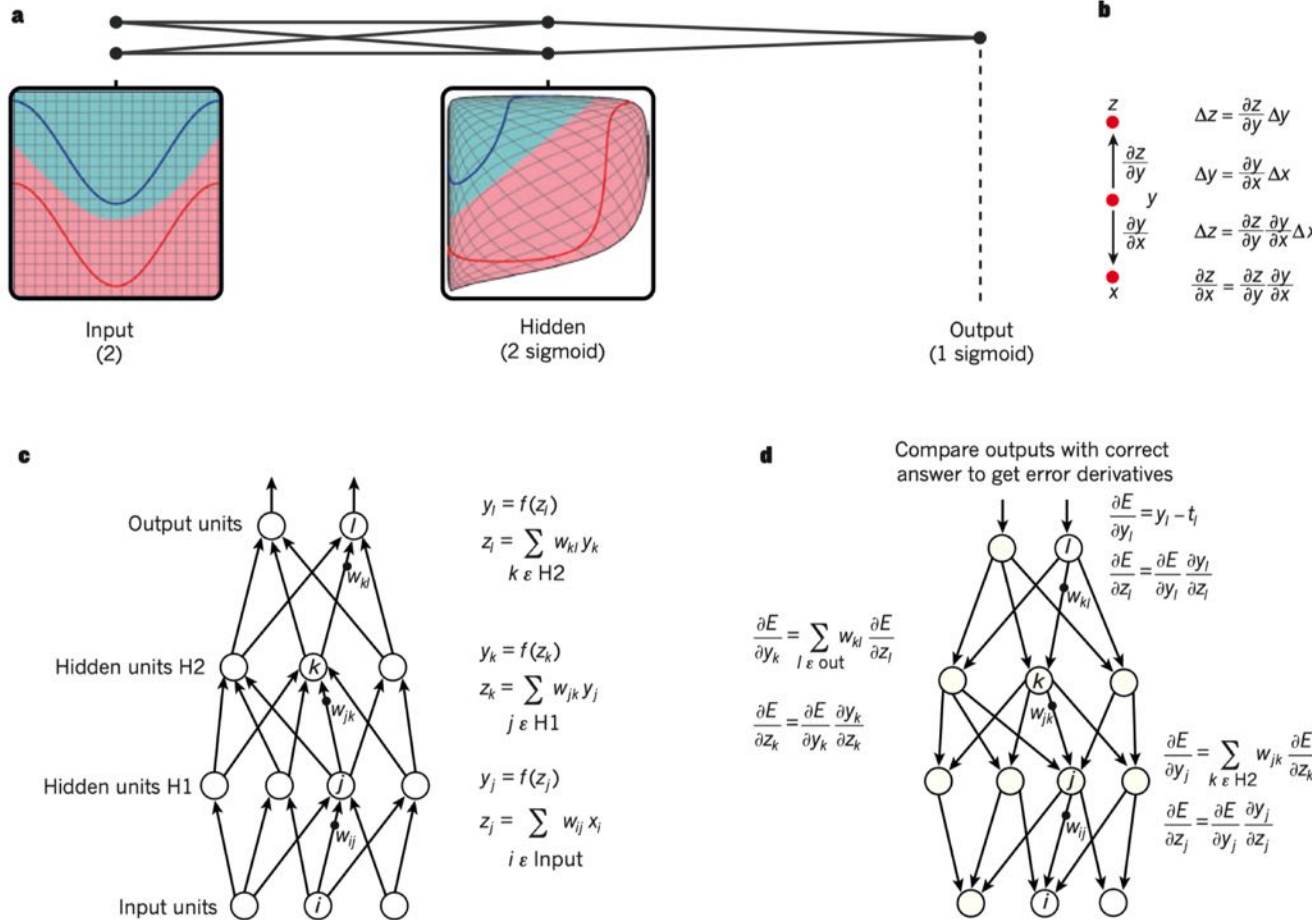


**Figure 2 | Inside a convolutional network.** The outputs (not the filters) of each layer (horizontally) of a typical convolutional network architecture applied to the image of a Samoyed dog (bottom left; and RGB (red, green, blue) inputs, bottom right). Each rectangular image is a feature map

corresponding to the output for one of the learned features, detected at each of the image positions. Information flows bottom up, with lower-level features acting as oriented edge detectors, and a score is computed for each image class in output. ReLU, rectified linear unit.

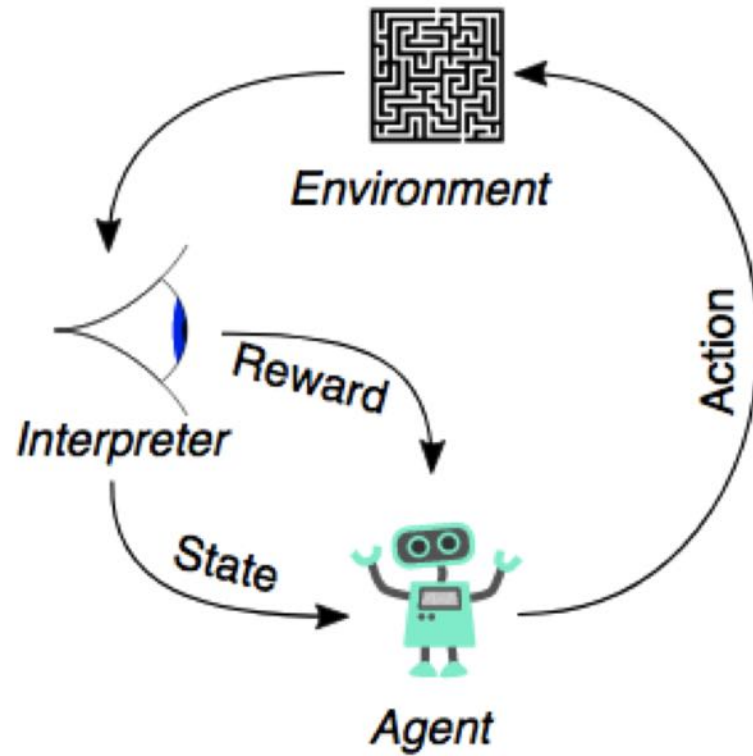
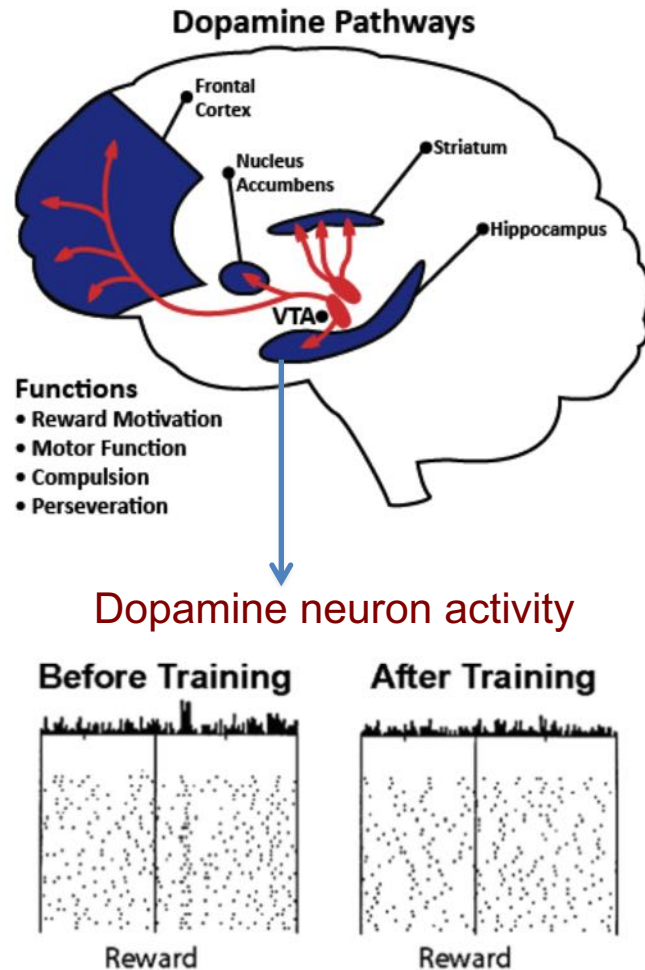
# 深度学习网络与BP学习算法？

## Deep learning network and BP



# Leap 5#: Reinforcement Learning

Inspired by rewarding system in the brain

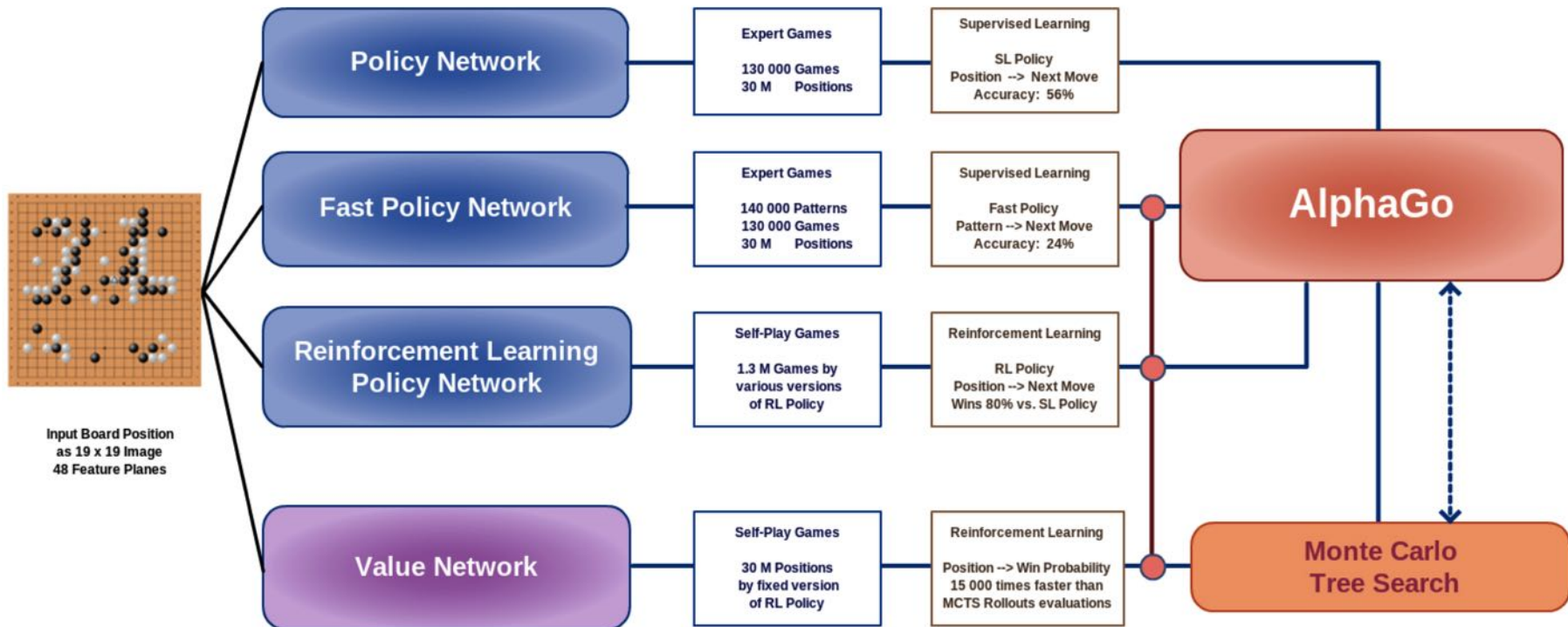


# Deep Reinforcement Learning

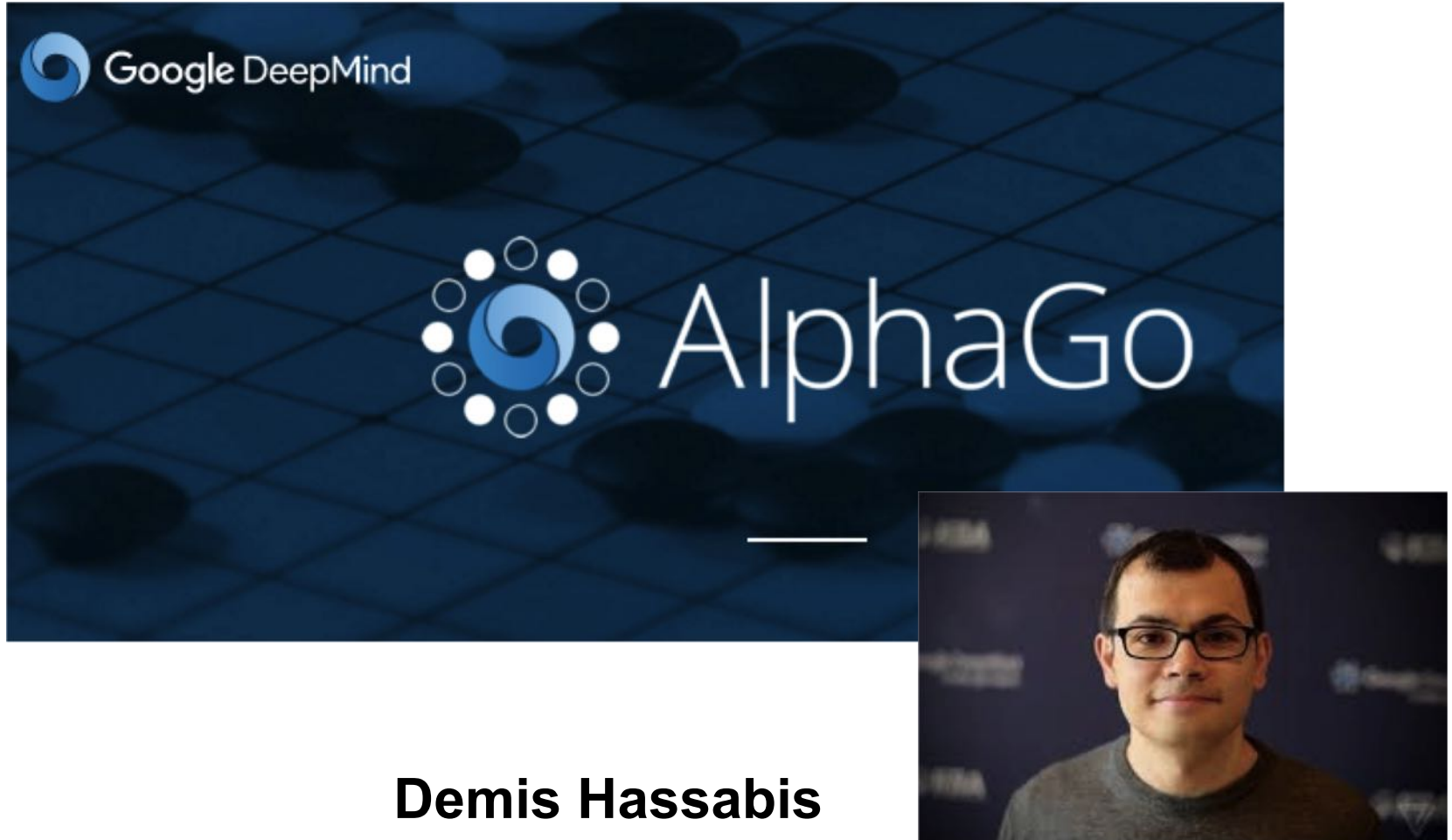
## Learn by itself with

### AlphaGo Overview

based on: Silver, D. et al. Nature Vol 529, 2016  
copyright: Bob van den Hoek, 2016



DeepMind is the AI that can **learn** by itself



The image is a collage of three distinct elements. On the left, there is a dark blue background with a faint grid pattern. In the top-left corner, the "Google DeepMind" logo is visible, consisting of a blue circular icon followed by the text "Google DeepMind". In the center, there is a white graphic of a blue and white circular logo with a central swirl, surrounded by smaller circles, followed by the text "AlphaGo" in a large, white, sans-serif font. A thin horizontal white line separates the central graphic from a portrait of a man on the right. The portrait shows a man with short brown hair and glasses, wearing a dark grey t-shirt, standing in front of a dark background with some blurred text or logos.

Demis Hassabis

# Neuroscience-Inspired Artificial Intelligence

Demis Hassabis,<sup>1,2,\*</sup> Dharshan Kumaran,<sup>1,3</sup> Christopher Summerfield,<sup>1,4</sup> and Matthew Botvinick<sup>1,2</sup>

<sup>1</sup>DeepMind, 5 New Street Square, London, UK

<sup>2</sup>Gatsby Computational Neuroscience Unit, 25 Howland Street, London, UK

<sup>3</sup>Institute of Cognitive Neuroscience, University College London, 17 Queen Square, London, UK

<sup>4</sup>Department of Experimental Psychology, University of Oxford, Oxford, UK

\*Correspondence: [dhcontact@google.com](mailto:dhcontact@google.com)

<http://dx.doi.org/10.1016/j.neuron.2017.06.011>

The fields of neuroscience and artificial intelligence (AI) have a long and intertwined history. In more recent times, however, communication and collaboration between the two fields has become less commonplace. In this article, we argue that better understanding biological brains could play a vital role in building intelligent machines. We survey historical interactions between the AI and neuroscience fields and emphasize current advances in AI that have been inspired by the study of neural computation in humans and other animals. We conclude by highlighting shared themes that may be key for advancing future research in both fields.



## 反馈连接与世界模型

Feedback connection and world model

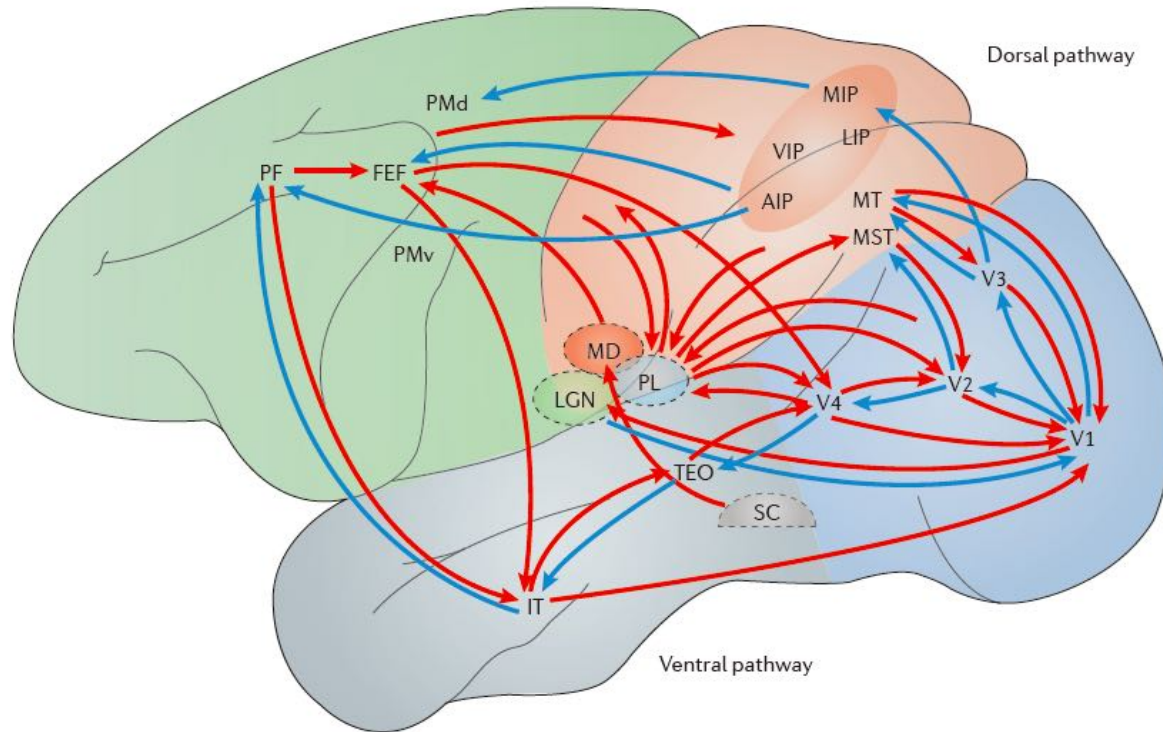


**Figure 1 | Feedback pathways carrying top-down information.** Processing visual information involves feedforward connections across a hierarchy of cortical areas (represented by the blue arrows). The visual cortical pathways begin in the primary visual cortex (V1), which receives subcortical input from the lateral geniculate nucleus (LGN). The feedforward connections extend through a ventral pathway into the temporal lobe and through a dorsal pathway into the parietal cortex and prefrontal cortex (PF). Matching these feedforward connections are a series of reciprocal feedback connections (represented by the red arrows), which provide descending top-down influences that mediate re-entrant processing. Feedback is seen in direct corticocortical connections (those directed towards area V1), in projections from area V1 to the LGN and in interactions between cortical areas mediated by the pulvinar (PL). Information about motor commands, or efference copy, is fed to the sensory apparatus by a pathway involving the superior colliculus (SC), medial dorsal nucleus of the thalamus (MD) and frontal eye fields (FEF). In addition to direct reciprocal connections, for example from area V2 to area V1, feedback can cascade over a succession of areas, for example, from the PF to FEF to area V4 to area V2 to area V1. As outlined in this Review, diverse information is conveyed across these pathways, including attention, expectation, perceptual tasks and efference copy. AIP, anterior intraparietal area; IT, inferior temporal area; LIP, lateral intraparietal area; MIP, medial intraparietal area; MST, medial superior temporal area; MT, medial temporal area; PMd, dorsal premotor area; PMv, ventral premotor area; TeO, tectum opticum. Figure is modified, with permission, from REF. 147 © (2012) McGraw-Hill Companies.

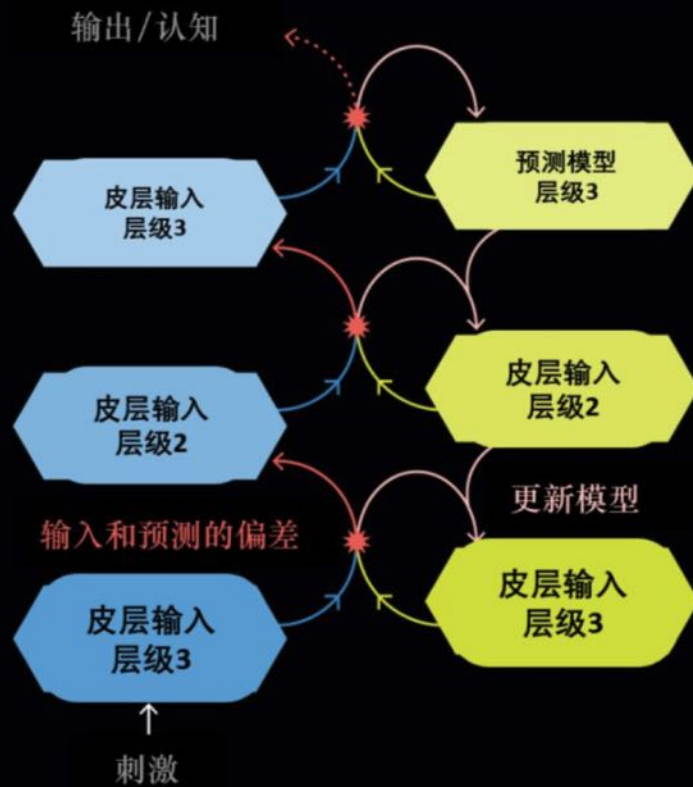
## 20世纪的观点

神经元接受并处理感觉输入，永远向认知层级的更高一级传输。



## 预测性编码的观点

大脑将它的预期/预测和接收到的数据作比较，将差别/预测误差传向更高级。这个过程让大脑得以更新它的预测性模型，来消除未来的误差。

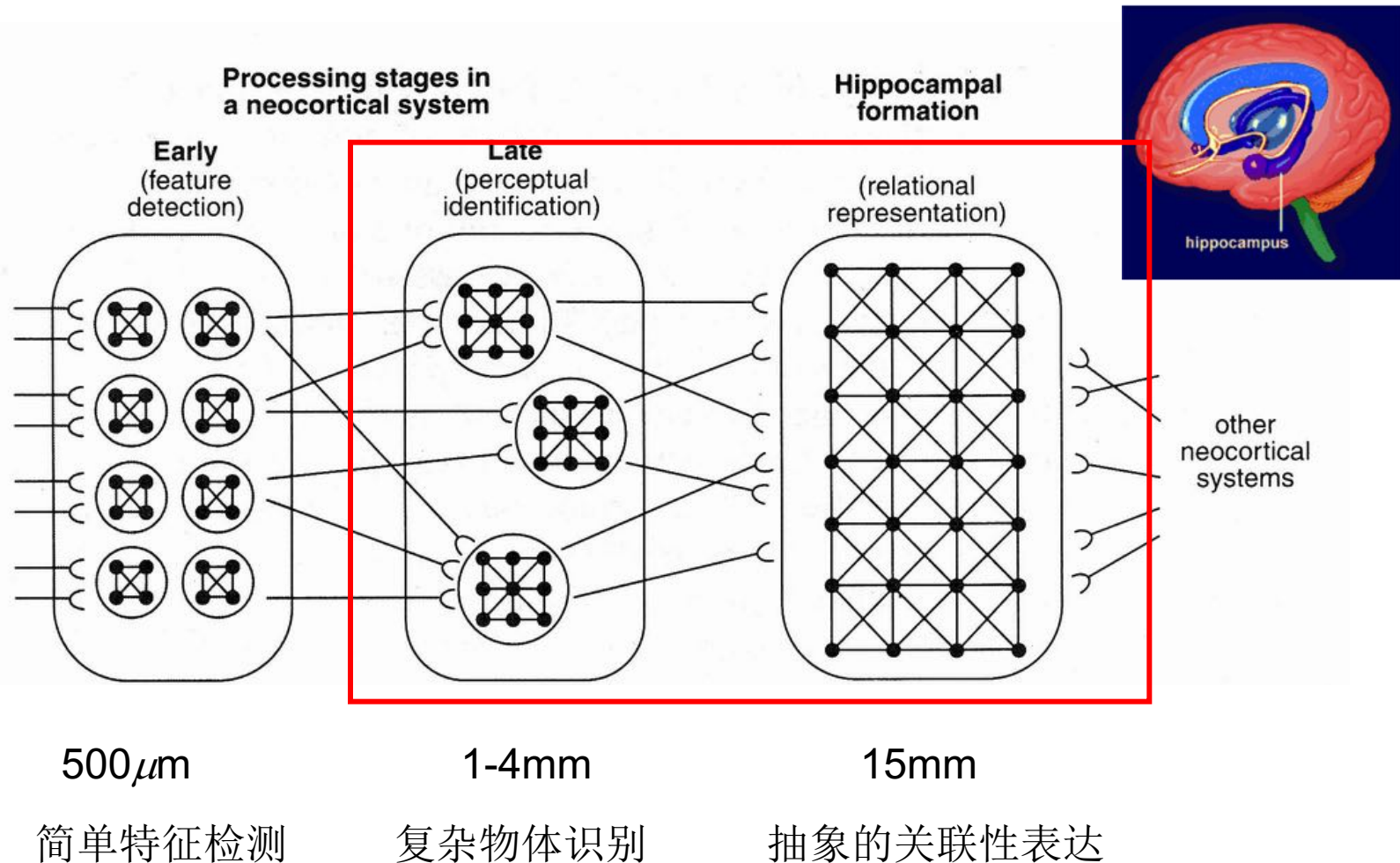




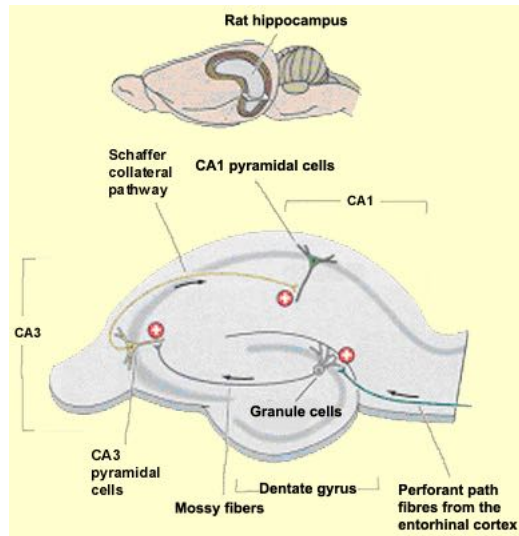
# 记忆与睡眠

Memory and Sleep

# Big picture of information processing in the brain



# 海马与前额叶交互实现记忆巩固

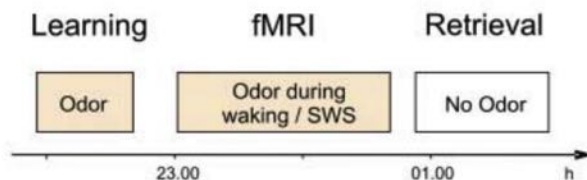


- \*Slow acquisition of structure
- \*Parametric
- \*Efficient representations for generalisation

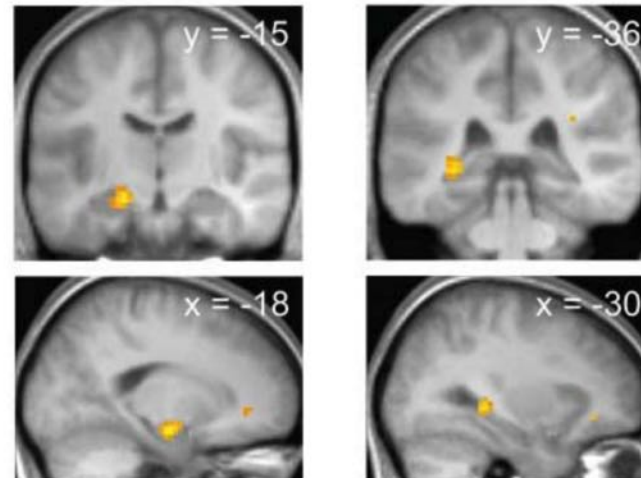
- \*Rapid storage: individual experiences
- \*Non-parametric instance-based system
- \*Sparse non-overlapping representations (poor generalization)

# 睡眠的学习价值

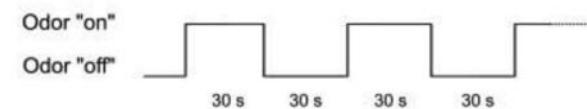
A



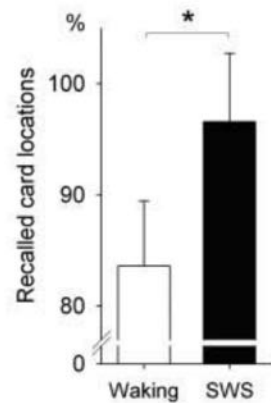
D



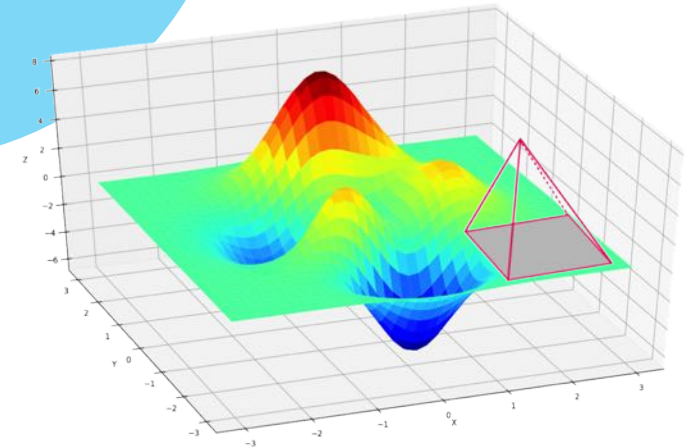
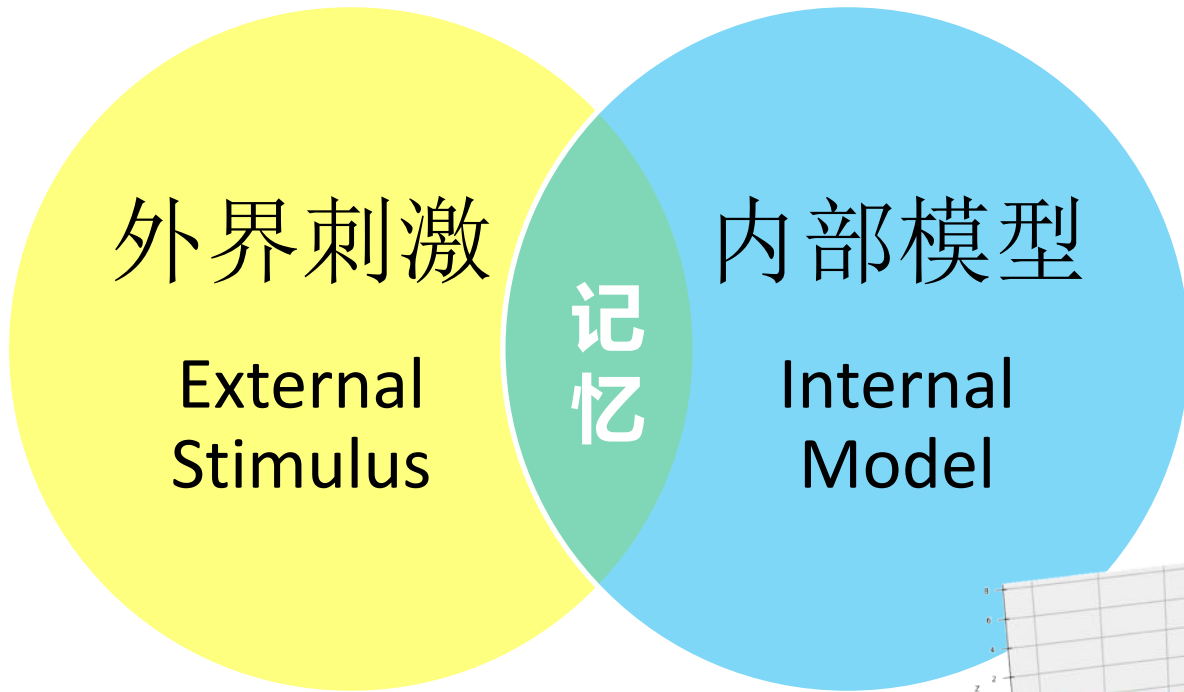
B



C



# 记忆的功能意义：一种学习方式

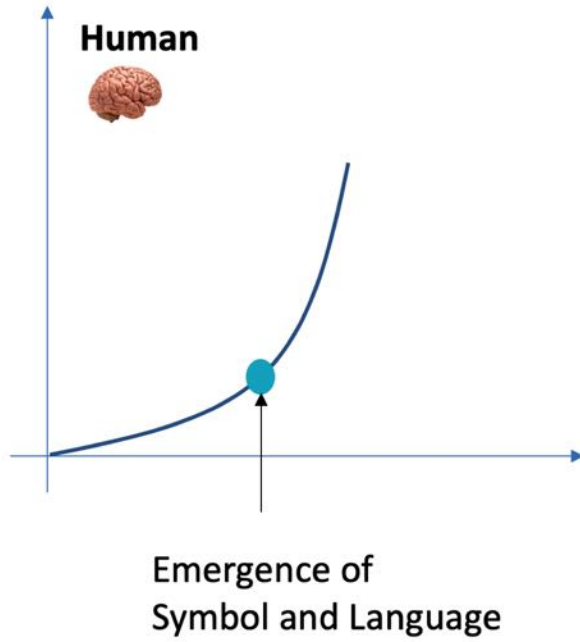




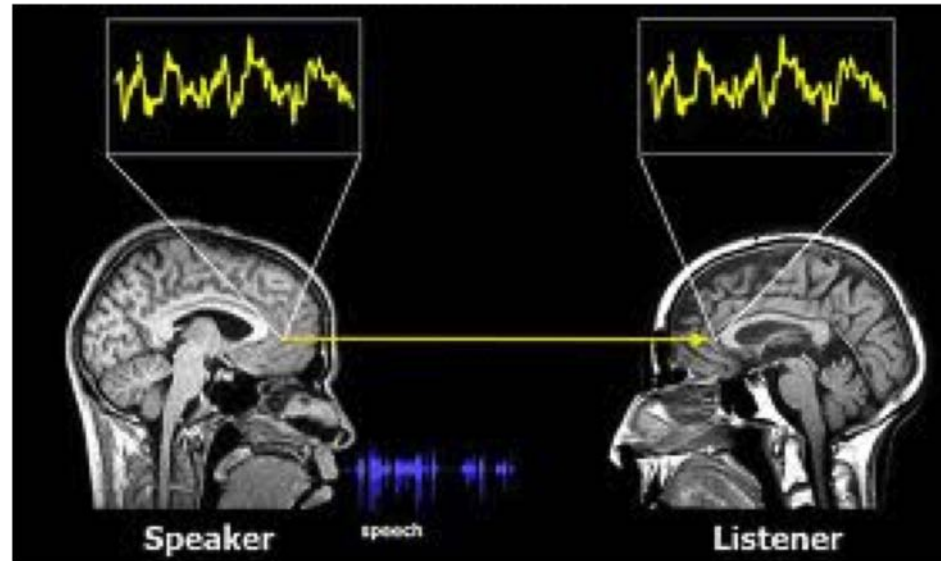
# 语言与符号推理

Language and Symbolic System

# Language pushed the boundary

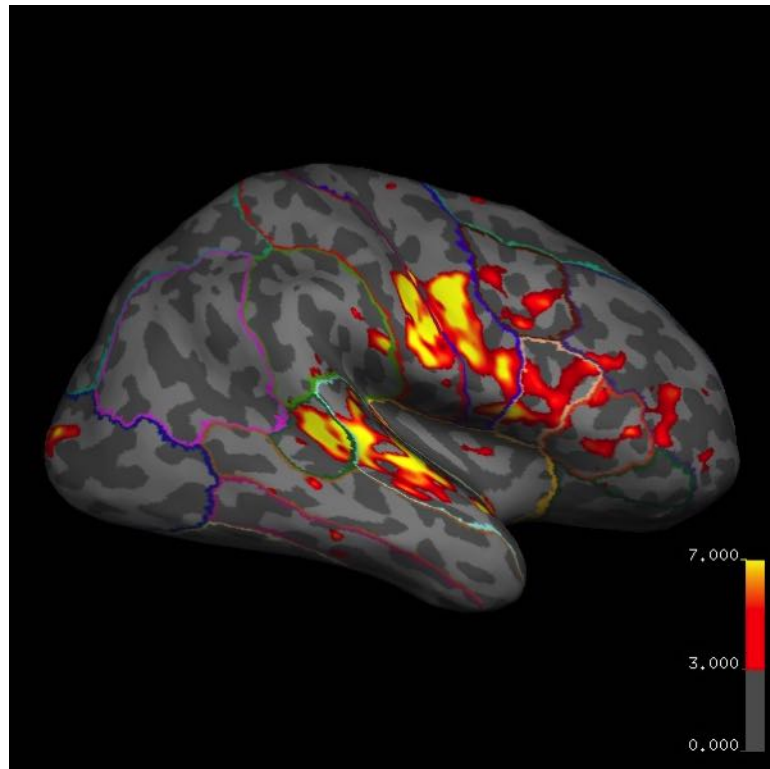
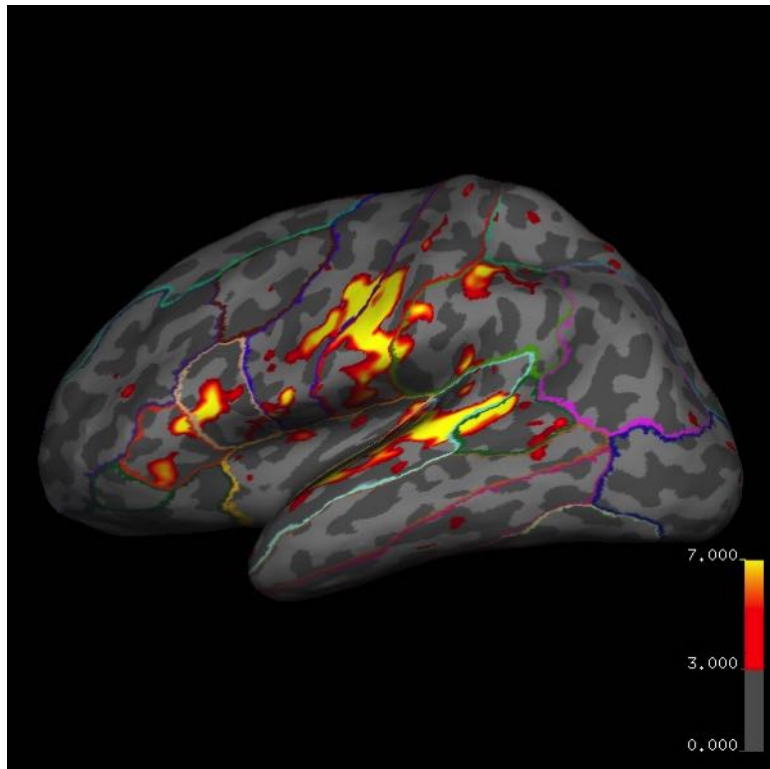


Yuval Harari, 2011



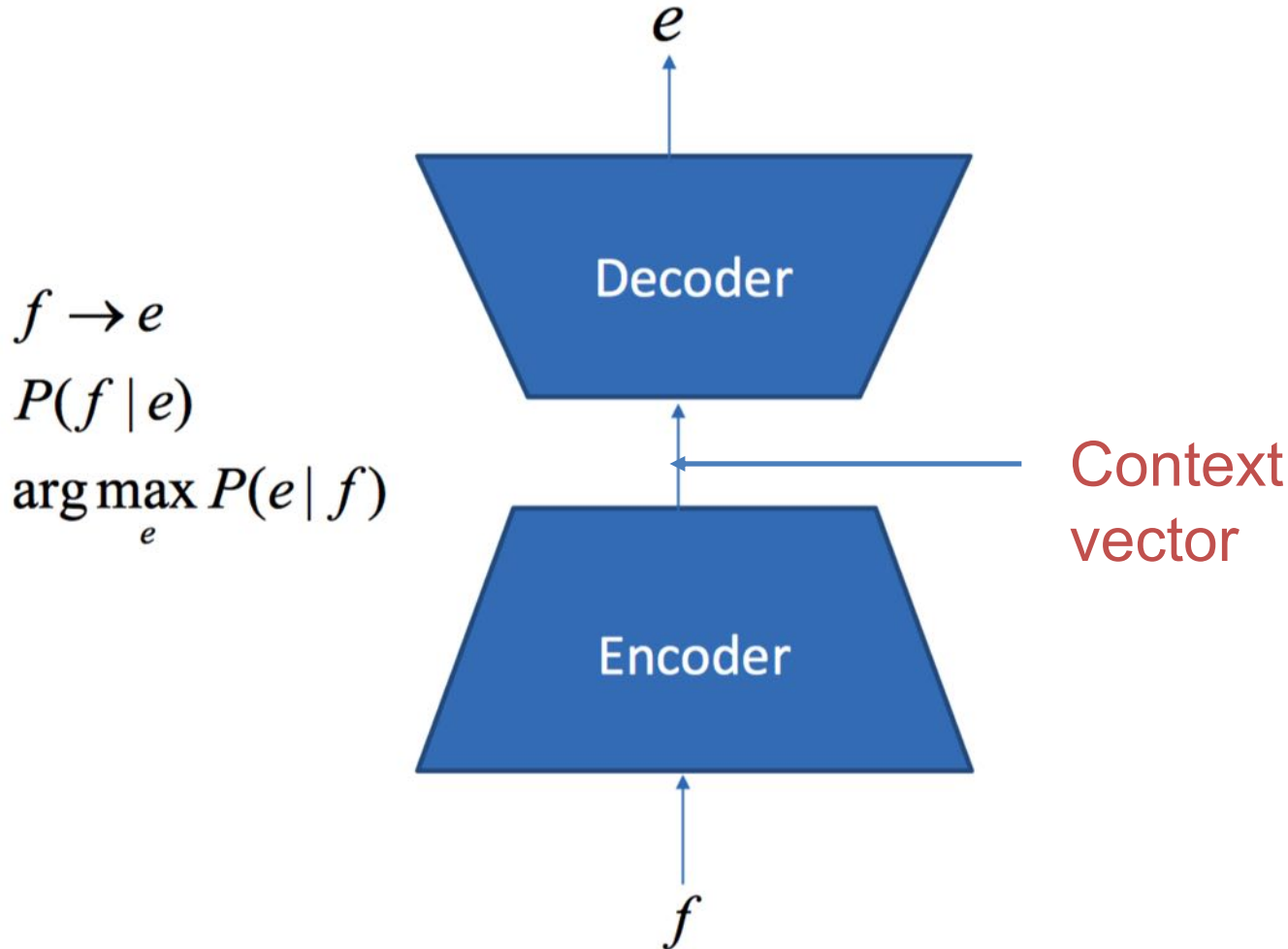
Penfield, 1950s

# fMRI mapping of speech network



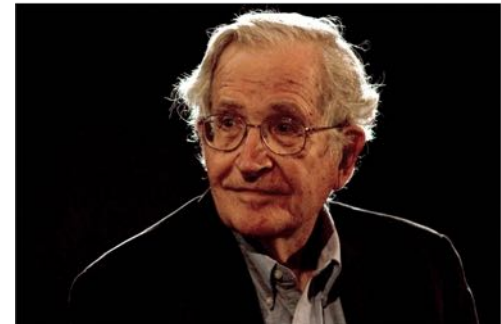
# 神经机器翻译

## Neural machine translation



# 通用语法

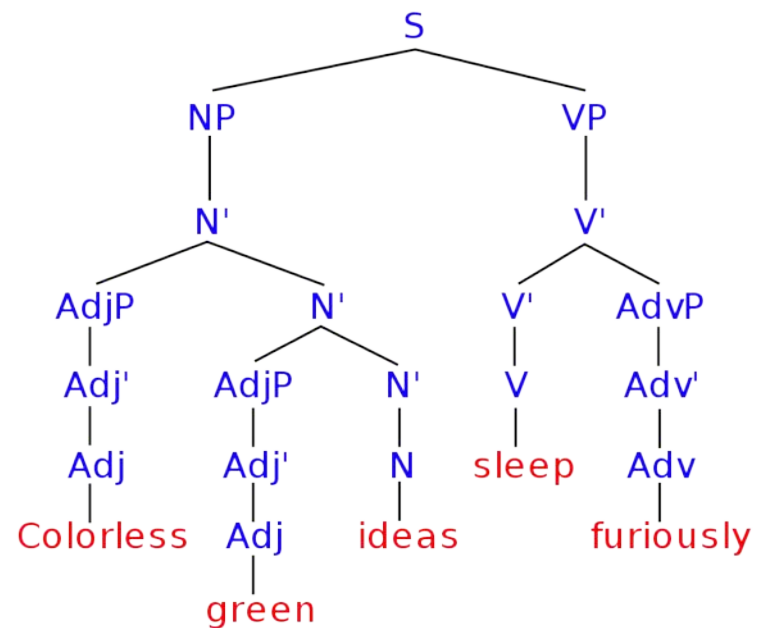
# Universal (Mental) Grammar



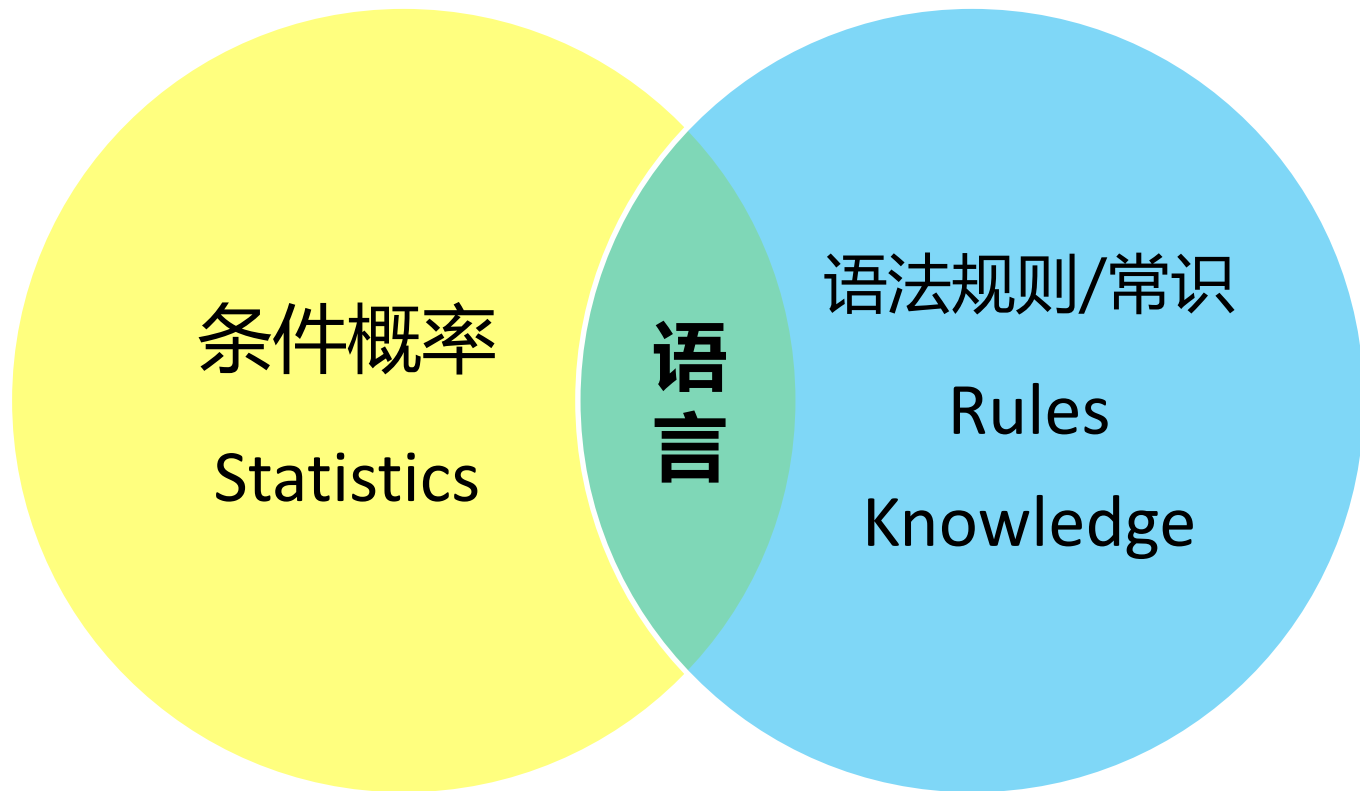
# ***Colorless green ideas sleep furiously***

by Noam Chomsky in his 1957 book *Syntactic Structures* as an example of a sentence that is grammatically correct, but semantically nonsensical.

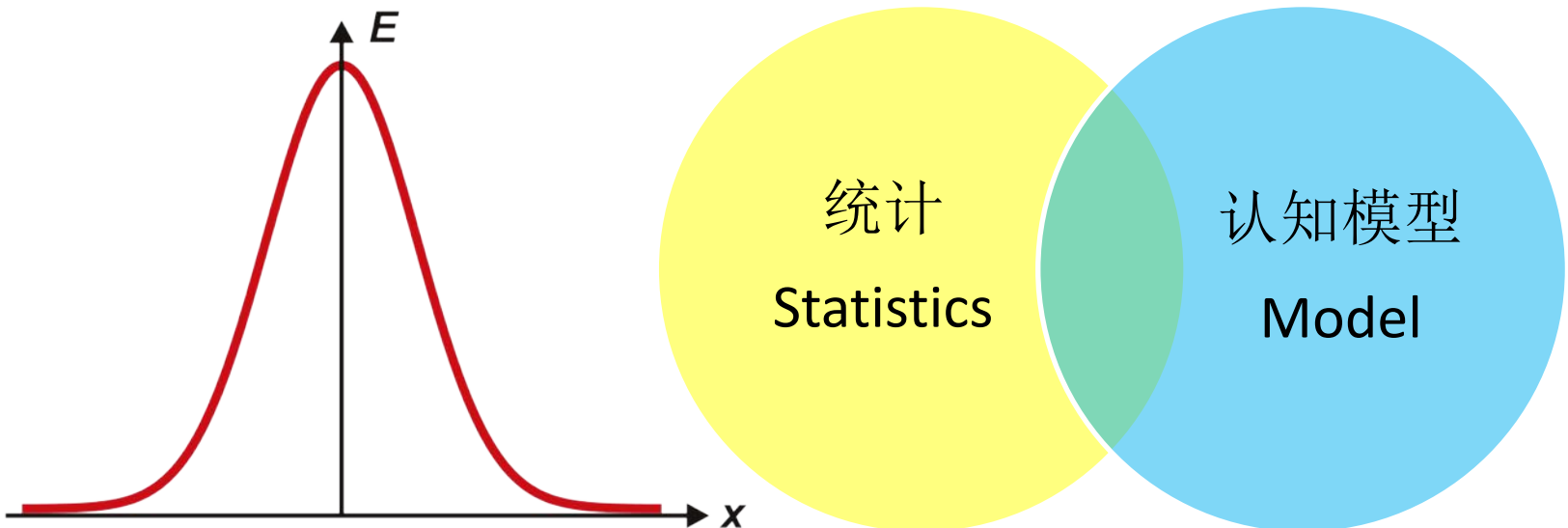
# Noam Chomsky



# 语言的本质：条件概率 or 语法规则



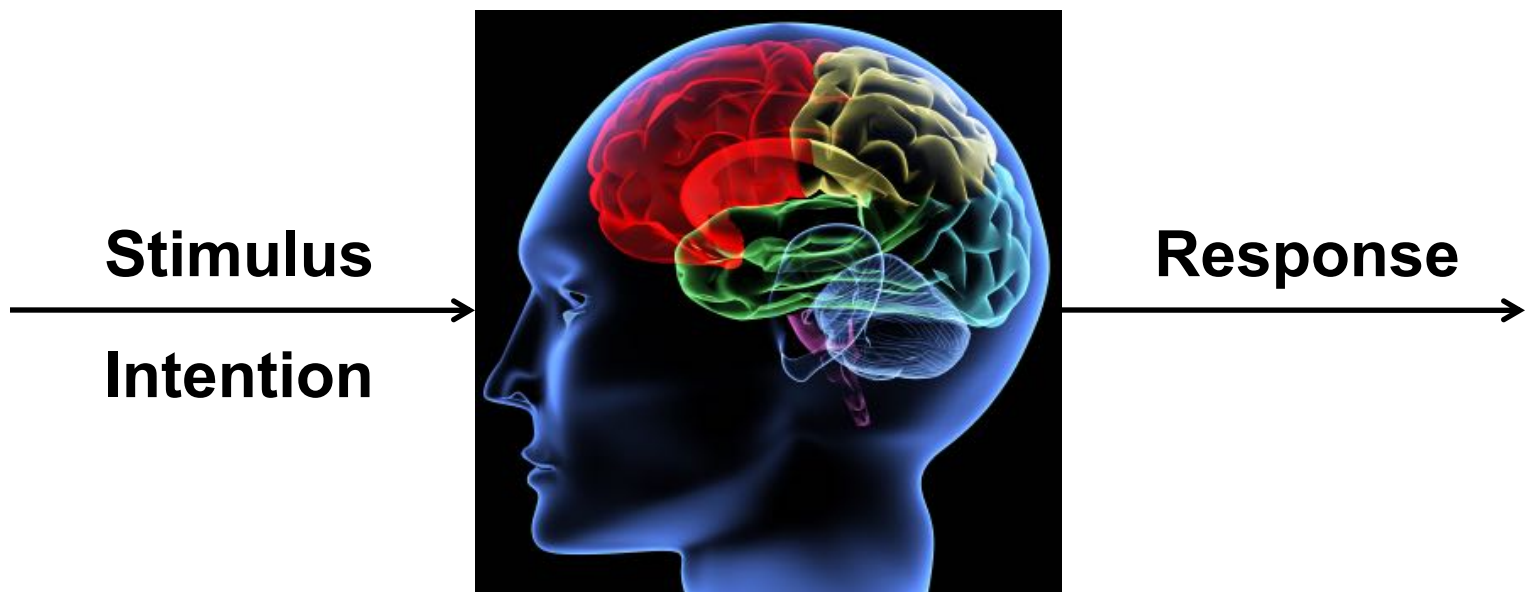
# 智能的核心难题：在不确定性中寻找确定性



# 人工智能帮助脑科学

## AI helps BI

# Encoding/Decoding Problem

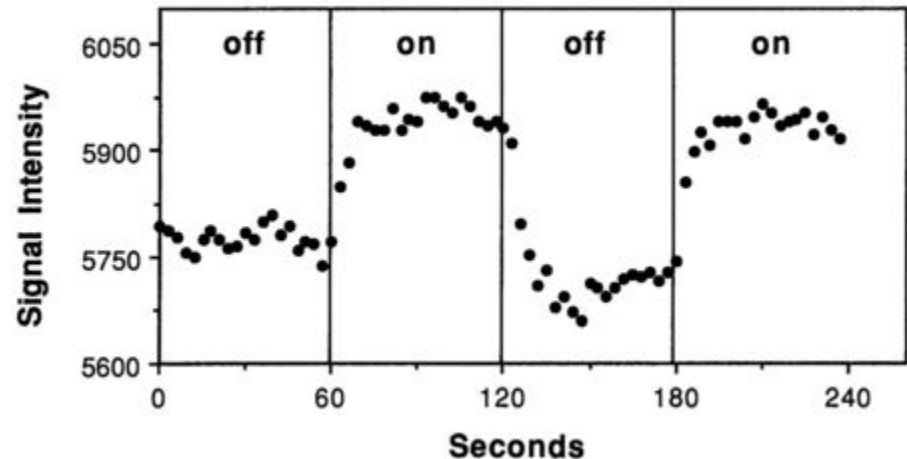
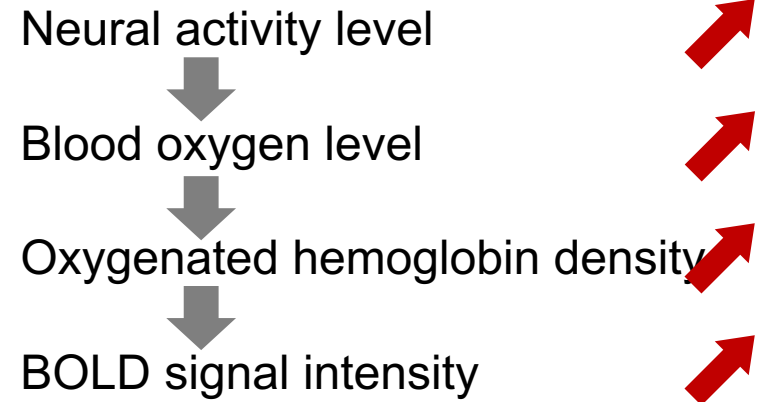
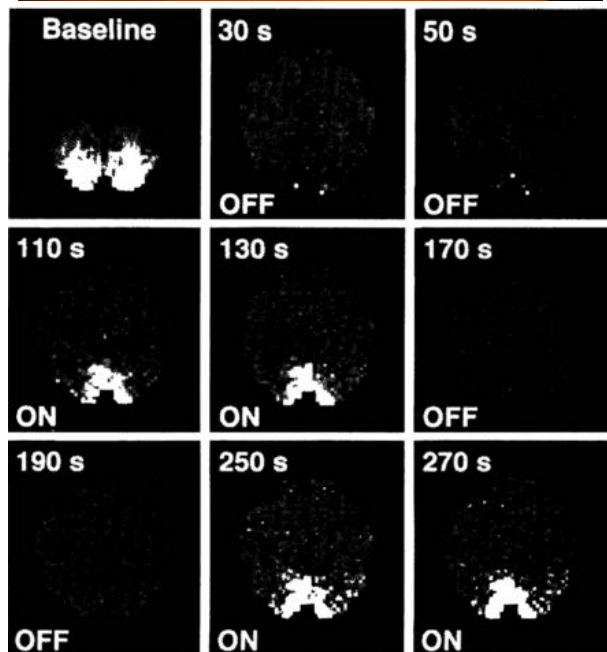


# 基于fMRI的神经解码

## Neural Decoding in fMRI

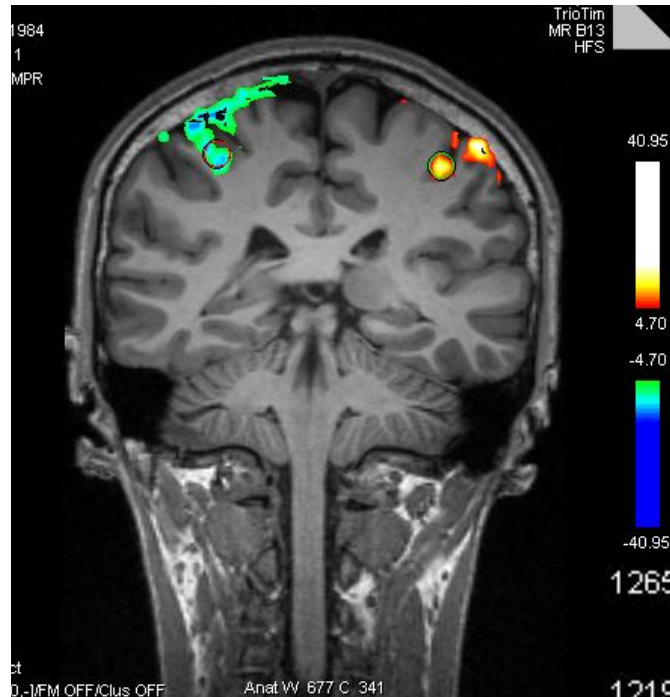
# Functional Magnetic Resonance Imaging (fMRI)

Blood-oxygen-level dependence (BOLD) fMRI: a non-invasive indicator of neural activity.



Kwong et al. 1992

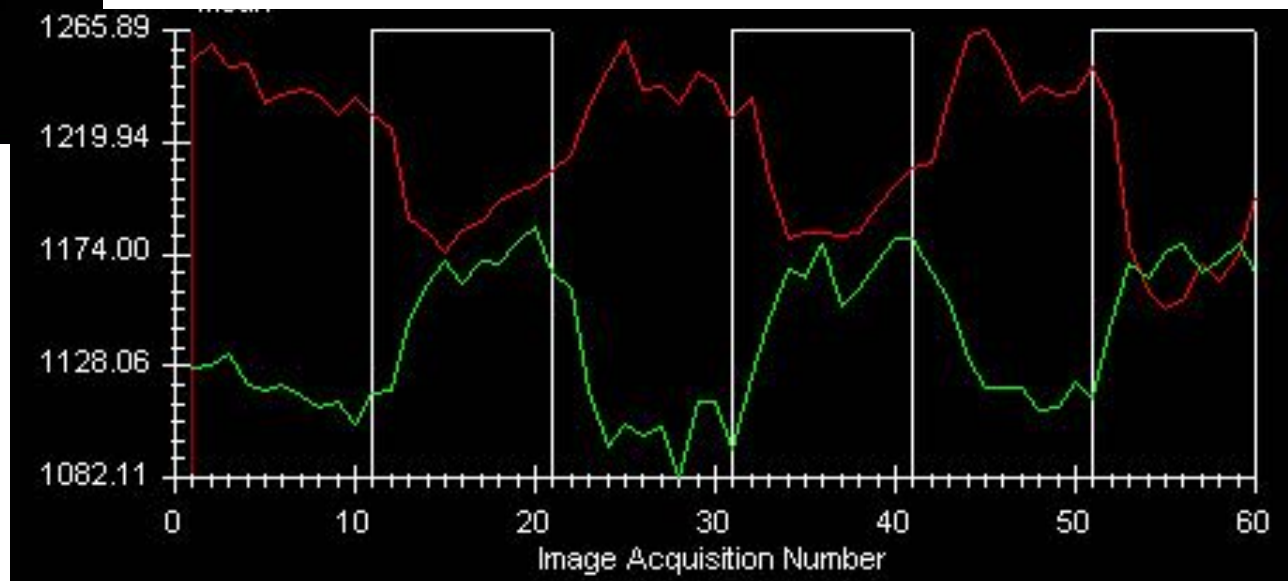
# Conventional fMRI data analysis



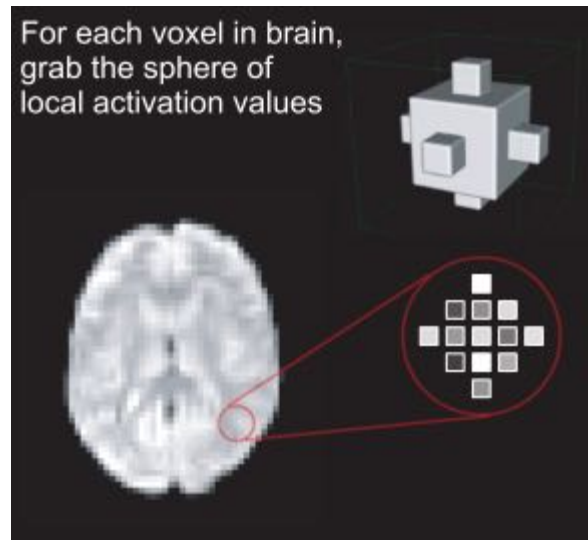
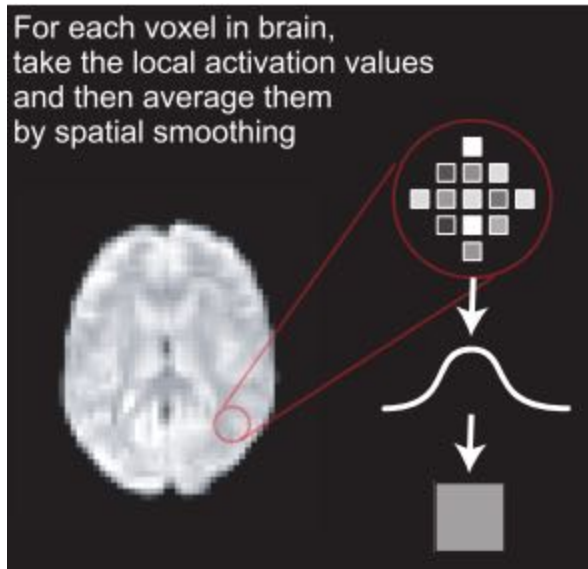
People usually model between-condition contrast in a voxel-wise, i.e. **univariate** fashion.

**Task:** Right/Left hand movement  
**Contrast:** Right minus Left

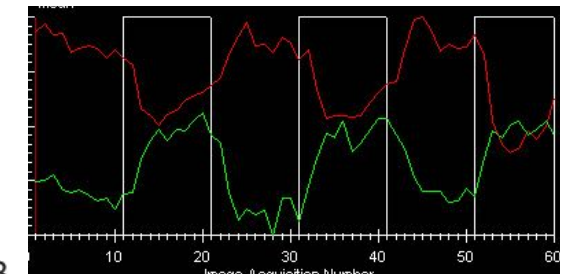
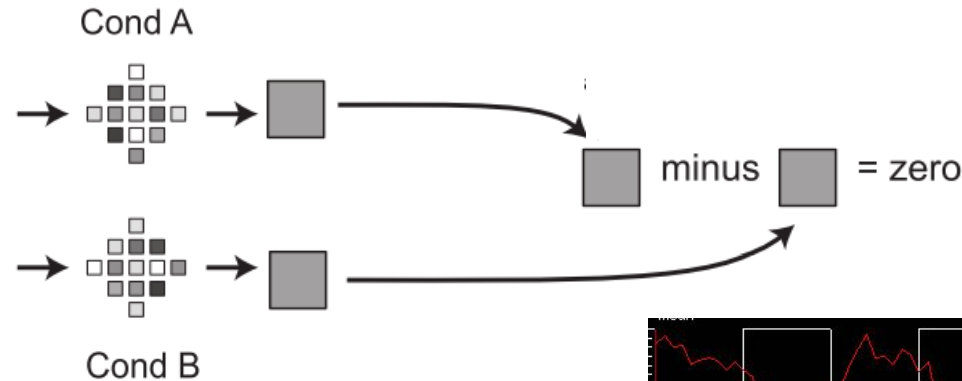
**Red** - right hand   **Green** - left hand



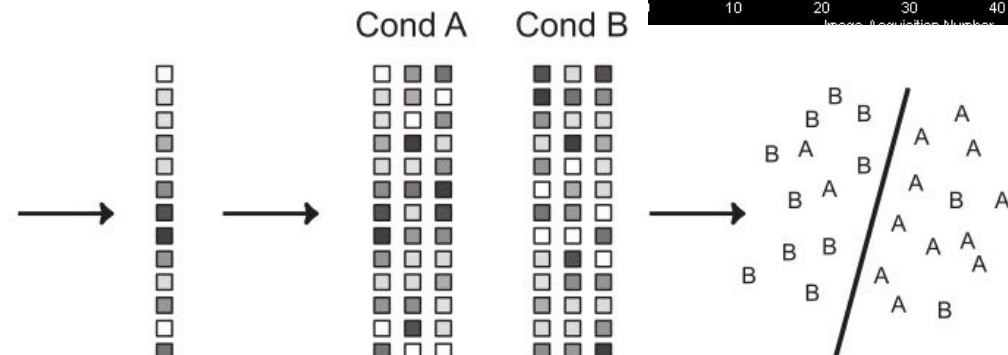
# Multi-voxel pattern analysis (MVPA)



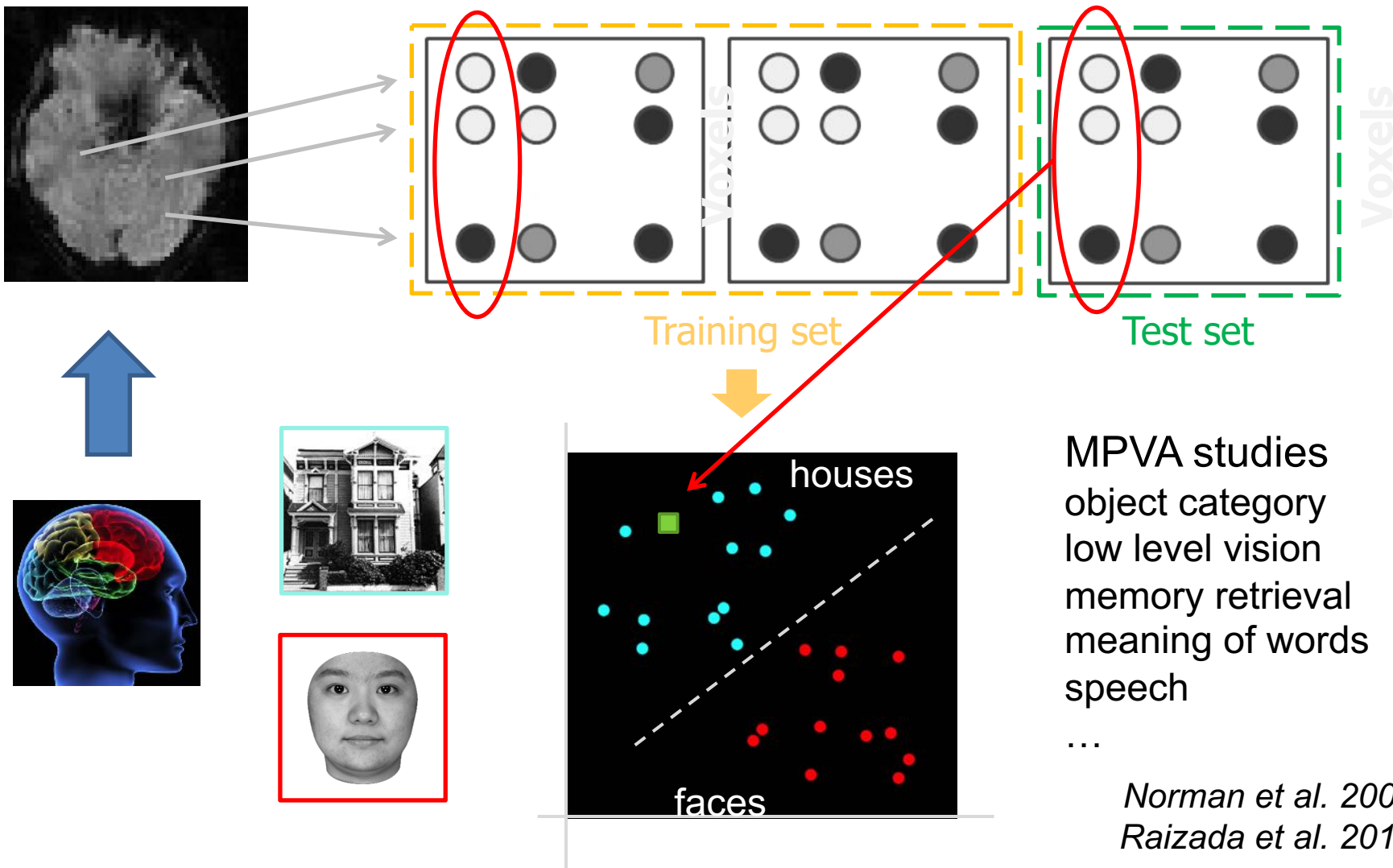
## Conventional approach



## MVPA



$n\text{Voxel} \times 1$     $n\text{Voxel} \times n\text{Sample}_{A/B}$



# MVPA for mind reading

Neuron  
**Article**

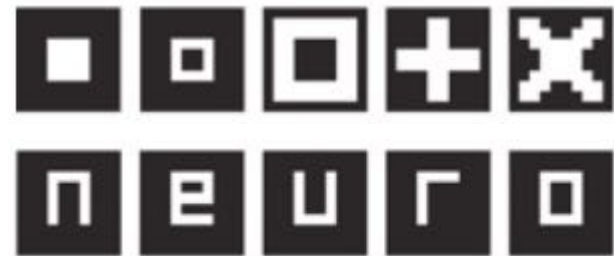
## **Visual Image Reconstruction from Human Brain Activity using a Combination of Multiscale Local Image Decoders**

60, 915–929, December 11, 2008

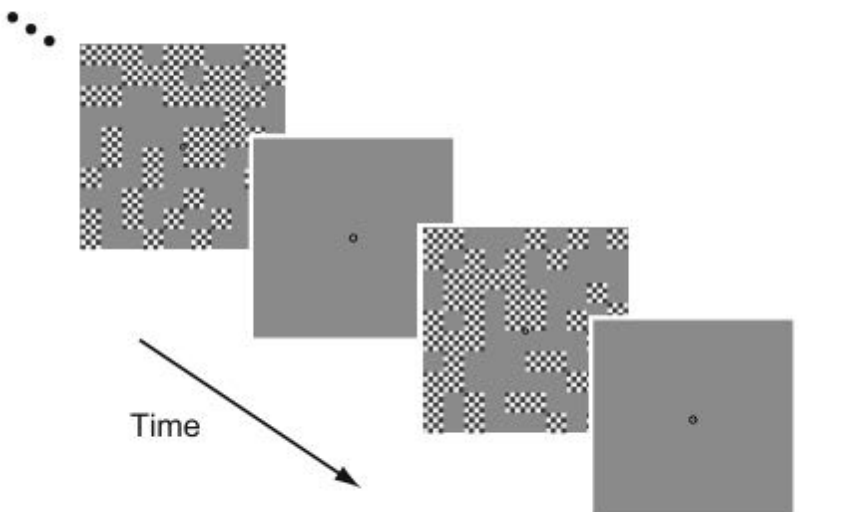
Yoichi Miyawaki,<sup>1,2,6</sup> Hajime Uchida,<sup>2,3,6</sup> Okito Yamashita,<sup>2</sup> Masa-aki Sato,<sup>2</sup> Yusuke Morito,<sup>4,5</sup> Hiroki C. Tanabe,<sup>4,5</sup> Norihiro Sadato,<sup>4,5</sup> and Yukiyasu Kamitani<sup>2,3,\*</sup>

# MVPA for reconstruction - Rationale

- Motivation: From classification to **constraint-free** visual image reconstruction.
- Goal: Reconstructing 10x10 binary-contrast visual images.



# MVPA for reconstruction - Methods

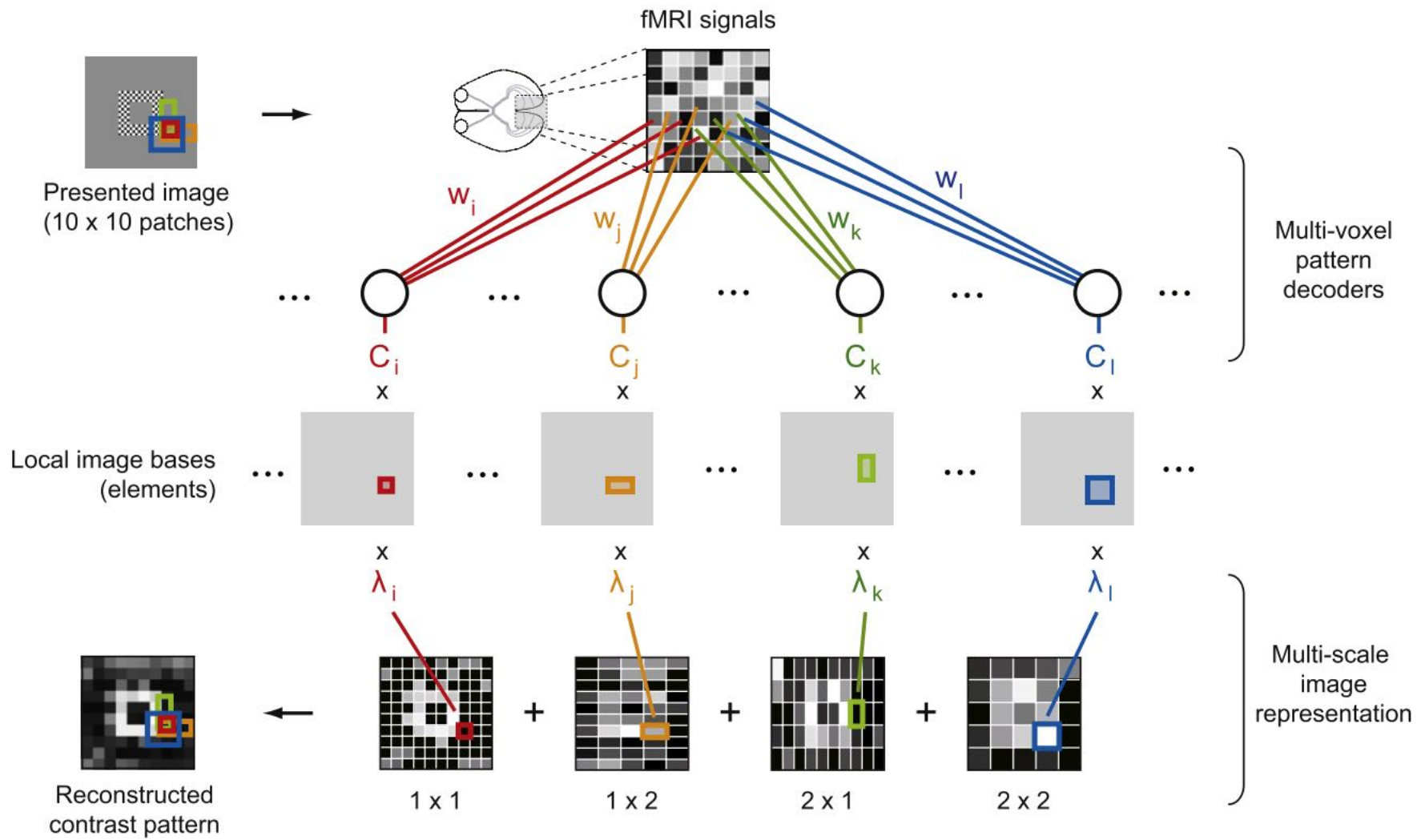


2 subjects  
1396/1550 voxels from **early visual cortex**

Training data: multi-voxel patterns corresponding to **440 random images**

Test data: multi-voxel patterns corresponding to five geometric shapes and five alphabet letters, **8 samples per shape/letter**

# MVPA for reconstruction - Methods



**Local discriminative models were built with sparse multinomial logistic regression**

# MVPA for reconstruction - Methods summary

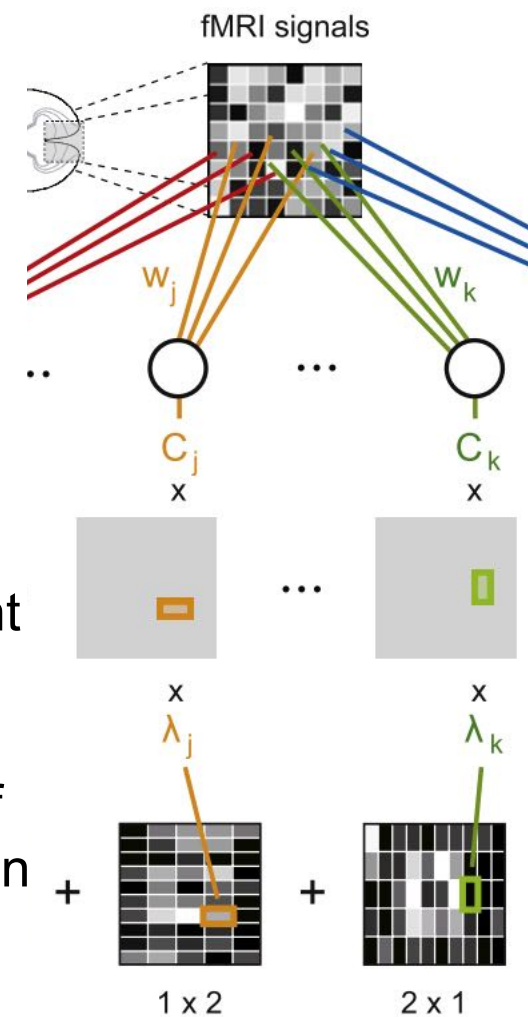
Features: 1396/1550 voxels from early visual cortex

Training samples: 440 samples of random images

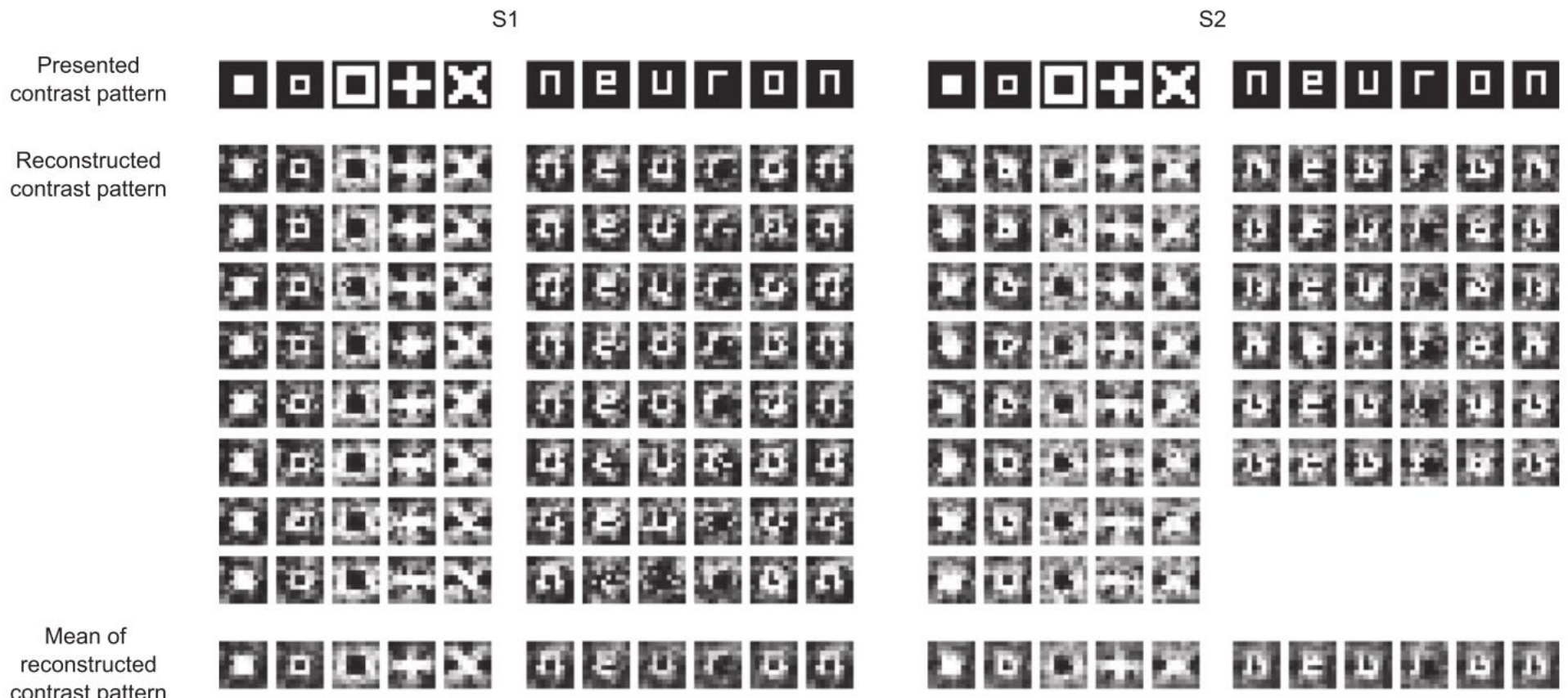
Test samples: 40 samples of geometric shapes  
alphabet letters

Classifier: 100 **1x1**, 90 **1x2**, 90 **2x1**, and 81 **2x2** local  
SLR classifiers, with **2/3/3/4** possible labels for different  
type of classifiers

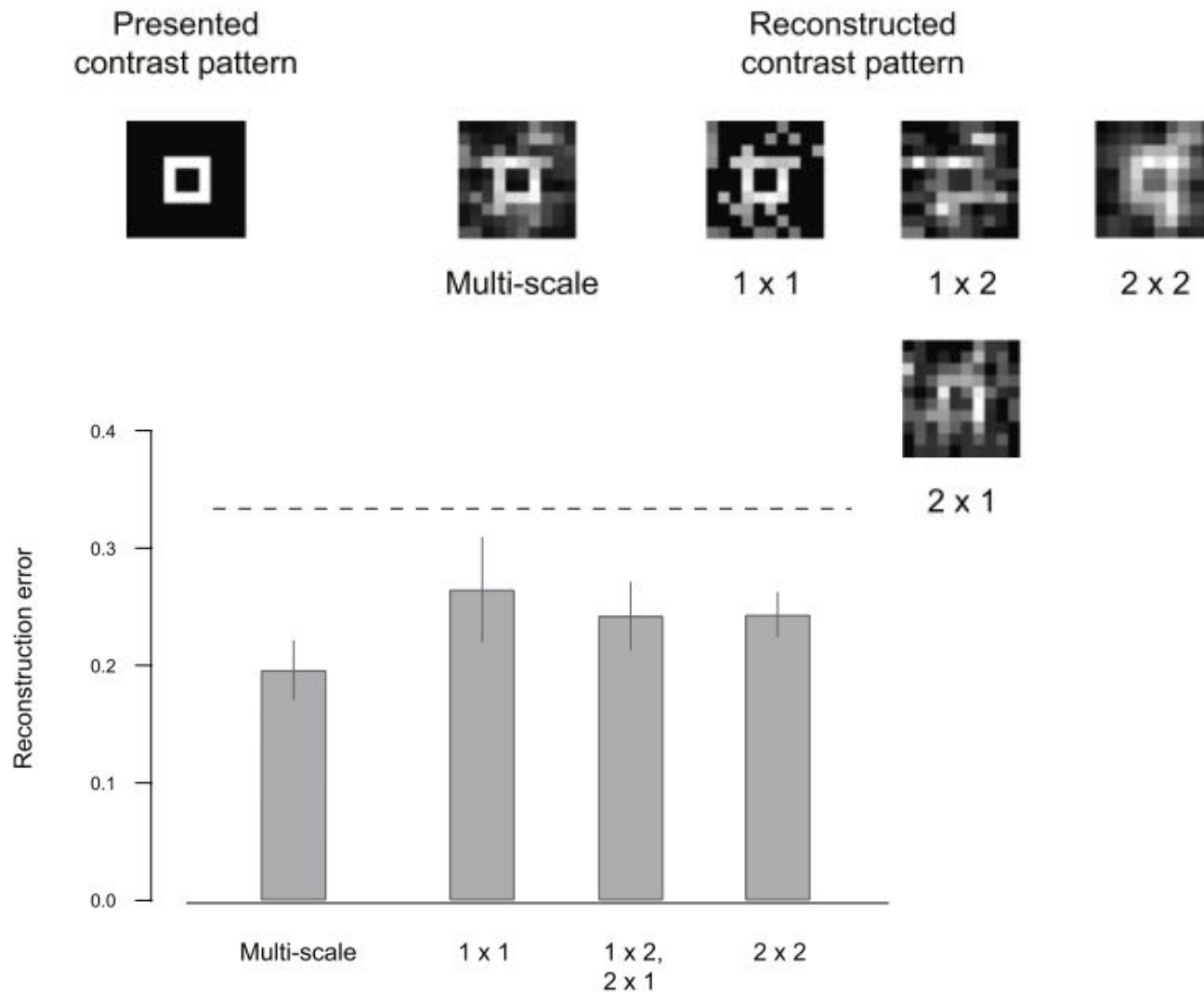
Post-processing: linear combination of different type of  
local classifiers that covered each of 10x10 locations, in  
which the combination coefficient was determined with  
least square method using training samples for each  
location respectively.



# MVPA for reconstruction - Results



# MVPA for reconstruction - Results



# References

- Norman, K. A., Polyn, S. M., Detre, G. J., & Haxby, J. V. (2006). Beyond mind-reading: multi-voxel pattern analysis of fMRI data. *Trends in cognitive sciences*, 10(9), 424-430.
- Kamitani, Y., & Tong, F. (2005). Decoding the visual and subjective contents of the human brain. *Nature neuroscience*, 8(5), 679-685.
- Miyawaki, Y., Uchida, H., Yamashita, O., Sato, M. A., Morito, Y., Tanabe, H. C., ... & Kamitani, Y. (2008). Visual image reconstruction from human brain activity using a combination of multiscale local image decoders. *Neuron*, 60(5), 915-929.

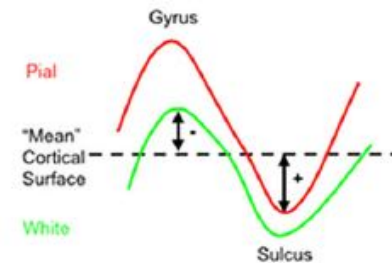
# 基于MRI影像的自闭症诊断

## SVM in autism diagnosis

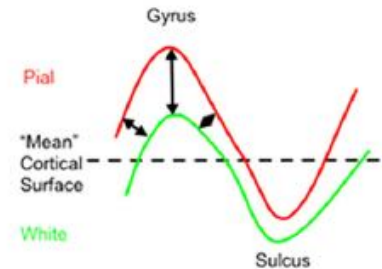
# Describing the Brain in Autism in Five Dimensions

MRI-Assisted Diagnosis of Autism Using a Multiparameter Classification

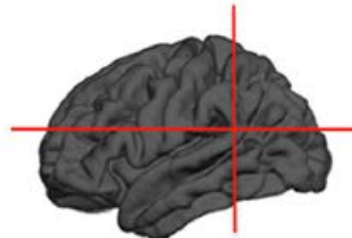
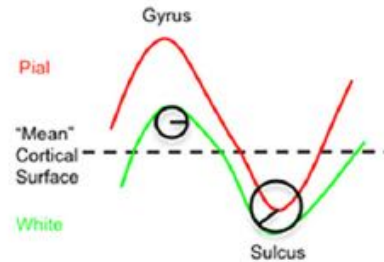
A Average Convexity



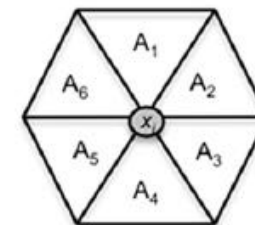
B Cortical Thickness



E Mean (radial) Curvature



C Area (pial)



$$\text{Area} = \sum A_i / 6$$

D Metric Distortion (Jacobian)

$$= \frac{k * \text{area of a triangle on registered sphere}}{\text{area of triangle on original g/w interface surface}}$$

$$k = \frac{\text{total surface area of original g/w interface surface}}{\text{total surface area of individual sphere}}$$

# Methods

1. SVM is applied to images feature vector  $\mathbf{x}$  coming from 5 different modalities, as in the current study, the number of dimensions equals the number of voxels/ vertices per image multiplied by 5.
2. Input data  $\mathbf{x}$  were then classified into two classes  $\mathbf{c}$  ( $\mathbf{c} = +1$  for patients,  $\mathbf{c} = -1$  for controls) by identifying a separating hyperplane or decision boundary.
3. The algorithm is initially trained on a subset of the data ( $\mathbf{x}, \mathbf{c}$ ) to find a hyperplane that best separates the input space according to the class labels
4. The linear kernel SVM used in the present study allows direct extraction of the weight vector as an image((i.e., the SVM discrimination map).

# Result

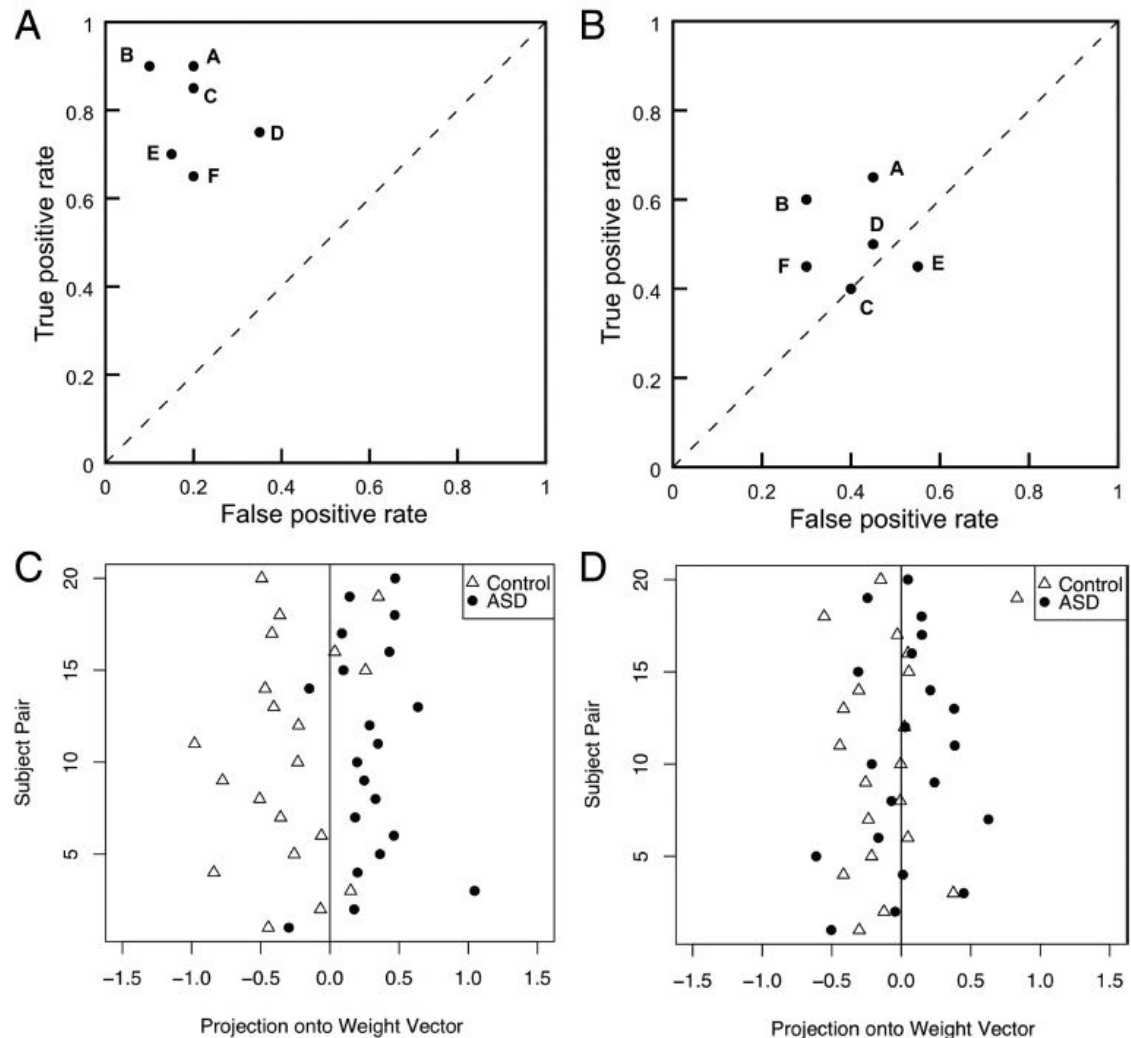


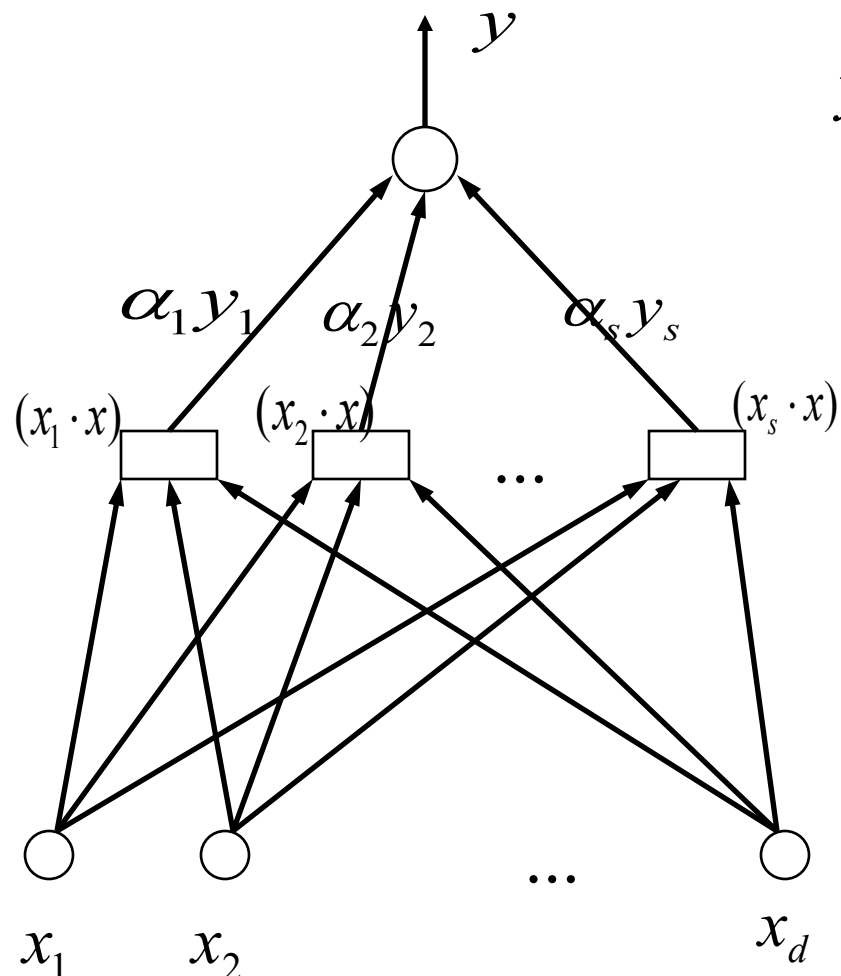
**Figure 2.** *A, B*, ROC graphs for the six discrete classifiers in the left hemisphere (*A*) and in the right hemisphere (*B*). Individual points on the graph depict classifiers on the basis of all parameters (A), cortical thickness (B), metric distortion/Jacobian (C), average convexity (D), pial area (E), and mean (radial) curvature (F). *C, D*, The classification plots for the left (*C*) and right (*D*) hemispheres.

**Table 4. Correlation coefficients between ADI diagnostic criteria and weight vector for the model combining all parameters**

Diagnostic test ( <i>n</i> = 17)	Left hemisphere		Right hemisphere	
	<i>r</i>	<i>p</i>	<i>r</i>	<i>p</i>
ADI-R social	0.414*	<0.04	-0.152	<0.28
ADI-R communication	0.620**	<0.01	-0.074	<0.38
ADI-R repetitive behavior	0.161	<0.26	-0.198	<0.22

\* denotes significant correlation on *p* < 0.05 (1-tailed); \*\* denotes significant correlation on *p* < 0.01 (1-tailed).

# 线性 Linear SVM



$$y = \text{sgn} \left( \sum_{i=1}^s \alpha_i y_i (\mathbf{x}_i \cdot \mathbf{x}) + b \right)$$

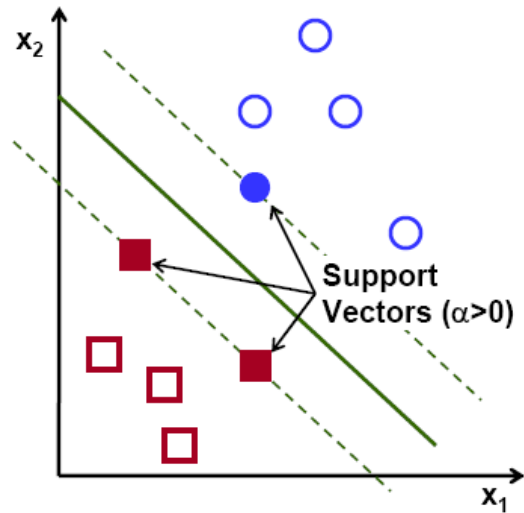
权值  $w_i = \alpha_i y_i$

基于s个支持向量的线性变换（内积）

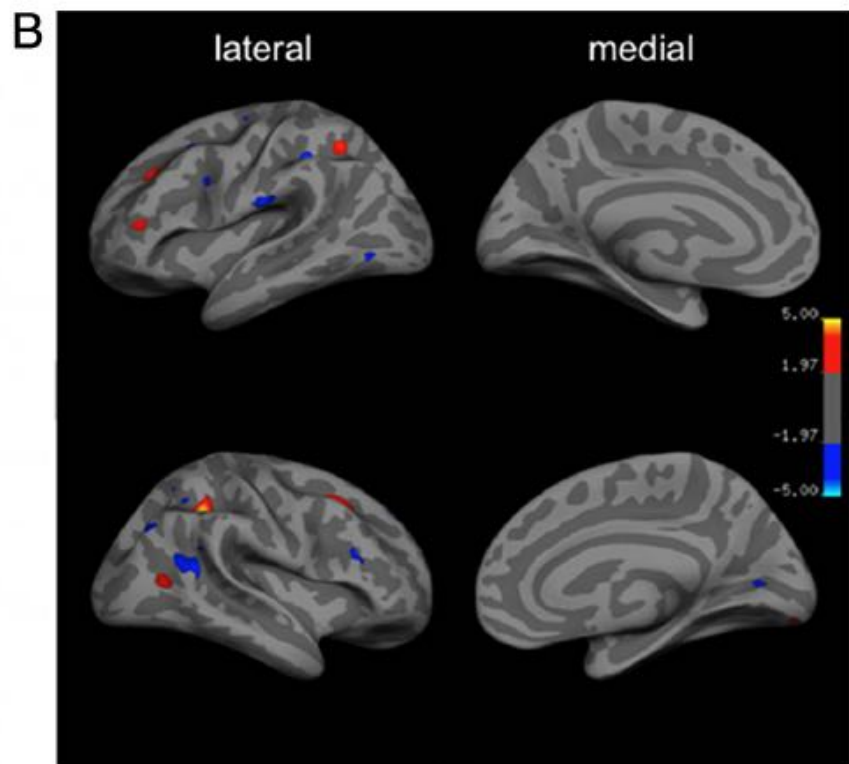
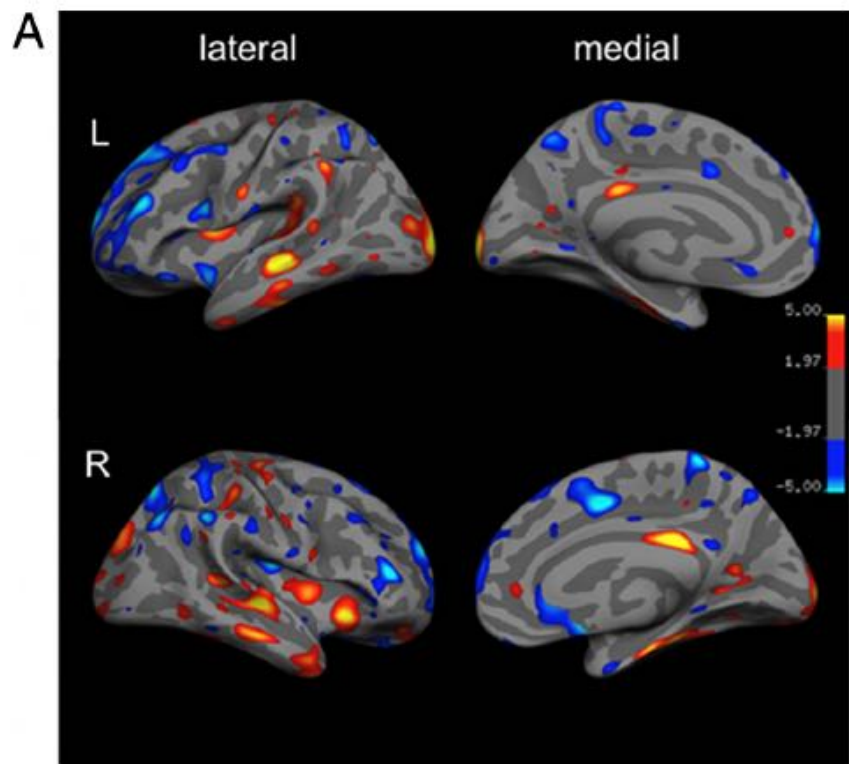
输入向量  $x = (x_1, x_2, \dots, x_d)$

# SVM discrimination map

- The weight vector has the same dimension as the feature vector and is normal to the hyperplane. It can be thought of as a ***spatial representation*** of the decision boundary, and thus represents a map of the most discriminating regions. Here, the feature vector had  $n \times 5$  dimensions, where  $n$  equals the number of voxels.
- To enable visualization of the discriminating pattern for each image modality, the weight vector was cut into its constituent parts, which were then mapped back onto the average white matter surface.
- Given two groups (ASD vs controls), a positive value in the discrimination map indicates relatively higher parameter values in patients than in controls with respect to the hyperplane, and a negative weight means relatively higher parameter values in controls than in patients with respect to the hyperplane.



# SVM Discrimination map



discrimination map for cortical thickness (**A**), average convexity (**B**)

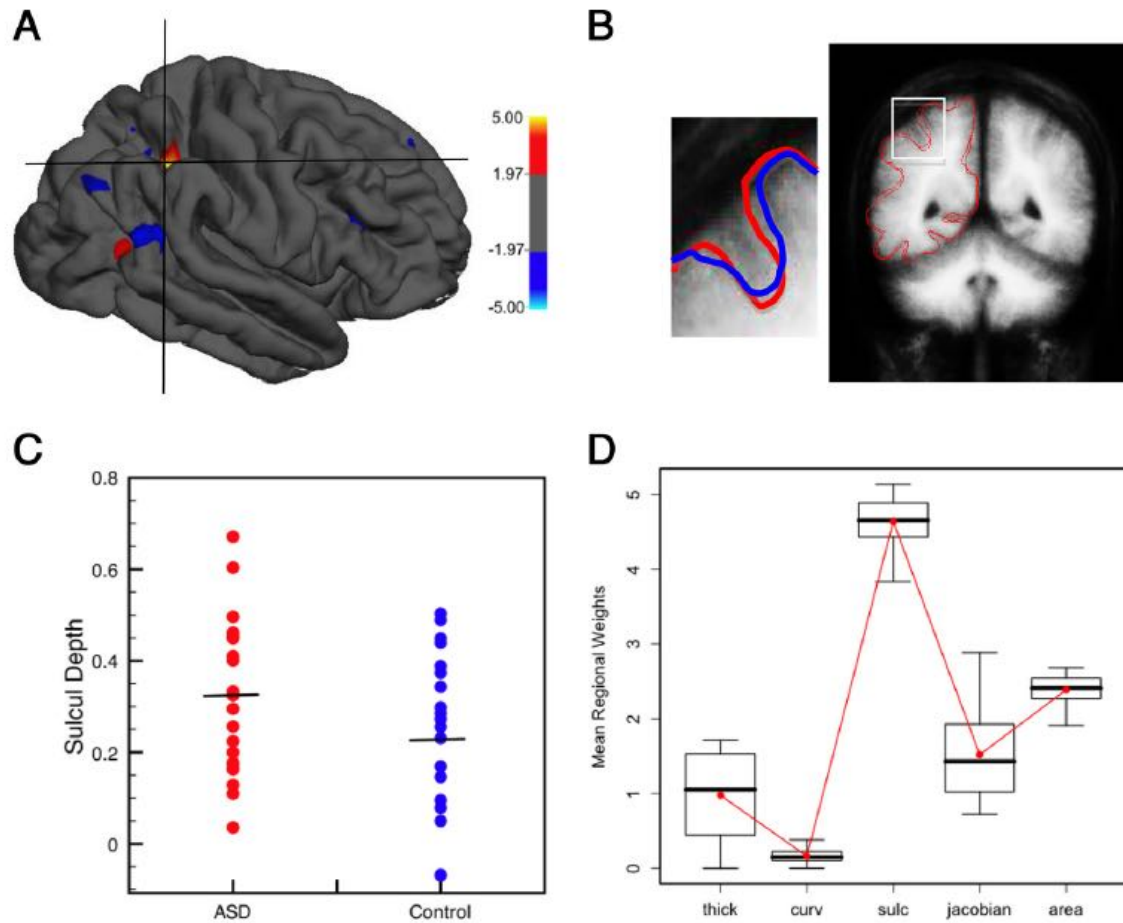


**Figure 5.** Visualization of the morphometric abnormalities in the right intraparietal sulcus. Color maps represent the weight vector score (**A**). **B**, Outlines of the cortical surface for ASD (red) and control (blue) group. This main discriminating factor in this group was an increase in sulcal depth in ASDs relative to controls. Differences in sulcal depth for this ROI are shown for both groups in **C**. **D**, Morphometric profile for this region. Profiles were derived by averaging the weight vector scores across vertices within this region of interest, and for the different morphometric parameters. Weights were identified on the basis of the concatenated SVM model, thus showing the relative contribution of parameters in this ROI.

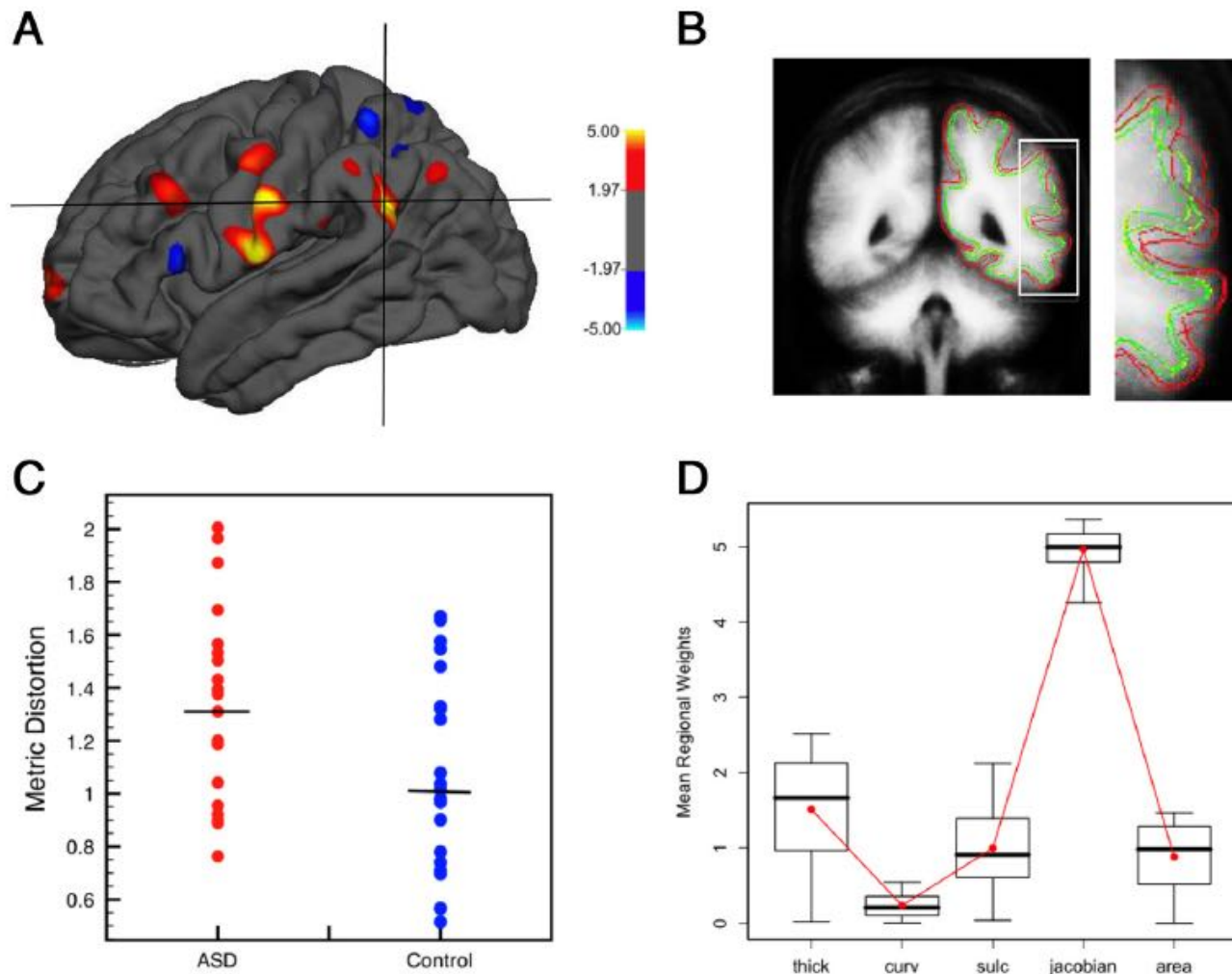


**Figure 6.** *A*, Visualization of the morphometric abnormalities in the left inferior parietal lobe (BA39). *B*, Outlines of the cortical surface for ASD and control group. Differences in metric distortion for this ROI are shown for both groups in *C*. *D*, Morphometric profile (see Fig. 4 legend).

**Table 7. Mean discrimination weights within regions of interest for individual morphometric features**

Region	Mean( <i>w</i> )				
	Cortical thickness	Mean curvature	Sulcal depth	Metric distortion	Surface area
Intraparietal sulcus (R)	0.97	0.16	<u>4.63</u>	1.51	2.38
Inferior parietal lobe (L)	1.51	0.23	0.99	<u>4.96</u>	0.88
Medial temporal sulcus (L)	<u>5.66</u>	0.07	0.17	0.48	0.62
Posterior cingulate gyrus (L)	<u>3.83</u>	0.09	0.78	3.79	0.20

R, Right hemisphere; L, left hemisphere; *w*, weight.

# References

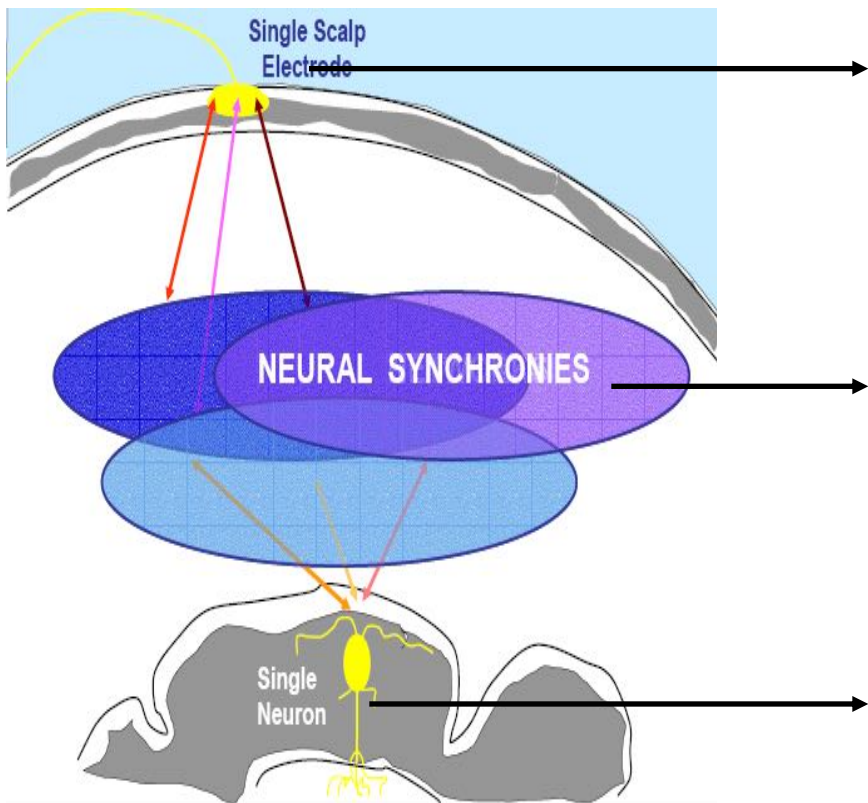
- Ecker, C., Marquand, A., Mourão-Miranda, J., Johnston, P., Daly, E. M., Brammer, M. J., ... & Murphy, D. G. (2010). Describing the brain in autism in five dimensions—magnetic resonance imaging-assisted diagnosis of autism spectrum disorder using a multiparameter classification approach. *The Journal of Neuroscience*, 30(32), 10612-10623.

# 基于头皮脑电的脑机接口

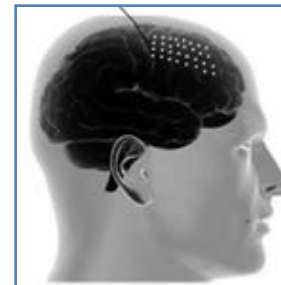
## BCI using scalp EEG

# Electrical brain signals

Macro-scale (mm-cm)



EEG



ECoG

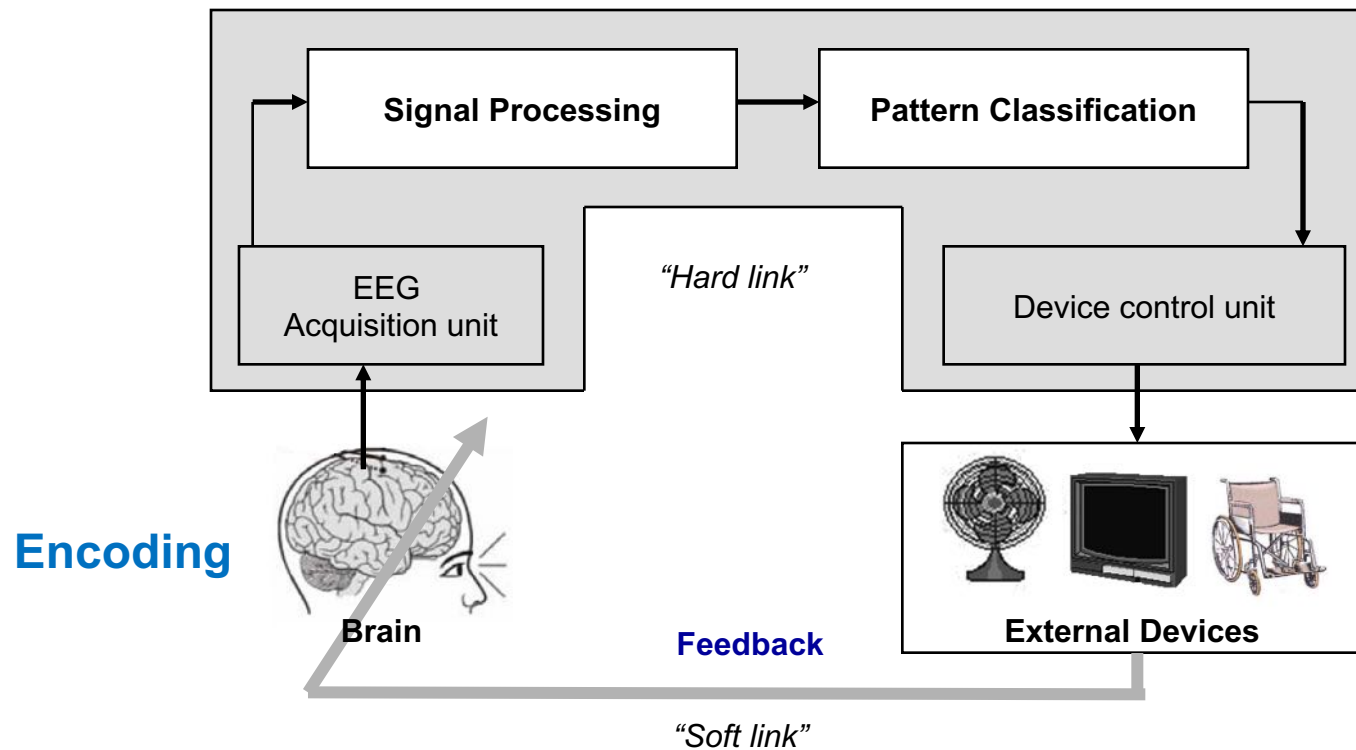
Micro-scale ( $\mu\text{m}$ )



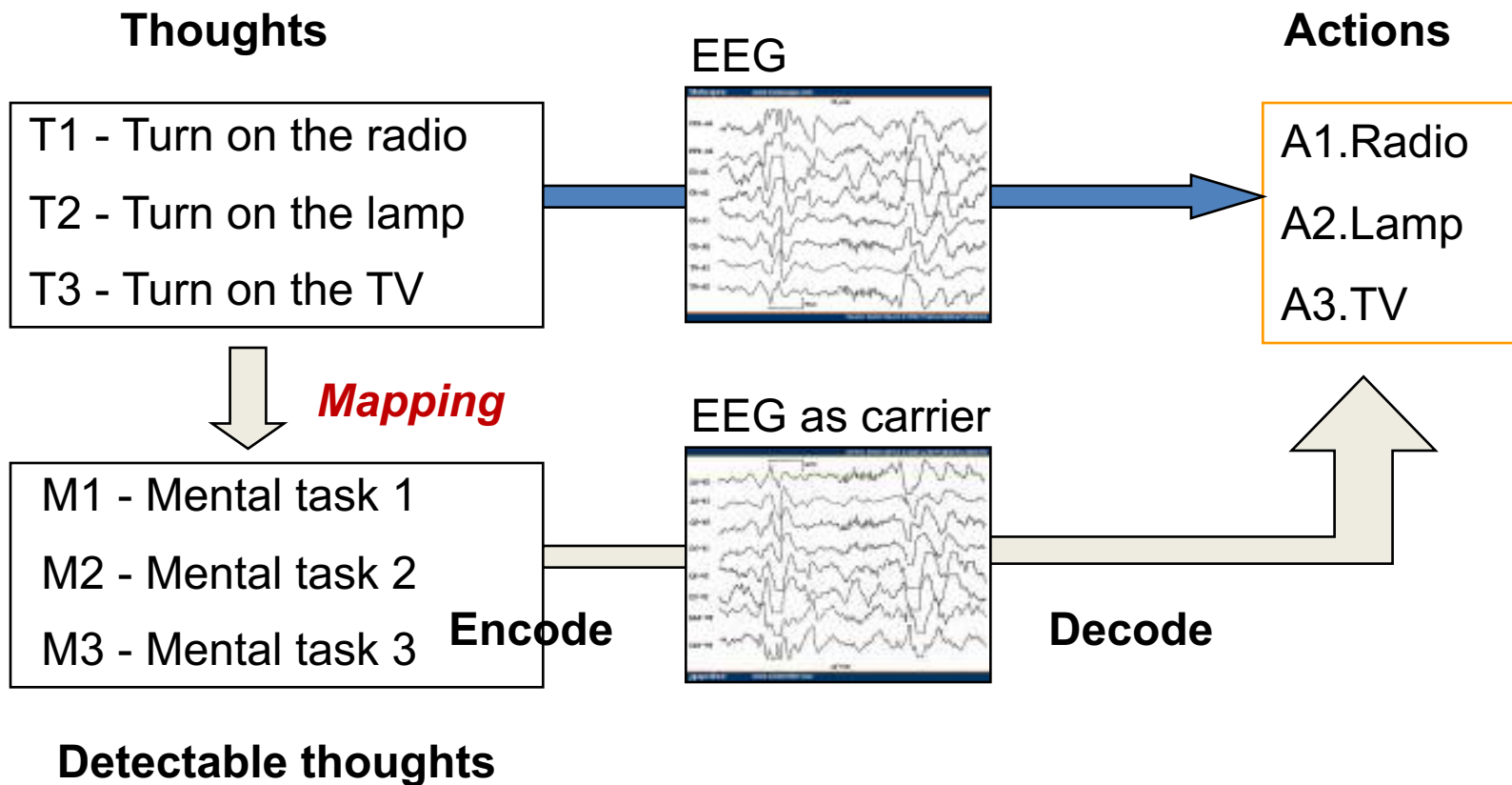
Neuronal firing  
(spike)

# EEG based Brain Computer Interface (BCI)

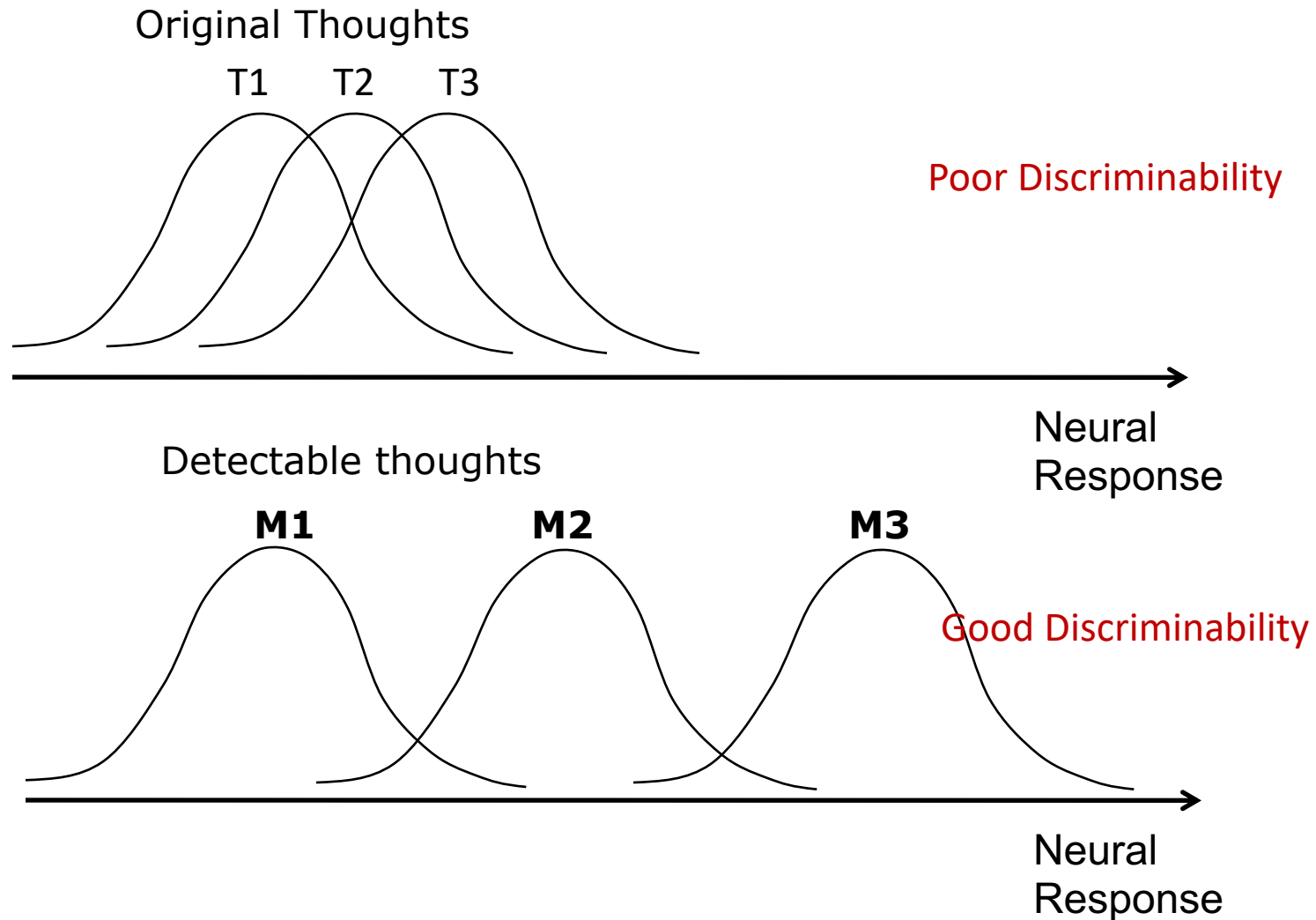
## BCI core for control command **decoding**



# Direct vs indirect mind reading



# Mapping and Classification in BCI



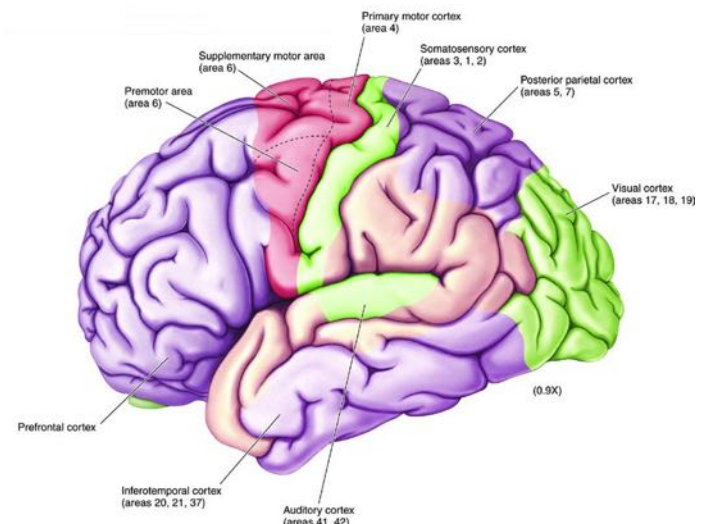
# Detectable brain activities for BCI

## – Event Related Potential (ERP)

- Visual evoked potential (VEP)
- Auditory evoked potential
- P300
- Error Related Potential

## – Self-modulated activity

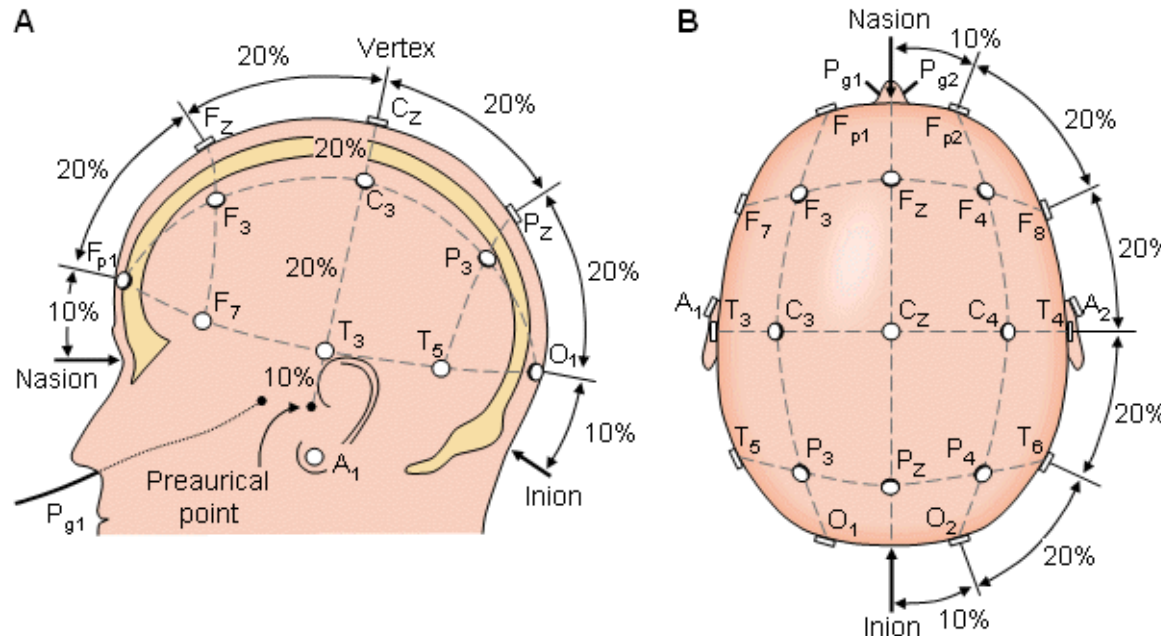
- Slow Cortical Potential (SCP)
- Sensori-motor rhythm (SMR)



J. J. Vidal, Real-time detection of brain events in EEG

*IEEE Proceedings*, vol. 65, 1977

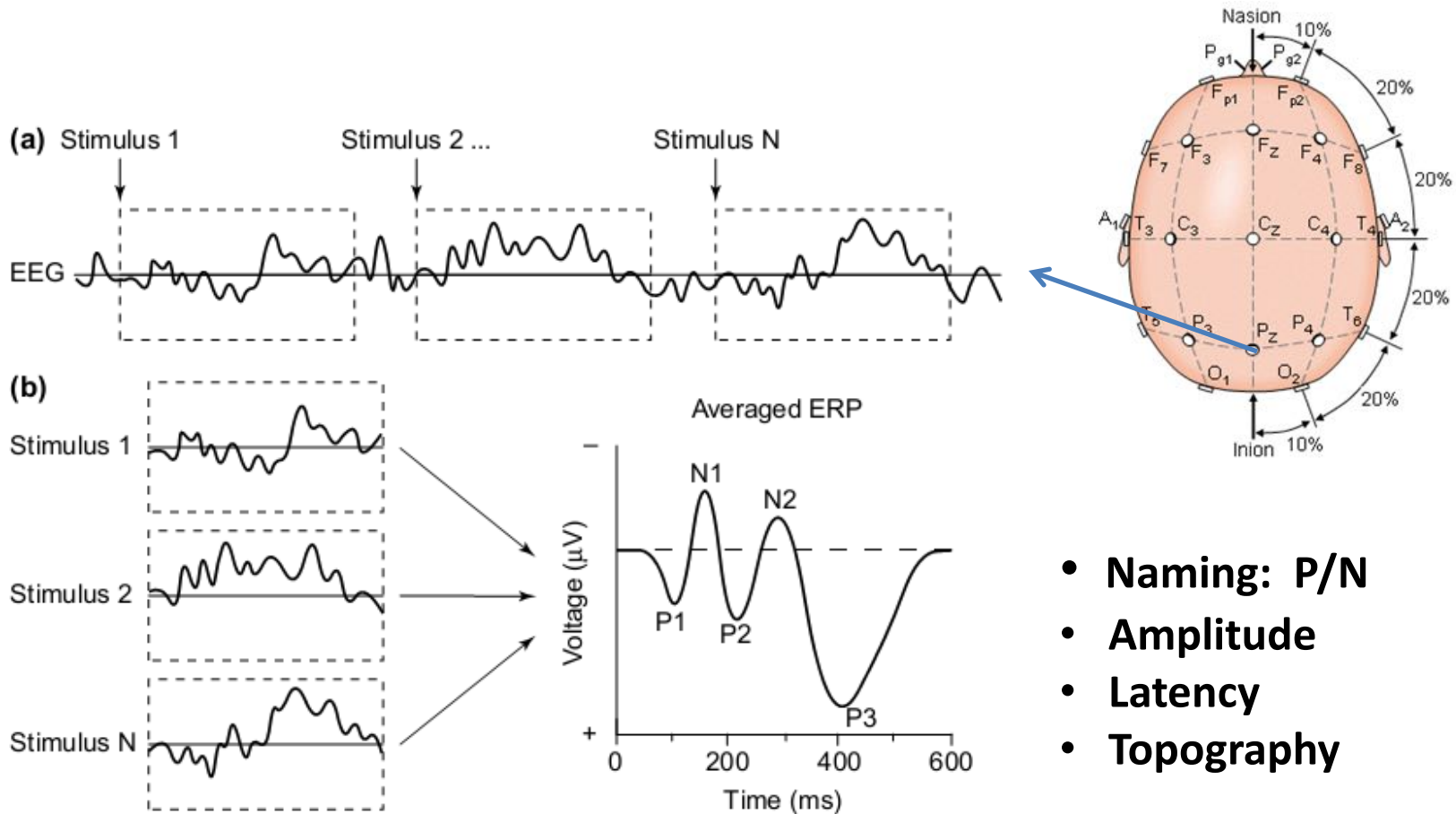
# EEG Electrode Placement



## International 10/20 EEG electrode system:

- The electrodes are placed at points that are 10% and 20% of the distances between certain fixed points on the head (Nasion and Inion as shown)
- Each electrode site is labelled with a letter and a number. The letter refers to the area of brain underlying the electrode e.g. F - Frontal lobe and T - Temporal lobe. Even numbers denote the right side of the head and odd numbers the left side of the head.

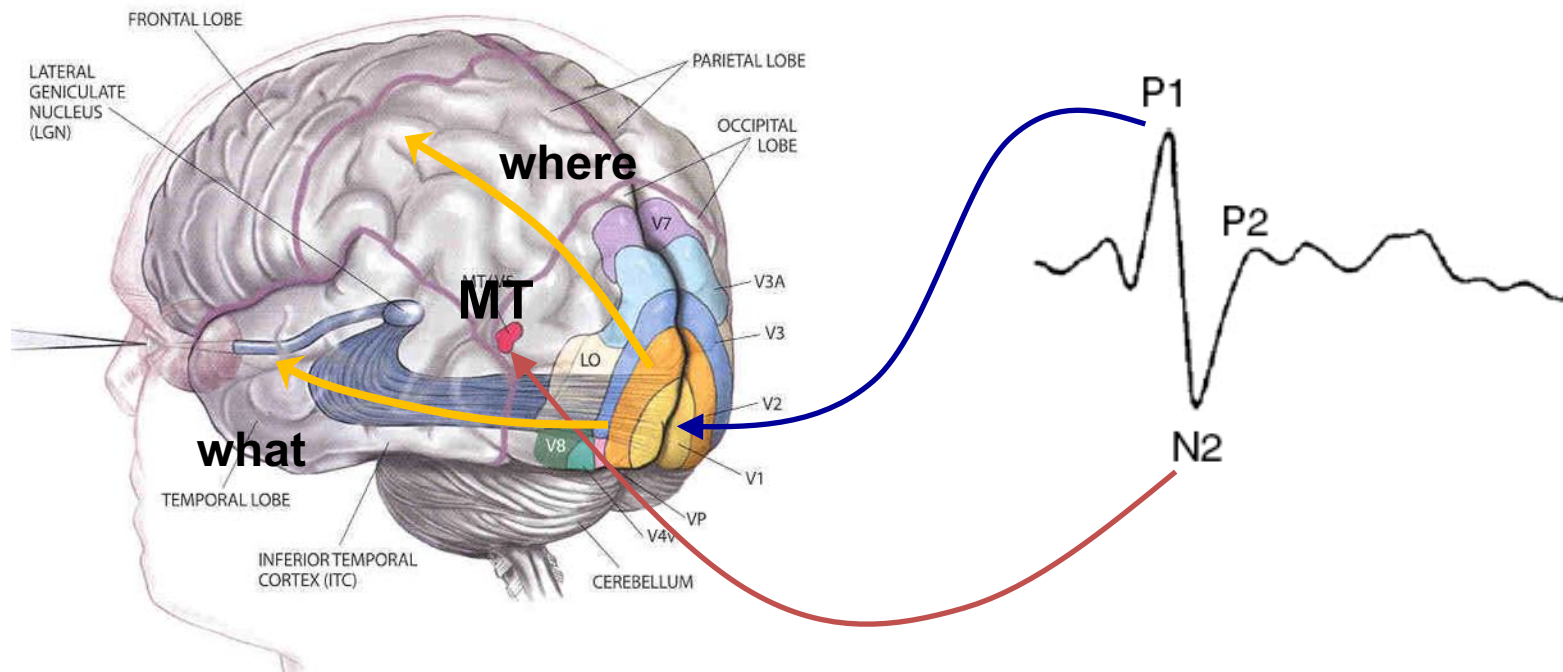
# Event Related Potential out of noisy EEG



- **Naming: P/N**
- **Amplitude**
- **Latency**
- **Topography**

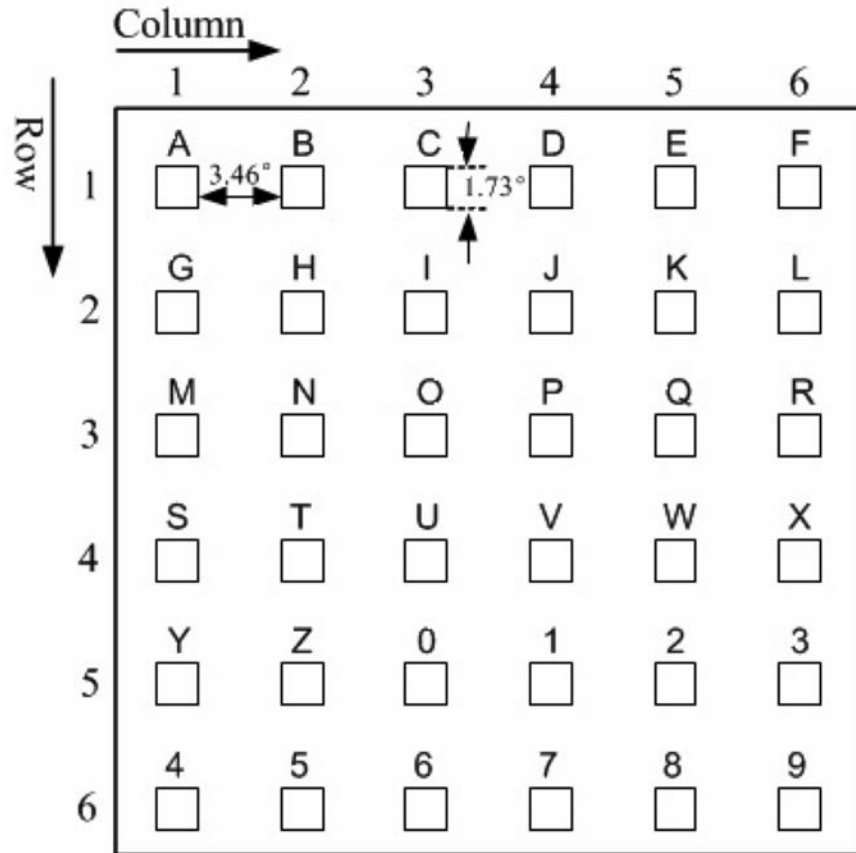
■ **N trial averaging provides N-fold increase of SNR**

# The brain area for non-flashing visual response



**Motion Visual Evoked Potential (mVEP)**

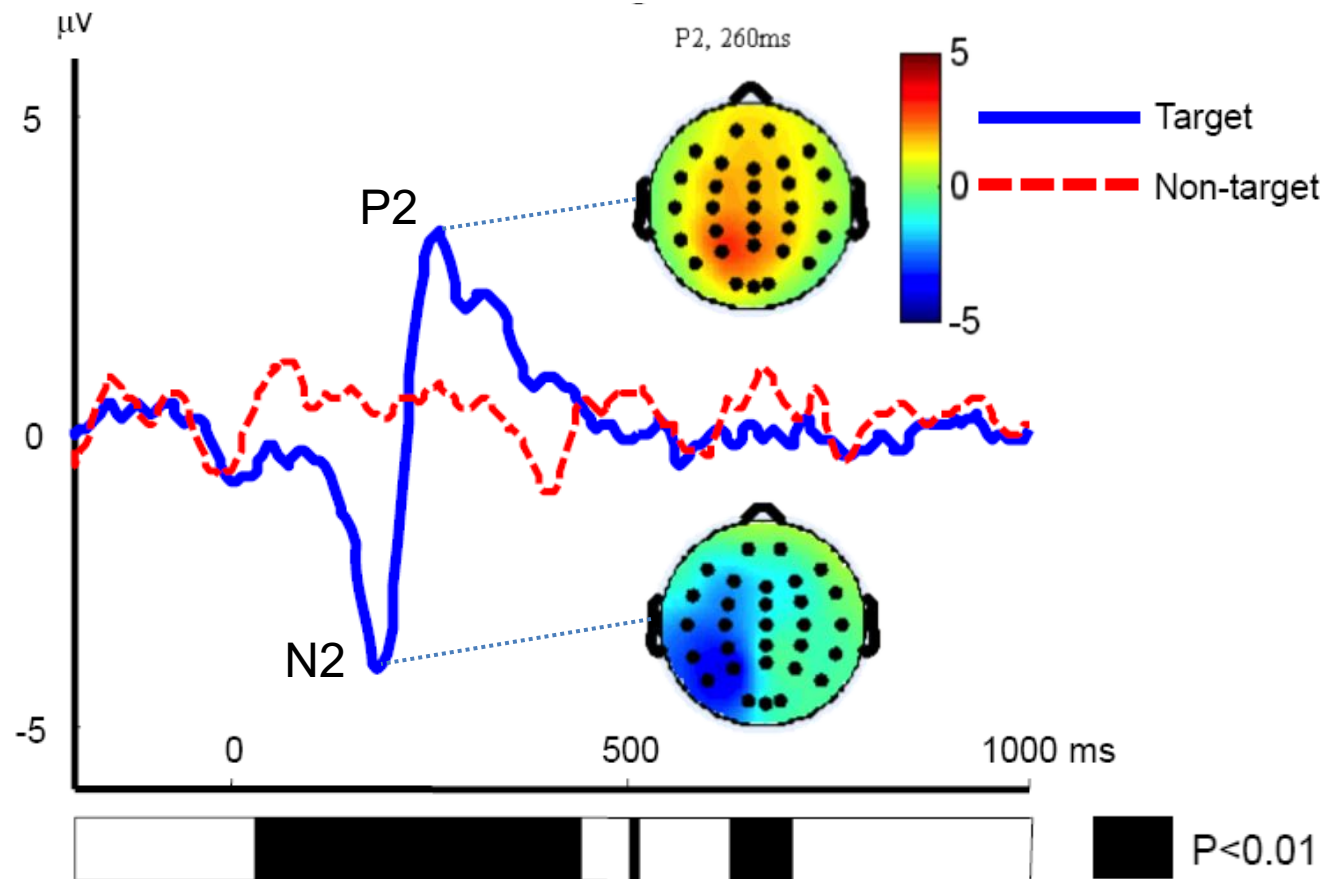
Kuba M and Kubova Z 1992



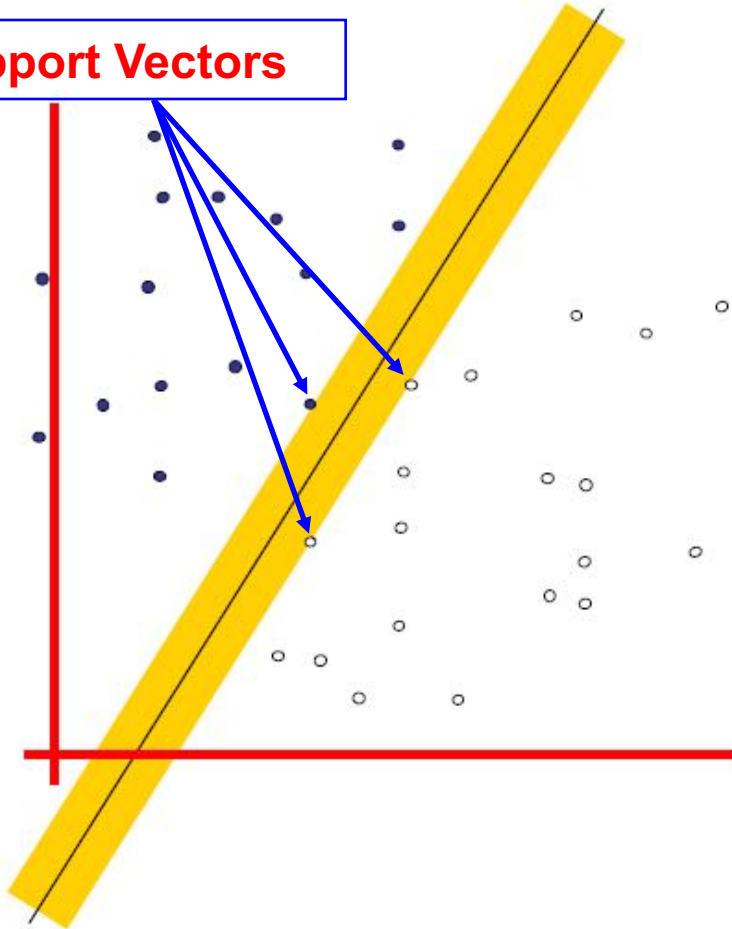
## ■ Brief motion

Direction: Leftwards , Velocity (3.1 deg/s), Motion duration (140 ms)

# Spatio-temporal pattern of motion-onset VEP (mVEP)



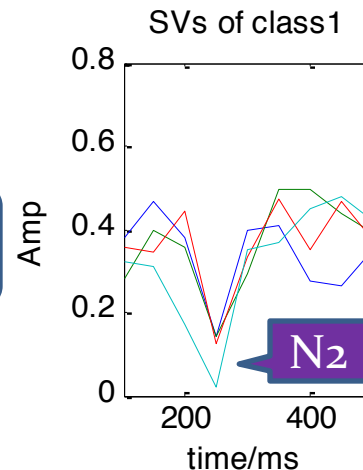
## Support Vectors



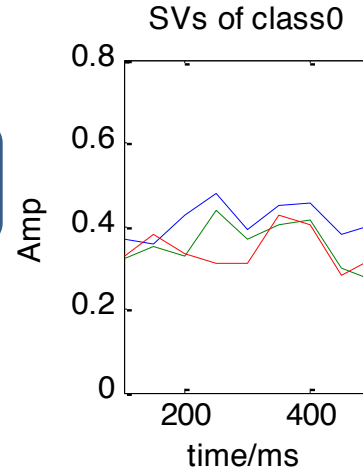
# Support Vectors

- subject 1 (dataset: 15 trials averaged)

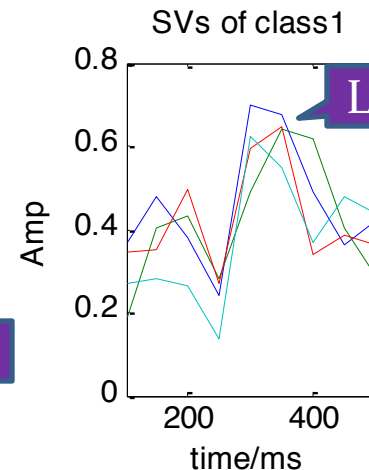
SVs of class 1



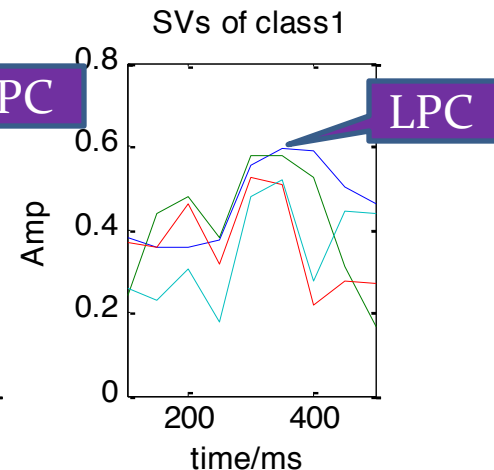
SVs of class 0



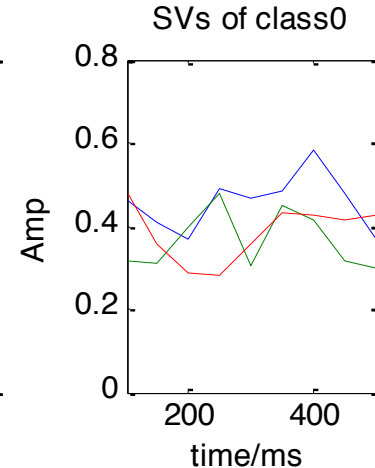
SVs of class1



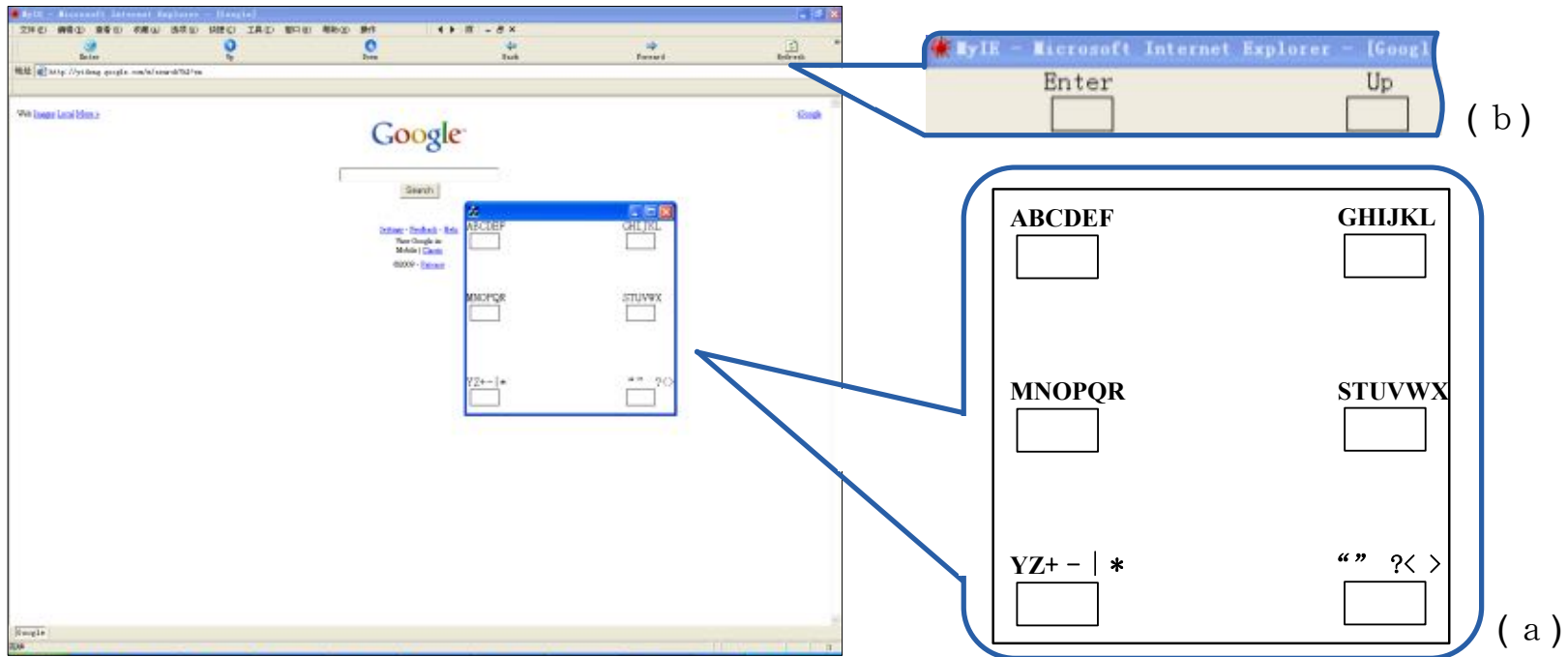
SVs of class1



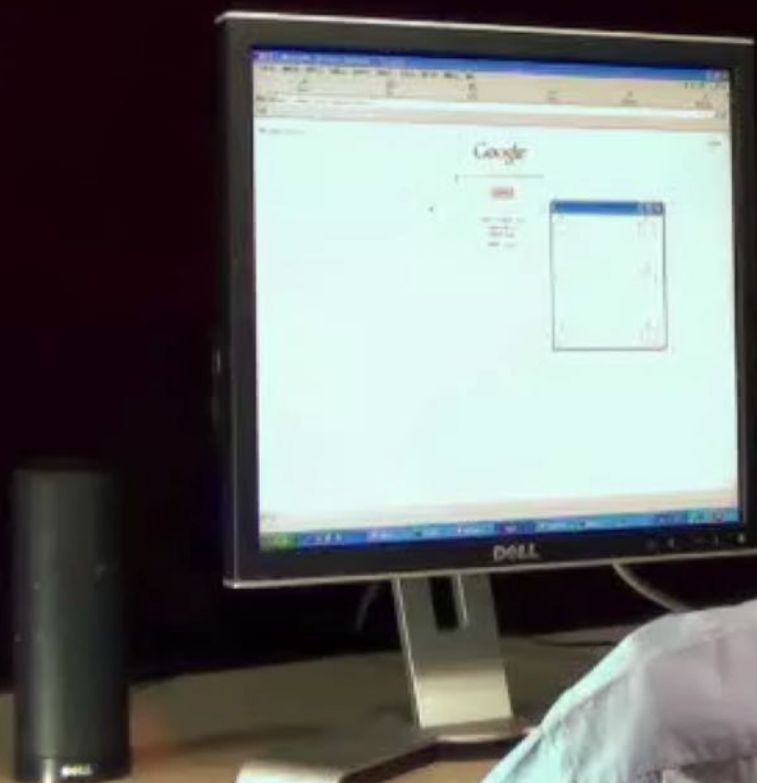
SVs of class0



# Google search by N200 BCI



Liu and Hong, 2010



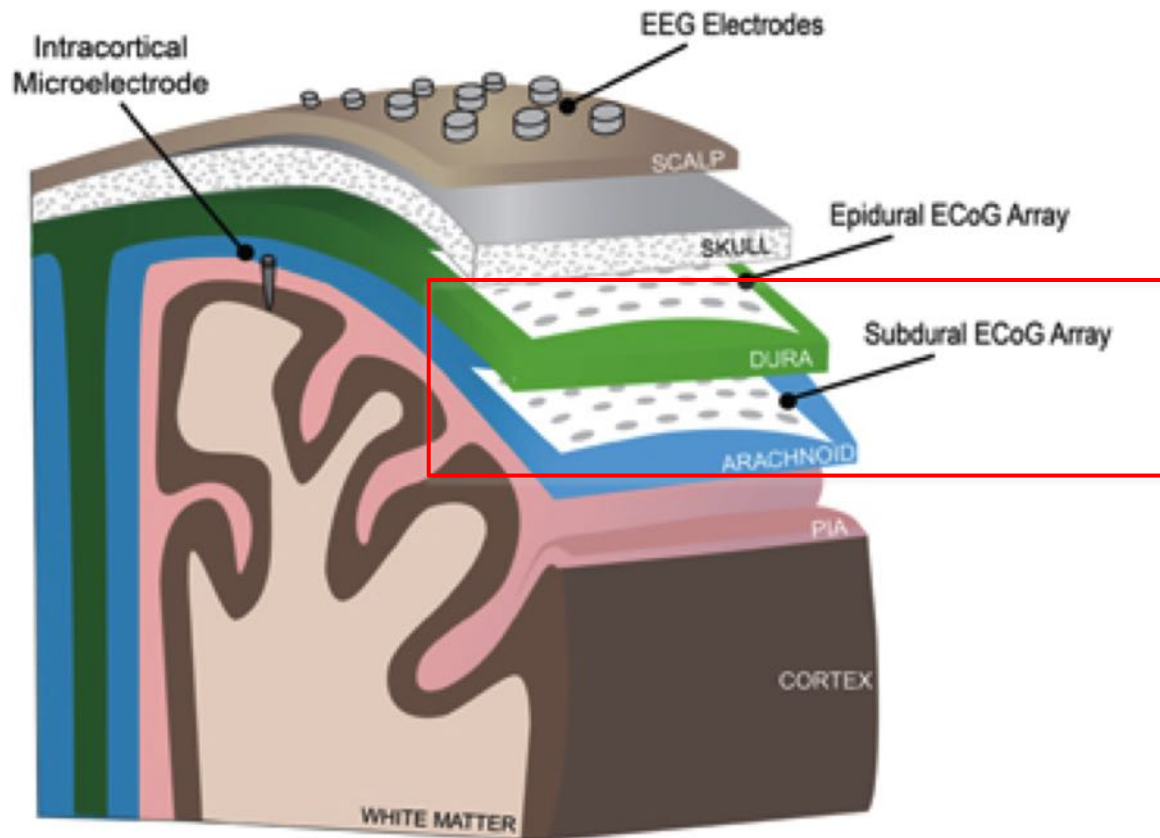
# Online testing result (copy typing)

Subject	Electrode	Input	Trials/operation	Accuracy	ITR (bits min <sup>-1</sup> )
S1	O1	AB <u>DDEF ABCDEE</u> ABCDED ABEDEF	1.9	0.83	45.3
S2	P3	ABBDEF ABC_BEE EBCDEF ABCCEA	2.3	0.79	31.6
S3	O1	ABCDEF CBCDEE EBCDEF ABCDBF	3.0	0.83	33.2
S4	P7	ABCDEF ADCDEE ABADEF ADCDEF	2.0	0.83	47.2
S5	O1	BBCFEC DBCDEF ABCDEF ABCDEF	3.4	0.83	28.5
S6	P7	ABADEF AFCDFF ABFFEF ABCFDF	1.9	0.67	23.5
S7	P3	ABCDED ABCDEF ABCDEF BBCDEF	2.2	0.88	49.9
S8	P3	AECDEF ABCDEB ABCDEF ABCDEF	2.2	0.92	51.9
S9	O1	ABCDED ABCDEF ABCDEF ABADEF	2.5	0.92	43.7
S10	P3	ABC_AED FBCDEB ABC_AEA ABCDEF	1.7	0.75	39.9
S11	P3	ABCDEF ABCDEF ABCDCF CBCDEF	1.5	0.92	76.5
S12	P7	ABBFEF ABCDEF ABCDEF CBCDDF	2.5	0.83	33.5
Average			2.3	0.83	42.1

# Online Google search result

Subject	Operations	Trials/ operation	Accuracy	Time (seconds)
S1	14	2.4	0.92	79.4
S2	10	4.3	1	77.3
S3	18	5.6	0.89	164
S4	26	5.5	0.77	234.2
S5	22	6.0	0.86	210.1
S6	18	5.3	0.89	159.6
S7	11	2.4	0.91	61.6
S8	14	4.7	0.93	114.6
S9	11	2.9	0.91	68.2
S10	14	3.2	0.93	91.5
S11	10	1.9	1	50.9
S12	14	4.9	0.93	117.9
Average	15.1	4.1	0.91	119.1

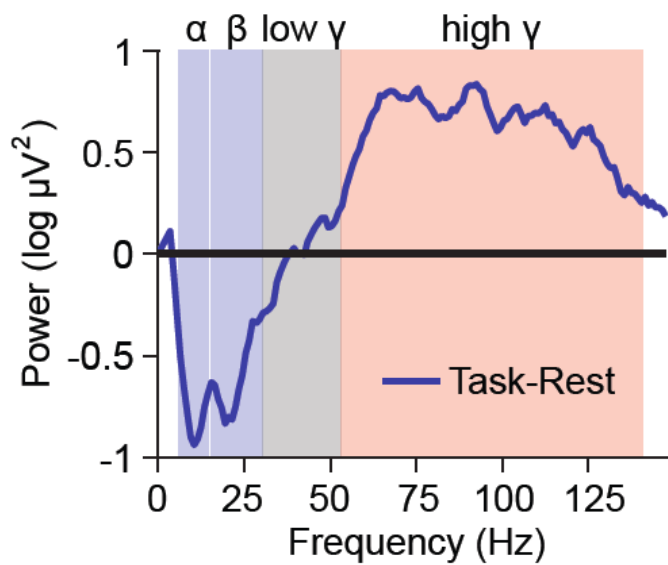
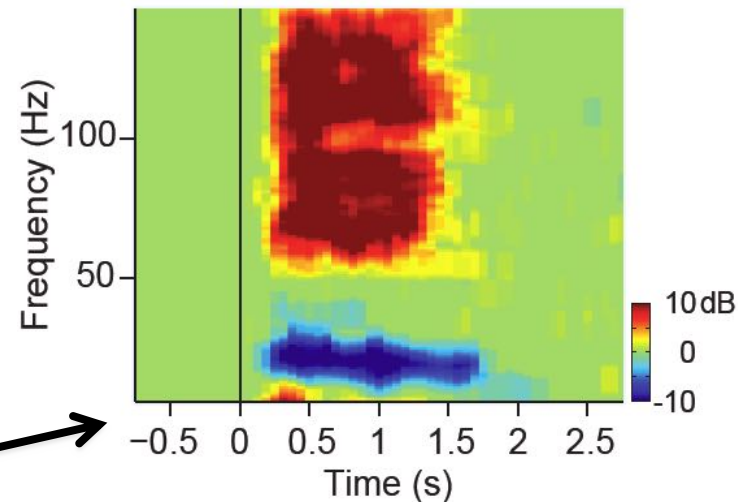
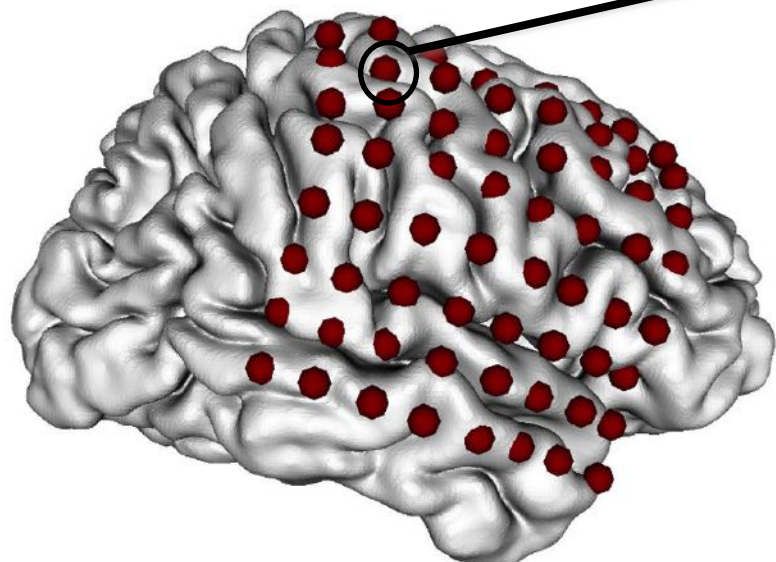
# Where to put the BCI electrodes?



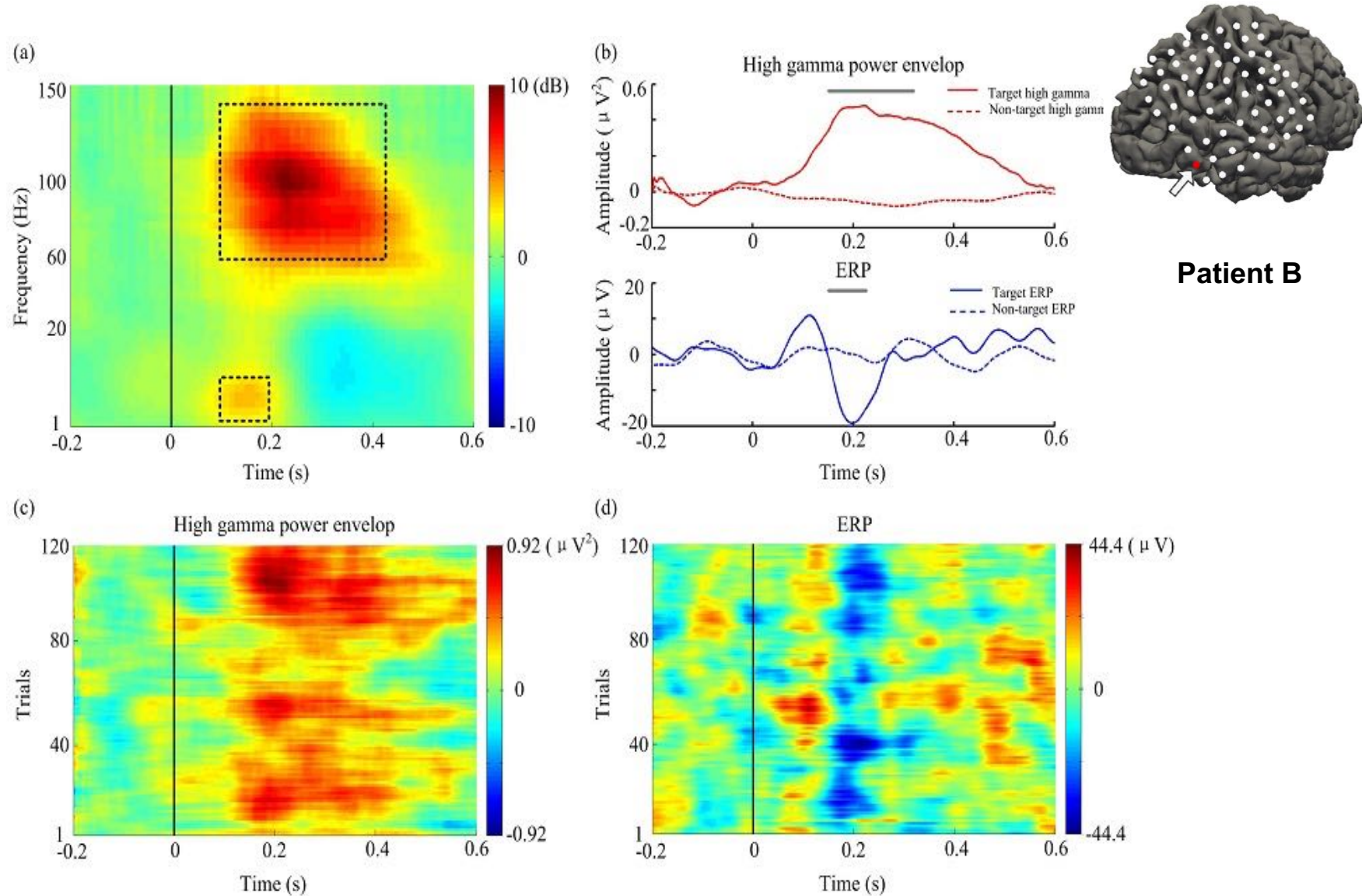
Jofri et al, 2014

# ECoG recording

- High temporal resolution
  - Rich spectral contents
  - Population neural activity
- 
- Moderate spatial resolution
  - Partial brain coverage

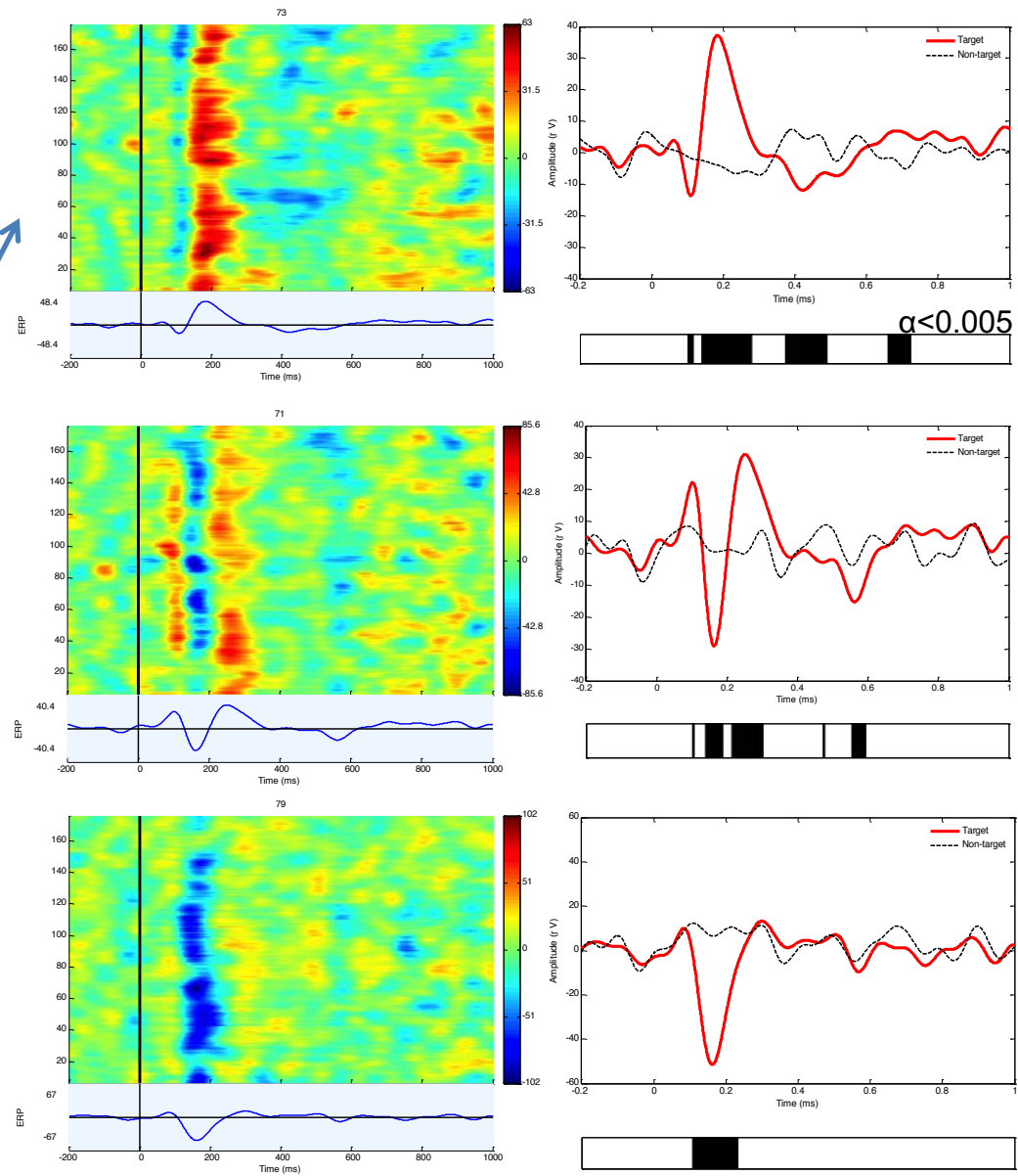
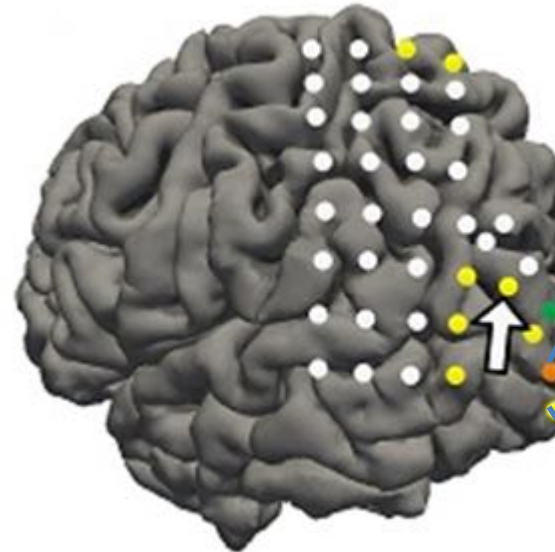


# Cortical visual motion response: High gamma + mVEP

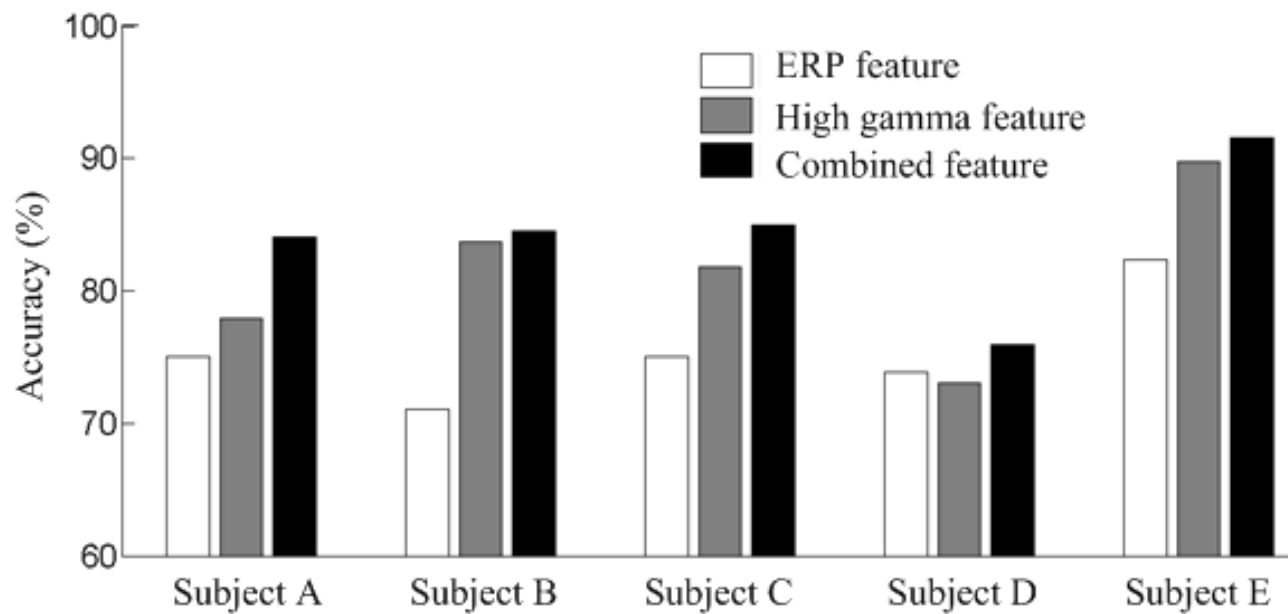


# Cortical visual motion responses : Electrode Variability

Patient D



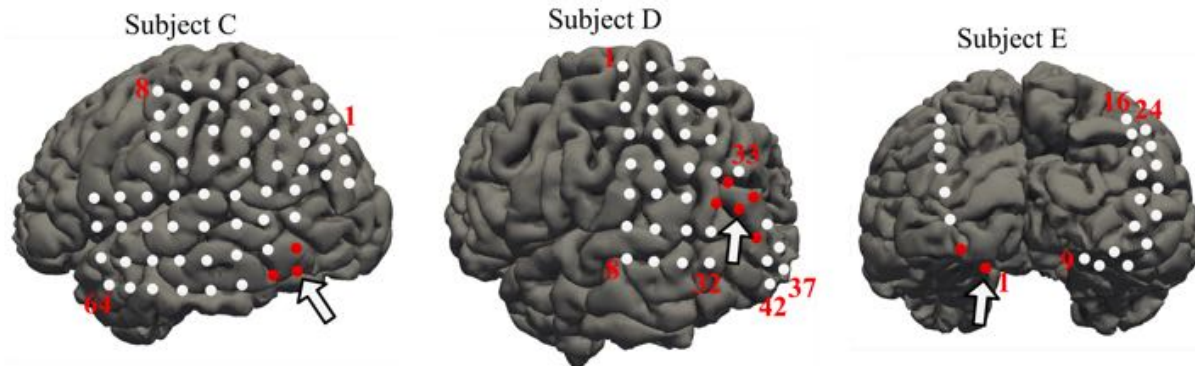
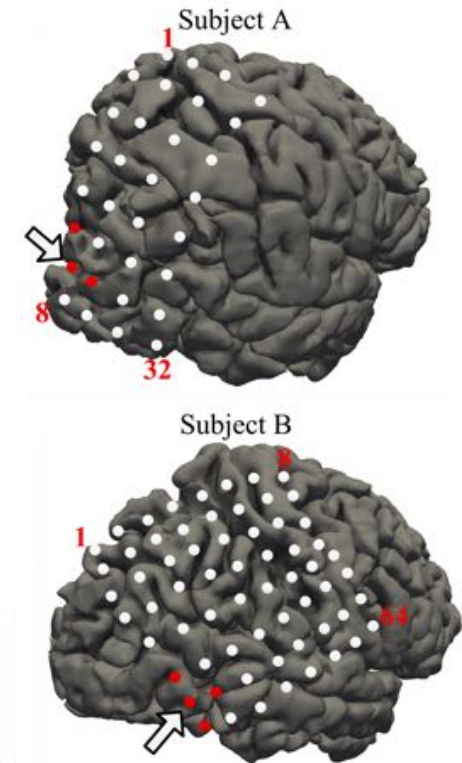
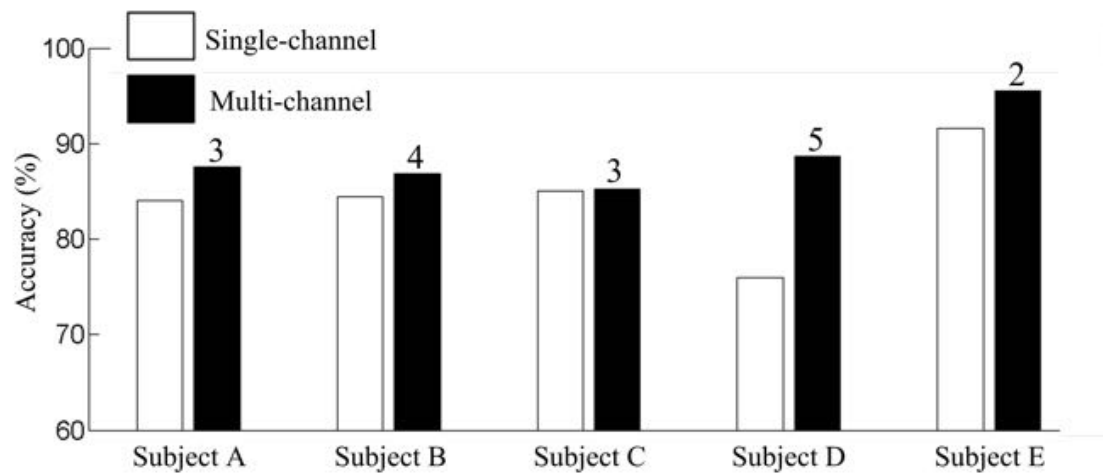
# High gamma feature enhance performance



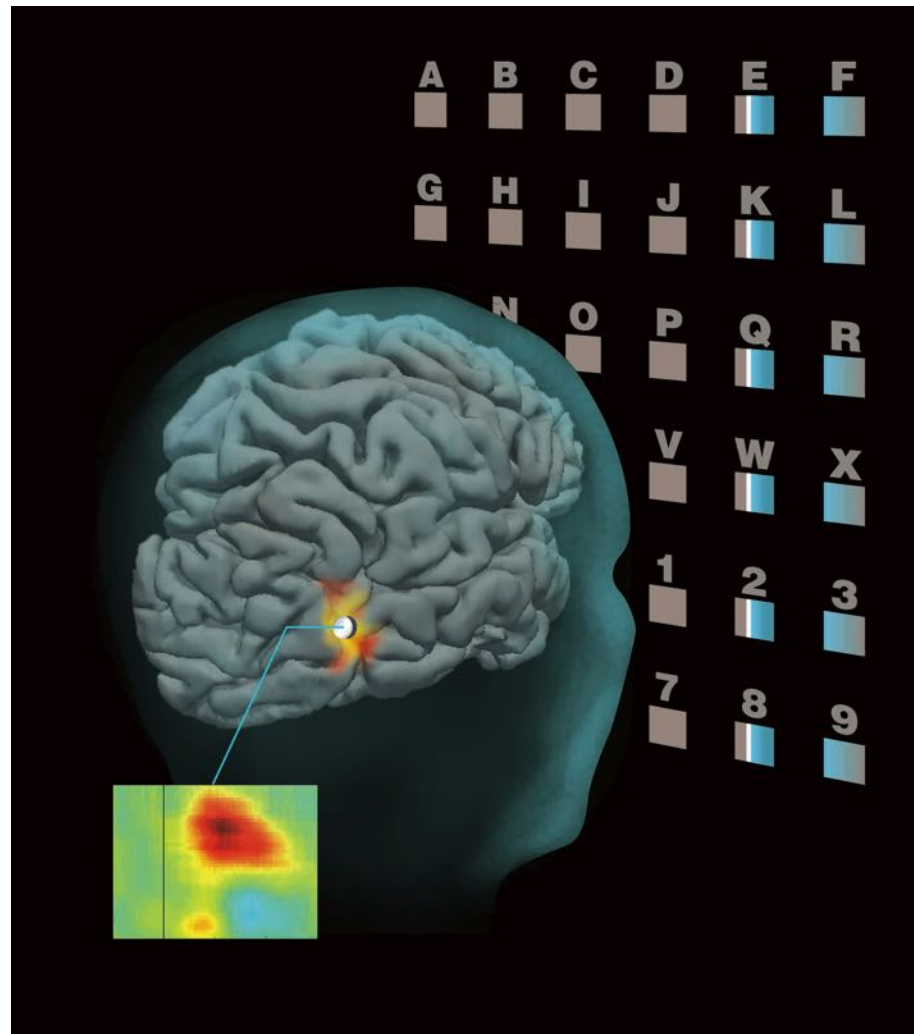
**3-trial averaging**

# Single ECoG electrode is good enough?

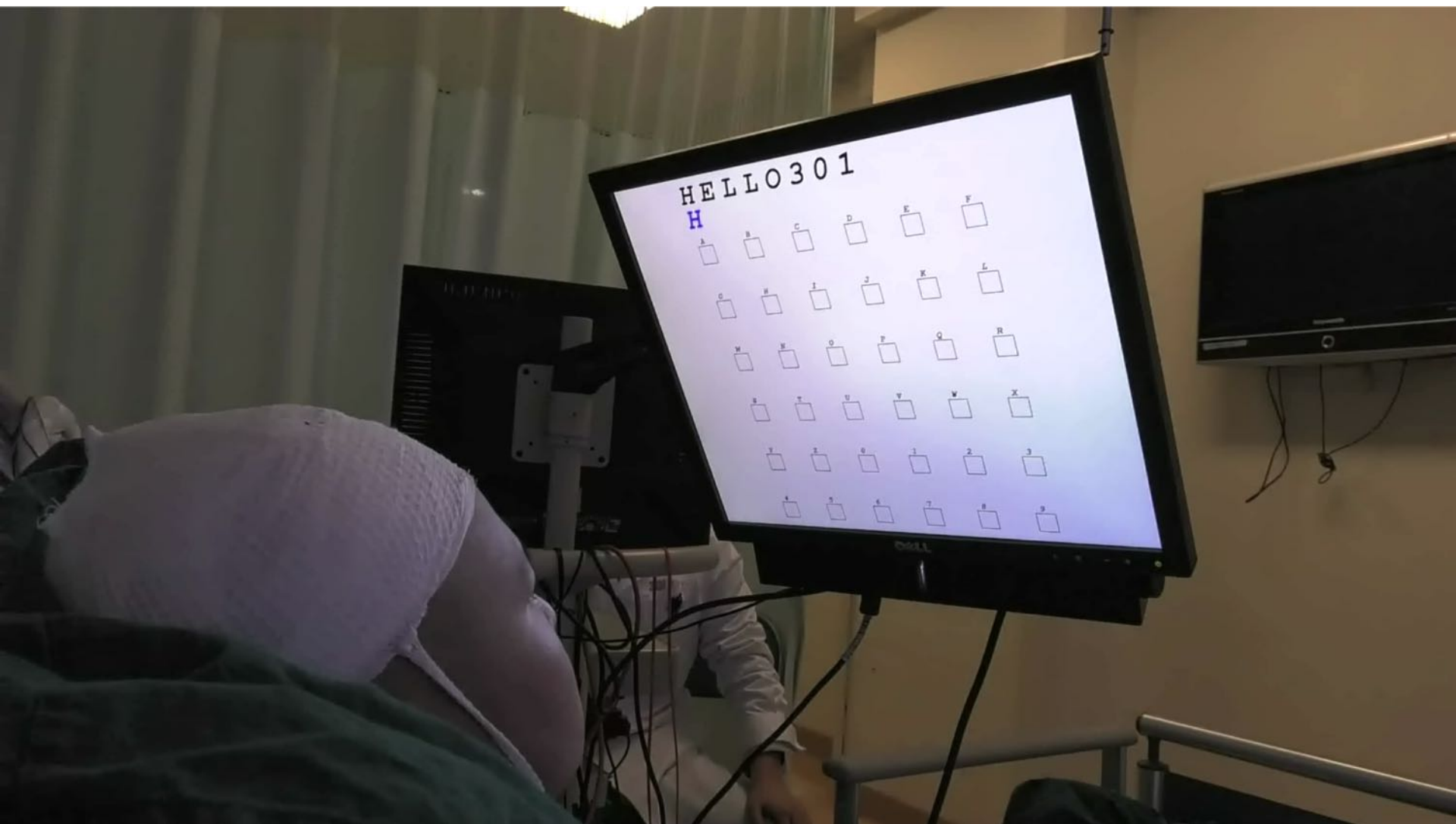
Yes



Minimally invasive with long-term stability



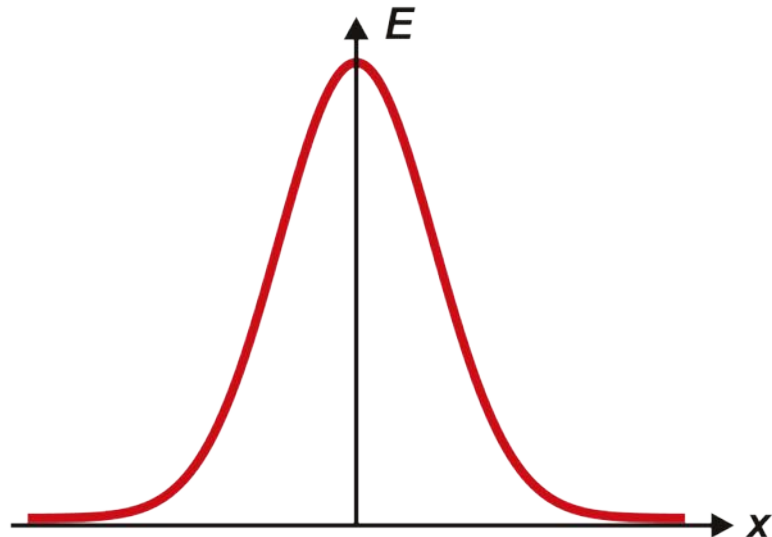
# BCI typing with one SEEG electrode



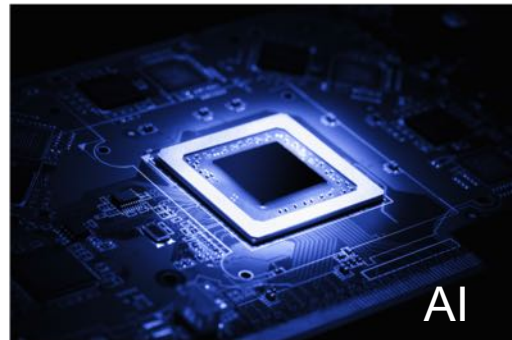
# References

- Zhang D, Song H, Xu R, Zhou W, Ling Z\*, Hong B\*. Toward a minimally invasive brain-computer interface using a single subdural channel: A visual speller study. *NeuroImage* 71:30-41, 2013.
- Liu T, Goldberg L, Gao S, Hong B\*. An online brain-computer interface using non-flashing visual evoked potentials. *Journal of Neural Engineering*, 7(3):036003.2010.
- Hong B\*, Guo F, Liu T, Gao XR, Gao SK. N200-speller using motion-onset visual response. *Clinical Neurophysiology*, 120:1658–1666, 2009.

# AI和BI – 你中有我，我中有你



BI



AI

智能 - 应对确定性和不确定性的能力

*Certainty and Uncertainty!*